

กระบวนการไฮบริดโดยใช้ไฮโดรไซโคลน โคแอกกูเลชัน ฟลอกกูเลชันและการลอยตะกอน
ในการบำบัดน้ำ



นางสาวประดิพัทธ์ บำรุงศรี

สถาบันวิทยบริการ จุฬาลงกรณ์มหาวิทยาลัย

วิทยานิพนธ์นี้เป็นส่วนหนึ่งของการศึกษาตามหลักสูตรปริญญาวิทยาศาสตรดุษฎีบัณฑิต

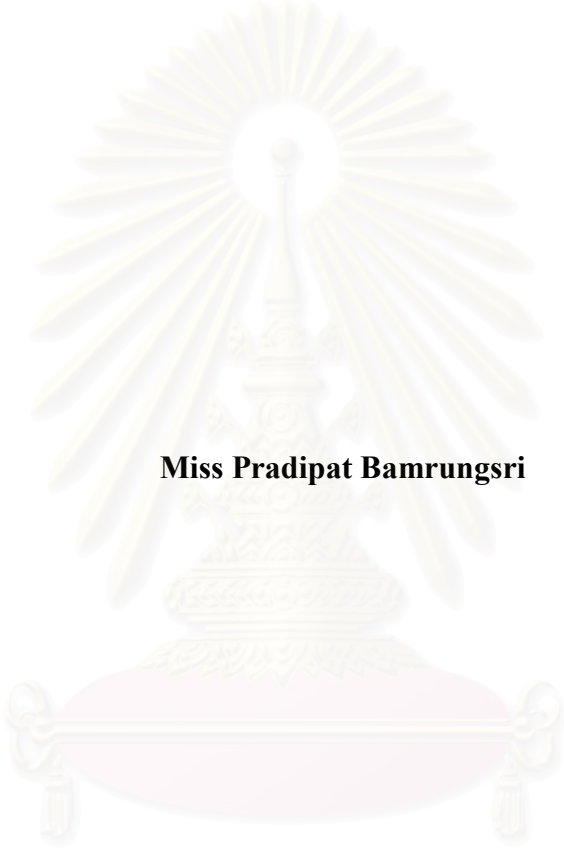
สาขาวิชาการจัดการสิ่งแวดล้อม (สหสาขาวิชา)

บัณฑิตวิทยาลัย จุฬาลงกรณ์มหาวิทยาลัย

ปีการศึกษา 2550

ลิขสิทธิ์ของจุฬาลงกรณ์มหาวิทยาลัย

**HYBRID PROCESS: HYDROCYCLONE, COAGULATION,
FLOCCULATION AND FLOATATION IN WATER TREATMENT PROCESS**



Miss Pradipat Bamrungsri

สถาบันวิทยบริการ
จุฬาลงกรณ์มหาวิทยาลัย

**A Dissertation Submitted in Partial Fulfillment of the Requirements
for the Degree of Doctor of Philosophy Program in Environmental Management
(Interdisciplinary Program)
Graduate School
Chulalongkorn University
Academic Year 2007**

Thesis Title HYBRID PROCESS: HYDROCYCLONE,
COAGULATION, FLOCCULATION AND
FLOATATION IN WATER TREATMENT PROCESS.

By Miss Pradipat Bamrungsri

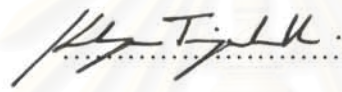
Field of Study Environmental Management

Thesis Advisor Chaiyaporn Puprasert, Ph.D.

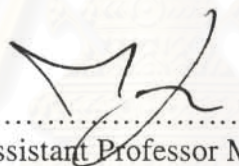
Thesis Co-advisor Professor Gilles Hébrard, Ph.D.

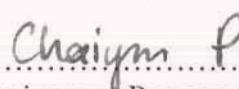
Accepted by the Graduate School, Chulalongkorn University in Partial
Fulfillment of the Requirements for the Doctoral Degree

Vice president

Acting Dean of the Graduate School
(Assistant Professor M.R. Kalaya Tingsabadh, Ph.D.)

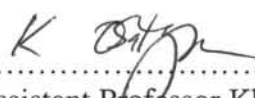
THESIS COMMITTEE

Chairperson
(Assistant Professor Manaskorn Rachakornkij, Ph.D.)

Thesis Principal Advisor
(Chaiyaporn Puprasert, Ph.D.)

Thesis Co-advisor
(Professor Gilles Hébrard, Ph.D.)

External Member
(Bowornsak Wanichkul, Ph.D.)

Member
(Assistant Professor Khemarath Osathaphan, Ph.D.)

Member
(Punjaporn Weschayanwiwat, Ph.D.)

ประดิพัทธ์ บำรุงศรี : กระบวนการไฮบริดโดยใช้ไฮโดรไซโคลน โคแอกกูเลชัน ฟล็อกกูเลชันและการลอยตะกอนในการบำบัดน้ำ. (HYBRID PROCESS: HYDROCYCLONE, COAGULATION, FLOCCULATION AND FLOATATION IN WATER TREATMENT PROCESS.) อ. ที่ปรึกษาวิทยานิพนธ์หลัก: อ.ดร. ชัยพร ภูประเสริฐ, อ. ที่ปรึกษาวิทยานิพนธ์ร่วม: Professor Gilles Hébrard. 164 หน้า.

วัตถุประสงค์ของการศึกษานี้เป็นไปเพื่อศึกษาลักษณะของภาวะทางชลศาสตร์ในไฮโดรไซโคลนและเพื่อทำการค้นหาสภาวะที่เหมาะสมในการเดินระบบไฮบริด โดยภาพรวมการทำการทดลองดำเนินไปเพื่อกำจัดอนุภาคของแข็งที่แขวนลอยอยู่ในน้ำ

สำหรับการศึกษาลักษณะทางชลศาสตร์ ได้ทำการสร้างเส้นแนวโน้มความเร็ว เส้นค่าแกระเดียนท์ของความเร็วในไฮโดรไซโคลน ในการศึกษาครั้งนี้ได้มีการนำเสนอวิธีในการศึกษาลักษณะทางชลศาสตร์ ซึ่งเป็นวิธีการในการใหม่ที่สะดวก รวดเร็ว และมีประสิทธิภาพ ทั้งนี้ผลการทดลองที่ได้สามารถนำมาใช้ในการอธิบายถึงปรากฏการณ์ที่เกิดขึ้นในระบบไฮบริด

การศึกษาเพื่อให้ได้มาซึ่งสภาวะที่เหมาะสมของระบบไฮบริด ได้มีการรวมระบบโคแอกกูเลชัน ฟล็อกกูเลชัน และระบบการแยกอนุภาคแขวนลอยให้อยู่ภายในหนึ่งถังปฏิกรณ์ พารามิเตอร์ต่างๆ ที่ส่งผลต่อระบบ เช่น ลักษณะของถังปฏิกรณ์ สัดส่วนของอากาศ และ ความเข้มข้นของโคแอกกูแลนต์ได้มีการทดลองในการศึกษาครั้งนี้ด้วย

สถาบันวิทยบริการ จุฬาลงกรณ์มหาวิทยาลัย

สาขาวิชา การจัดการสิ่งแวดล้อม

ลายมือชื่อนิสิต..... Pradipat B.....

ปีการศึกษา 2550

ลายมือชื่ออาจารย์ที่ปรึกษาวิทยานิพนธ์. Guaiem...P.

478 97024 20 MAJOR: ENVIRONMENTAL MANAGEMENT

KEYWORDS: HYDRODYNAMICS / HYBRID PROCESS / SEPARATION / HYDROCYCLONE / WATER TREATMENT.

PRADIPAT BAMRUNGSRI: HYBRID PROCESS: HYDROCYCLONE, COAGULATION, FLOCCULATION AND FLOATATION IN WATER TREATMENT PROCESS.

THESIS PRINCIPLE ADVISOR: CHAIYAPORN PUPRASERT, Ph.D.,

THESIS CO-ADVISOR: PROFESSOR GILLES HEBRARD, Ph.D., 164 pp.

The aims of this research are to characterize the hydrodynamics in the hydrocyclones and find out the optimum operating conditions for the hybrid process. The objective of this hybrid process is to separate the solid particle from the turbid raw water.

The hydrodynamics characterization study is carried out in the hydrocyclones to investigate the velocity profiles and velocity gradients. In this study, a new, simple and effective method is developed to study the hydrodynamics for the further research. The obtained experimental results are used as the background knowledge to design and explain the found phenomena in the hybrid process.

This hybrid process is the integration of the conventional coagulant, flocculation and separation process in a reactor which is an innovation for the water treatment. Many operating conditions are tested in the hydrocyclone to find out the optimum condition such as the hydrocyclone geometry, air fraction, and coagulant concentration.

สถาบันวิทยบริการ
จุฬาลงกรณ์มหาวิทยาลัย

Field of study: Environmental management

Student's signature: Pradipat B.

Academic Year: 2007

Principal Advisor's signature: Chaiyaporn P.

ACKNOWLEDGEMENT

First of all, I would like to thank Prof. Gilles Hébrard, Dr. Chaiyaporn Pupasert, and Assist. Prof. Christelle Guigui for their great advices to carry out this research. Thank for a great chance that allowed me to study in this innovative equipment.

I would like to thank as well for

- Monsieur Alain Grasmick, professor of USTL de Montpellier II and Assist. Prof. Manaskorn Rachakornkij for the acceptance of the referees.
- Monsieur Yves Aurelle, professor of INSA de Toulouse, for the acceptance of the chairman for this thesis.
- Monsieur Philippe Marteil, the research and development engineer from VEOLIA WATER for the acceptance of the invitee of this thesis.
- In addition, I would like to thank for the National Center of Excellence for Environmental and Hazardous Waste Management (NCE-EHWM), Chulalongkorn University, Thailand, the Chemical and Environmental Engineering, Institut National des Sciences Appliquées de Toulouse (INSA-Toulouse), French Embassy in Thailand and VEOLIA WATER Company for the financial supports along the research.
- A great thank you for the administrative officers and technicians in the laboratory of LISBP to help to me to settle in France. Thank to Louis Lopez, Dominique Auban, Bernard Reboul, Nathalie Clergerie, Vincent Fontanaz and a great secretary, Daniele Corradi.
- Thank you for the administrative officers at NRC-EHWM for the kindly assistance of the administrative documents and special thank for Akiko for her kindness and English consults of this thesis.

Finally, I would like to dedicate the great thank you for the patience and love for my parents. I really appreciate to be your daughter and I hope that one day I can return of everything that you gave to me.

CONTENTS

	page
Abstract (Thai)	IV
Abstract (English).....	V
Acknowledgement.....	VI
Contents.....	VIII
List of Tables.....	XIV
List of Figures.....	XVI
List of Abbreviations.....	XXII
CHAPTER I INTRODUCTION.....	1
The objectives of the study	1
CHAPTER II BIBLIOGRAPHY	3
Part 1 Coagulation and flocculation.....	3
1.1 Introduction.....	3
1.2 Coagulation mechanisms in water production.....	5
1.2.1 Electrostatic coagulation	5
1.2.2 Coagulation by chemical reaction.....	5
1.2.3 Adsorption/charge neutralization and Polymer bridging.....	6
1.2.4 Sweep coagulation	6
1.3 Mixing and contact time for coagulant and flocculation.....	7
Part 2 Hydrocyclone.....	10
2.1 Components and operating principle of classical hydrocyclone.....	10
2.2 The advantages of utilizing a hydrocyclone	12
2.3 The disadvantages of utilizing a hydrocyclone.....	12

2.4	Basic theories of the hydrocyclone	13
2.4.1	The velocity components	13
2.4.1.1	The liquid tangential velocity.....	14
2.4.1.2	The liquid axial velocity.....	15
2.4.1.3	The liquid radial velocity	16
2.4.2	The velocity profile study in the hydrocyclone.....	17
2.4.2.1	Flow pattern in conical and cylindrical hydrocyclone	17
2.4.3	The liquid angular velocity	20
2.4.4	The liquid velocity gradient	20
2.4.5	Particle motion into a hydrocyclone	24
2.4.6	Physico-chemical parameters.....	25
2.5	Applications of hydrocyclones in water treatment processes	27
2.6	The application of coagulation and flocculation in a hydrocyclone.....	33
Part 3	Micro bubble production	36
3.1.1	The available approaches that produce micro bubbles	36
3.1.2	Dissolved air floatation (DAF).....	37
3.1.3	New processes using microbubble injections inside flocs	37
Part 4	Conclusion of the useful bibliography.....	42
4.1.1	The principles of the coagulation and flocculation process	42
4.1.2	The required properties for the coagulation and flocculation process	42
4.1.3	The separation potential of the hydrocyclone	42
4.1.4	The constant angular velocity in the hydrocyclone.....	43
4.1.5	Micro bubble production.....	43
Part 5	Hybrid process	45
5.1	Principle and expected phenomena of the hybrid process	45
5.2	The controlled parameters for the hybrid process.....	46
5.2.1	Coagulant concentration.....	47
5.2.2	Air fractions	47
5.2.3	Velocity gradient and raw water flow rate.....	47
5.2.4	Water inlet diameter	48
5.2.5	Geometry of the hydrocyclone.....	48

5.3 Application of coagulation and flocculation in the hydrocyclone.....	48
Part 6 Mission and objectives of this Thesis.....	52

CHAPTER III MATERIALS AND METHODS..... 53

Part 1 Materials and methods for the hydrodynamic study.....	53
1.1 Materials for the hydrodynamic study.....	53
1.1.1 Oil tracer solution.....	53
1.1.2 Hydrocyclones.....	54
1.1.3 Digital high-speed camera.....	55
1.2 Hydrodynamic experiment methods.....	55
1.2.1.1 Injection of oil droplets in the hydrocyclones.....	55
1.2.1.2 Picture acquisition.....	56
1.2.1.3 Operating conditions.....	58
1.2.1.4 The calculation of the axial and tangential velocities of the water.....	58
1.2.1.5 The tangential velocity gradient.....	62
Part 2 Materials and methods of the hybrid process study.....	65
2.1 Materials of the hybrid process study.....	65
2.1.1 Pilot experiment description.....	65
2.1.2 Preparation of raw water.....	66
2.1.3 Hydrocyclone.....	66
2.1.4 Raw water inlet diameter.....	68
2.1.5 Coagulant.....	69
2.1.6 Pressurized water preparation.....	69
2.1.7 Experimental description.....	70
2.1.8 Experimental feeding procedure.....	71
2.1.8.1 Rapid start-up (Method 1).....	71
2.1.8.2 Progressive start-up (Method 2).....	71
2.2 Calculation methods for the hybrid process.....	71
2.2.1 Calculation of air fractions.....	71
2.3 Operating conditions.....	73

2.3.1 Summarized operating conditions in the hybrid process study.....	73
2.3.2 Observed parameters for the hybrid process study	75

CHAPTER IV EXPERIMENTAL RESULTS..... 77

Part 1 The hydrodynamic characterization study.....	78
1.1 Validation of the oil droplet tracer method.....	78
1.2 The trajectory line of the oil droplets.....	79
1.2.1 Conclusions of the trajectory line for the hybrid process	81
1.3 The velocity profiles inside the hydrocyclones	82
1.3.1 The different diameter cylindrical hydrocyclone, HC1	82
1.3.1.1 Effects of the water flow rate	82
1.3.1.2 Effects of the water inlet diameter	84
1.3.2 Conical hydrocyclone HC2.....	86
1.3.2.1 Effects of the water flow rate	86
1.3.2.2 Effects of the water inlet diameter	88
1.3.3 Constant diameter cylindrical hydrocyclone HC3	89
1.3.3.1 Effects of the water flow rate	89
1.3.3.2 Effects of the inlet diameter	90
1.4 Comparison of tangential velocity for the different hydrocyclones: HC1, HC2, and HC3.....	92
1.5 Prediction of tangential velocity (V_z) versus the radius (R)	94
1.6 Discussion and conclusions on the velocity field for the hybrid process.....	97
1.7 Tangential velocity gradient	98
1.7.1 Different diameter cylindrical hydrocyclone HC1.....	98
1.7.1.1 Effects of the water flow rate	98
1.7.1.2 Effects of the water inlet diameter	99
1.7.2 Conical hydrocyclone HC2.....	101
1.7.2.1 Effects of the water flow rate	101
1.7.2.2 Effects of the inlet diameter	102
1.7.3 Constant diameter cylindrical hydrocyclone, HC3	103

1.7.3.1	Effects of the water flow rate	103
1.7.3.2	Effects of the inlet diameter	105
1.7.4	Comparison of the different hydrocyclone configurations	106
1.7.5	Tangential velocity gradient modeling.....	108
1.7.6	Experimental velocity gradient conclusions	109
1.8	Hydrodynamic characterization study	110
Part 2	The hybrid process study	111
2.1	The main objective of the hybrid process	111
2.2	The effects of important parameters on floating floc production.....	114
2.2.1	Influence of hydrodynamics on the floating floc production.....	114
2.2.2	The effects of axial velocity on bubble coalescence.....	116
2.2.2.1	The experimental results of HC1	116
2.2.2.2	The experimental results of HC2	118
2.2.2.3	The experimental results of HC2 and HC3.....	118
2.2.3	Influence of the air fraction on the production of floating floc.....	119
2.2.3.2	Modification of air fractions by varying the raw water flow rates.....	120
2.2.3.3	A variation of the total pressure in pressurized tank.....	121
2.2.3.4	The synthesis the global range of air fraction	123
2.2.4	The influence of the coagulant concentration on the floating floc production.....	124
2.2.5	Influence of the location of pressurized water on the floating floc percentage.....	126
2.2.6	The conclusions and selection of HC3 or HC4.....	127
2.3	The effects of the significant parameters on the separation efficiency.....	128
2.3.1	The influence of the raw water flow rate in HC3.....	128
2.3.1.1	Raw water inlet diameter = 0.50 cm	128
2.3.1.2	For raw water inlet diameter = 0.30 cm	130
2.3.2	The influence of the velocity inlet	131
2.3.3	The influence of the raw water flow rate	132

2.3.4	The influence of the air fraction.....	133
2.3.5	The influence of the coagulant concentration	134
2.3.6	The influence of G^*t on the separation efficiency	136
2.4	Global performances of the hybrid process for the optimum conditions.....	137
2.4.1	The influence of the start-up method	137
2.4.2	Optimum condition for the hybrid process in HC3.....	138

CHAPTER V GENERAL CONCLUSION AND PERSPECTIVES.....	140
General conclusions	140
Perspective of this study.....	142
REFERENCES	143
APPENDICES	146
BIOGRAPHY	163

สถาบันวิทยบริการ
จุฬาลงกรณ์มหาวิทยาลัย

LIST OF TABLES

Table	page
II-1. The recommended criteria for the coagulation and flocculation process	8
II-2. Expression of various forces on the different axes	25
III-1. The main dimensions of each hydrocyclone.....	55
III-2. Operating conditions of the hydrodynamics study	58
III-3. The operating conditions and experimental values in this study	73
III-4. The velocity inlet and detention time for each operating condition	74
III-5. The observed parameter and observation methods used in this study.....	75
IV-1. Axial direction of the flow streams of each hydrocyclone at a water flow rate of 200 l/hr and water inlet diameter of 0.50 cm	80
IV-2. Axial Direction of flow stream of each hydrocyclone at a water flow rate of 400 l/hr and water inlet diameter of 0.50 cm.....	80
IV-3. Axial direction of the flow streams of each hydrocyclone at a water flow rate of 200 l/hr and water inlet diameter of 0.30 cm	81
IV-4. Relations between the tangential velocity, V_z , and the radius, R, with a constant inlet diameter of 0.50 cm.....	97
IV-5. The average calculated and predicted velocity gradients at the constant water inlet diameter of 0.5 cm.	108
IV-6. Production of floating floc and hydrodynamic result for HC2 and HC3.....	115
IV-7. A comparison of the hydrodynamics results of the different raw water inlet diameters for HC1.....	117
IV-8. A comparison of the hydrodynamics results of the different raw water inlet diameters for HC2.....	118
IV-9. The hydrodynamic experimental results for HC2 and HC3.	119
IV-10. Bubble coalescence observations and the percentage of floating floc in HC3 and HC4 at different coagulant concentrations.....	126

IV-11. The relationship of $G_{z,exp} * t$ and the separation efficiency of each raw water flow rate.	136
IV-12. The influence of the start-up method on the separation efficiency.....	137
V-1. The optimum operating condition for the hybrid process	141



สถาบันวิทยบริการ
จุฬาลงกรณ์มหาวิทยาลัย

LIST OF FIGURES

Figure	page
II-1. A negative colloidal particle with its electrostatic field.	4
II-2. Basic components of classical hydrocyclone.....	11
II-3. Velocity directions of the three axes.....	14
II-4. Velocity profile expressions of a free vortex, forced vortex, and combined vortex in a hydrocyclone.....	15
II-5. Axial velocity profile in a hydrocyclone	16
II-6. Radial velocity profile in a hydrocyclone.....	17
II-7. Velocity profiles for cylindrical (a and b) and conical hydrocyclone	18
II-8. Experimental hydrocyclone (sketch not proportional)	19
II-9. Tangential velocity profiles for different concentrations, level 1(lower part of reactor).	19
II-10. The evolution of the tangential velocity in the hydrocyclone compared to the radius of the hydrocyclone.....	21
II-11. The configuration of the hydrocyclone used in Puprasert, (2004) study.....	23
II-12. Various forces applied on the particle from different axes.....	24
II-13. The hydrocyclone used in the study of D.N. Modge et al., (2004).....	27
II-14. Schematic diagram of hydrocyclones for the study of Chu et al., (2004).	29
II-15. Schematic of CANMET hydrocyclone.....	29
II-16. Schematic diagram of a concurrent three-phase hydrocyclone	31
II-17. Two-phase hydrocyclone hybridization process for.....	31
II-18. The schematic diagram of the hydrocyclone used in the.....	32
II-19. Generation and growth of aerated flocs inside the FGR for the study of Carissimin and Rubio, (2005).....	39
II-20. The Floated Floc pilot system for the study of Rosa and Rubio, (2005).....	40
II-21. Bubble size distribution (number) at different saturation pressures.	41

II-22.	Sauter mean bubble diameter at different saturation pressures (including the calculated standard deviation).....	41
II-23.	The expected phenomena of the hybrid process.....	46
III-1.	The studied hydrocyclones in the hydrodynamics study.....	54
III-2.	The studied hydrodynamics positions in the hydrocyclones.....	56
III-3.	The schematic diagram for the hydrodynamics experiment.....	57
III-4.	The trajectory line of an oil tracer droplet at different times.....	57
III-5.	Movement of the red oil droplet after leaving the tip of the syringe within the hydrocyclones at t_1 and t_2	59
III-6.	Trajectory line of the droplet at different times (top view).....	60
III-7.	Schematic diagram of the pilot hybrid process.....	65
III-8.	Photo of the pilot hybrid apparatus.....	66
III-9.	The studied hydrocyclones in the hybrid process.....	67
III-10.	Photos of the hydrocyclones for the hybrid process experiments.....	68
III-11.	Raw water inlet diameter.....	68
III-12.	Photos of the pressurized water system.....	70
IV-1.	The trajectory lines of the oil tracer droplets at different times.....	78
IV-2.	Trajectory lines of the droplets of HC3 at a water flow rate of 200 l/hr and water inlet diameter of 0.50 cm.....	79
IV-3.	Tangential and axial water velocity at different studied points in HC1, which was operated with a constant inlet diameter (0.50 cm) and at different water flow rates (200 and 400 l/hr).....	83
IV-4.	Tangential and axial water velocity at different studied points in the HC1, which was operated at a constant water flow rate (200 l/hr) and with different inlet diameters (0.30 and 0.50 cm).....	85
IV-5.	Tangential and axial water velocity at different studied points in HC2, which was operated with a constant inlet diameter (0.50 cm) and at different water flow rates (200 and 400 l/hr).....	87

IV-6.	Tangential and axial water velocity at different studied points in HC2, which was operated at a constant water flow rate (200 l/hr) with different inlet diameters (0.30 and 0.50 cm).....	88
IV-7.	Tangential and axial water velocity at the studied points in HC3, which was operated with a constant inlet diameter (0.50 cm) and at different water flow rates (200 and 400 l/hr).....	90
IV-8.	Tangential and axial water velocity at different studied points in HC3, which was operated at a constant water flow rate (200 l/hr) and with different inlet diameters (0.30 and 0.50 cm).....	91
IV-9.	The tangential velocities values obtained for the three hydrocyclones (HC1, HC2, and HC3) with an inlet injection diameter of 0.5 cm and a water flow rate of 200 l/hr.	92
IV-10.	Tangential water velocity at the studied points in HC1, HC2, and HC3 at a water flow rate of 400 l/hr and an inlet diameter of 0.50 cm.....	92
IV-11.	The tangential velocity values of the three hydrocyclones (HC1, HC2, and HC3), which were operated at a water flow rate equal to 200 l/hr and with a water inlet diameter equal to 0.30 cm.	93
IV-12.	Tangential water velocity at the studied points in HC1, HC2, and HC3, which were operated with an inlet diameter equal to 0.50 cm and at a water flow rate equal to 200 l/hr.....	94
IV-13.	Linear regression used to determine the relation between the tangential velocity, V_z , and the radius, R, for HC1 with an inlet diameter of 0.50 cm.....	95
IV-14.	Linear regression used to determine the relation between the tangential velocity, V_z , and the radius, R, for HC2 with an inlet diameter of 0.50 cm.....	96
IV-15.	Linear regression used to determine the relation between the tangential velocity, V_z , and the radius, R, for HC3 with a constant inlet diameter of 0.50 cm.	96

IV-16. Average tangential velocity gradients in HC1 at different flow rates, 200 and 400 l/hr, and with a constant inlet diameter (0.5 cm).	99
IV-17. Average tangential velocity gradients in HC1, which was operated using different inlet diameters (0.3 and 0.5 cm) and at a constant flow rate of 200 l/hr.....	100
IV-18. Average tangential velocity gradients in HC2, which was operated at different flow rates, 200 and 400 l/hr, with a constant inlet diameter (0.50 cm).....	102
IV-19. Average tangential velocity gradients in HC2, which was operated with different inlet diameters (0.30 to 0.50 cm) and at a constant flow rate of 200 l/hr.....	103
IV-20. Average tangential velocity gradients in HC3, which was operated at different flow rates, 200 and 400 l/hr, and with a constant inlet diameter, 0.50 cm.....	104
IV-21. Average tangential velocity gradients in HC3 at two water inlet diameters, 0.30 and 0.50 cm.	105
IV-22. Average tangential velocity gradients for HC1, HC2, and HC3 at a constant inlet diameter of 0.50 cm and a constant liquid flow of 400 l/hr.....	106
IV-23. Average tangential velocity gradients for HC1, HC2, and HC3 at a constant inlet diameter of 0.50 cm for a constant water flow of 200 l/hr.....	107
IV-24. Average tangential velocity gradients for HC1, HC2, and HC3 at a constant inlet diameter of 0.30 cm and a constant water flow of 200 l/hr....	107
IV-25. The photos of the floating floc at the top of hydrocyclone.....	113
IV-26. The photos of the microbubbles inside the floating flocs which taken by the microscope.	113
IV-27. Separation lines in the hydrocyclone (HC3).....	114
IV-28. The coalescence of bubbles in (a) HC2 and (b) HC3	116
V-29. The relation of the floating floc percentage and air fraction at different raw water flow rates for HC3.	121

IV-30.	The relation of the floating floc percentage and air fraction at different total pressures in the pressurized tank for HC3.....	122
IV-31.	The relationship of the floating floc percentage and different air fractions of HC3.....	123
IV-32.	The relation between the floating floc percentage and coagulant concentration in HC3.....	125
IV-33.	The relationship of the raw water flow rate and separation efficiency (%) in HC3 using a raw water inlet diameter equal to 0.50 cm.....	129
IV-34.	The relationship of the raw water flow rate and the separation efficiency (%) in HC3 using a raw water inlet diameter equal to 0.30 cm.....	130
IV-35.	The relationship of the velocity inlet and separation efficiency at different raw water flow rates and different water inlet diameters.....	132
IV-36.	Relationship of raw water flow rate and separation efficiency in the HC3 at different water inlet (0.50 and 0.30 cm).....	133
IV-37.	The variation of the air fraction and separation efficiency (%) at the different pressurized water flow rates of 40, 55, 70 and 90 l/hr.	134
IV-38.	The relation of the coagulant concentration and separation efficiency in HC3.....	135
IV-39.	Photo of the settled flocs in the sampled waters from in the center and wall zones of the hydrocyclone that show a 70% separation efficiency.	138
V-1.	The sketch of perspective reactor of this study.....	142

LIST OF ABBREVIATIONS

Latin letters

A_i	Water inlet area
C_c	Coagulant concentration
C_d	Drag coefficient
$D_1,$	Diameter of the lower part of the hydrocyclone
$D_2,$	Diameter of the upper part of hydrocyclone.
D_3	Diameter of injection of water inlet
D_i	Diameter of the water inlet
d_d	Diameter of a oil droplet (m)
d_p	Diameter of particle
fps	Frame per second
F_1	Centrifugal force in x-axis
F_2	Drag force in x-axis
F_3	Buoyancy force in y-axis
F_4	Drag force in y-axis
F_5	Tangential force in z-axis
G_a	Angular velocity gradient
$G_{g, b}$	The global velocity gradient which calculated by principle of Bradley
$G_{a, m}$	The average velocity gradient which calculated by principle of mixing tank
G_z	The tangential velocity gradient
$G_{z, exp}$	The experimental tangential velocity gradient
g	Acceleration of gravity

H	Henry's law constant.
H_1 ,	Height of the upper of the hydrocyclone of HC1
H_2	Height of the lower part of the HC1
H_{hc}	Height of the hydrocyclone
HC1	The first hydrocyclone
HC2	The second hydrocyclone
HC3	The third hydrocyclone
HC4	The fourth hydrocyclone
h_f	Head loss
K	Constant value
m	Numbers of considered tangential velocity data
n	Empirical constant.
n_g	Mole of gas
n_w	Mole of water
t_i	Time of considered droplet at $i = 1, 2, 3, \dots, n$
P	Dissipated energy
P_g	Mole fraction of gas in air, mole gas/mole air
P_t	Total pressure, atm
Q	Raw water flow rate
Q_w	Water flow rate
Q_p	Pressurized water flow rate
R	Radius of hydrocyclone
R^2	Coefficient of determination
Re	Reynolds number

r	Constant radius of the hydrocyclone
S.D.	Standard deviation
SS_{center}	Suspended solid at the center of hydrocyclone
SS_{wall}	Suspended solid at the wall of hydrocyclone
T_{center}	Turbidity at the center of hydrocyclone
T_{wall}	Turbidity at the wall of hydrocyclone
Δt	Time difference of two considered photos from t_1 to t_2
V_b	Volume of basin
V_d	Terminal velocity of the droplet
V_{hc}	Volume of hydrocyclone
V_i	Water inlet velocity
V_l	Axial velocity of water
V_p	Terminal settling velocity of particle
V_x	Radial velocity
V_y	Axial velocity
$V_{y,d}$	Axial velocity of droplet
$V_{y,w}$	Axial velocity of water
V_z	Tangential velocity
\bar{V}_z	Mean value of tangential velocity of each droplet
V_{zi}	Tangential velocity of considered droplet at $i = 1, 2, 3, \dots, n$
$V_{z,d}$	Tangential velocity of droplet
X_g	Mole fraction of gas in water (mole gas/mole water)
x	Radial axis of hydrocyclone.
y	Axial axis of hydrocyclone

y_1	Coordinate of a droplet at t_1 on the axial axis (y-axis)
y_2	Coordinate of a droplet at t_2 on the axial axis (y-axis)
Δy	The distance in axial axis
z	Tangential axis of hydrocyclone
z_1	Coordinate of a droplet at t_1 on the tangential axis (z-axis)
z_2	Coordinate of a droplet at t_2 on the tangential axis (z-axis)
Δz	The distance in tangential axis
Δz_{ex1}	The first example of tangential distance selection.
Δz_{ex2}	The second example of tangential distance selection.

Greek Letters

α	Empirical constant.
δR	Difference of the radius of two positions
δV_z	Difference of the tangential velocity of two positions
μ	Dynamic viscosity of continuous phase
μ_w	Dynamic viscosity of water
$\delta \omega$	Difference of angular velocity of two points
ω	Angular velocity
ρ_d	Density of the oil droplet
ρ_L	Density of liquid (water)
ρ_m	Density of dispersion
ρ_p	Density of solid particle
ρ_w	Density of the water
$\Delta \rho$	Difference in the densities of the oil and the water
θ	Angle of hydrocyclone

ζ Average centrifugal acceleration.



สถาบันวิทยบริการ
จุฬาลงกรณ์มหาวิทยาลัย

CHAPTER I

INTRODUCTION

In a tap water treatment plant, four important unit operations are performed: the coagulation, flocculation, settling and filtration. The objective of first two processes is to remove the suspended solid particles that cause turbidity in treated water. The range of these particles is generally varied in the colloidal dimension. The principle of the coagulation and flocculation processes is to destabilize the colloids to induce micro floc formation. The flocculation allows enhancing the floc collision to increase floc size. Hence, these big flocs can be removed further from the raw water by settling and/or filtration processes. In water treatment processes, alumina and iron salts, lime and polyelectrolyte or a combination of them can be used as the coagulant.

Usually, coagulation and flocculation are performed in agitated tanks or basins. Although they appear to be quite simple processes, they present problems such as short circuits, dead zones, high mechanical and electrical energy requirements, fairly high maintenances costs and large footprints. Bhole, (1993) stated that even though mechanical flocculator is an efficient machine used in many water treatment plants, it requires paddles, a shaft, bearing, a gear box system, a motor, energy and skilled process supervision– in other words, it requires, high operating costs.

In order to perform water treatments at lower costs and with smaller energy footprints, a new hybrid process had been developed. In this process, physical and chemical water treatment processes such as coagulation, flocculation and separation by centrifugal acceleration are integrated in a hydrocyclone reactor. Coagulation and flocculation are performed with corresponding gradients of classical unit separation, and no agitated reactor is required. This highly reliable new process requires a small footprint and low capital costs, and it contains no moving parts. As a result, it is a new and interesting water treatment system.

The objectives of the study

The main objective of this study is to find out the optimum conditions for the hybrid process, which is an innovative process for water treatment. This hybrid process integrates coagulation, flocculation, and separation by hydrocyclone, three

conventional water treatment processes, in one reactor. Therefore, there are many relevant parameters such as the strength of the water vortex, the water inlet diameter, coagulant concentration in the hydrocyclone, and the air fraction.

To fulfill the objective of identifying the optimal conditions for the hybrid process, it was first necessary to understand the hydrodynamic conditions in hydrocyclones, such as the velocity profile in hydrocyclones, the direction of the water stream, and the tangential velocity gradient. This knowledge was applied as the background knowledge for the hybrid process; for example, the velocity gradient in a hydrocyclone was used to identify the appropriate mixing intensity for coagulation and flocculation in the hydrocyclone.

In conclusion, the main objectives of this study were divided into two parts:

(1) To study the hydrodynamic conditions in terms of the velocity profile, tangential velocity gradient and the trajectory of the water flow.

(2) To find out the optimum operating conditions for performing the hybrid process, such as the optimum water inlet diameter, coagulant concentration in the hydrocyclone, and air fraction.

CHAPTER II

BIBLIOGRAPHY

The hybrid process which has been developed in this work integrates three important processes: coagulation, flocculation and separation by the hydrocyclone. The following sections deal with the basic concepts of these three processes.

Part 1 Coagulation and flocculation

1.1 Introduction

In natural resources, solid particles or colloid particles are stable as they are suspended in water due to the state of hydration and surface electric charge. In addition, since colloidal sizes range between 1 and 1000 nanometres (nm), these particles take a long time to settle. Therefore, the process of particle agglomeration, i.e., coagulation and flocculation, was introduced into the water treatment process to remove these colloidal particles. Coagulation is defined as the addition and rapid mixing of a coagulant that destabilizes the colloidal and fine suspended solids. Flocculation involves the slow stirring or gentle agitation necessary to aggregate the destabilized particles and form a rapid settling floc.

In water treatment, the principle use of coagulation and flocculation is to agglomerate solid particles and some organic compounds before settling and sand filtration. In water treatment, alumina and iron salts, lime, and polyelectrolyte are employed as coagulants. In most colloidal systems, the colloids are maintained in suspension (i.e., in a stabilized form) as a result of the electrostatic forces of the colloids themselves. Since most naturally occurring colloids are negatively charged (and like charges are repulsive) the colloids can remain in suspension for a long time because of the action of the repulsive forces.

Negative colloidal particles attract to their surface ions the opposite charge (i.e., counterions) from the surrounding water, as depicted in Figure II-1. The compact layer of counterions is frequently termed the *fixed layer*; outside the fixed layer is the *diffused layer*. Both layers contain positively and negatively charged ions; however,

there are much larger numbers of positive ions than negative ions. The two layers represent the region surrounding the particle where there is an electrostatic potential due to the particle, as illustrated in Figure II-1. The concentration of the counterions is greatest at the particle surface; it decreases to that of the bulk solution at the outer boundary of the diffused layer. The shear plane or shear surface surrounding the particle encloses the volume of water which moves with the particles. The zeta potential is the electrostatic potential at the shear surface, as shown in Figure II-1. This potential measures the charge to the colloidal particle, and it is dependent on the distance through which the charge is effective. It follows that the greater the zeta potential, the greater the repulsion forces between the colloids and, therefore, the more stable the colloidal suspension.

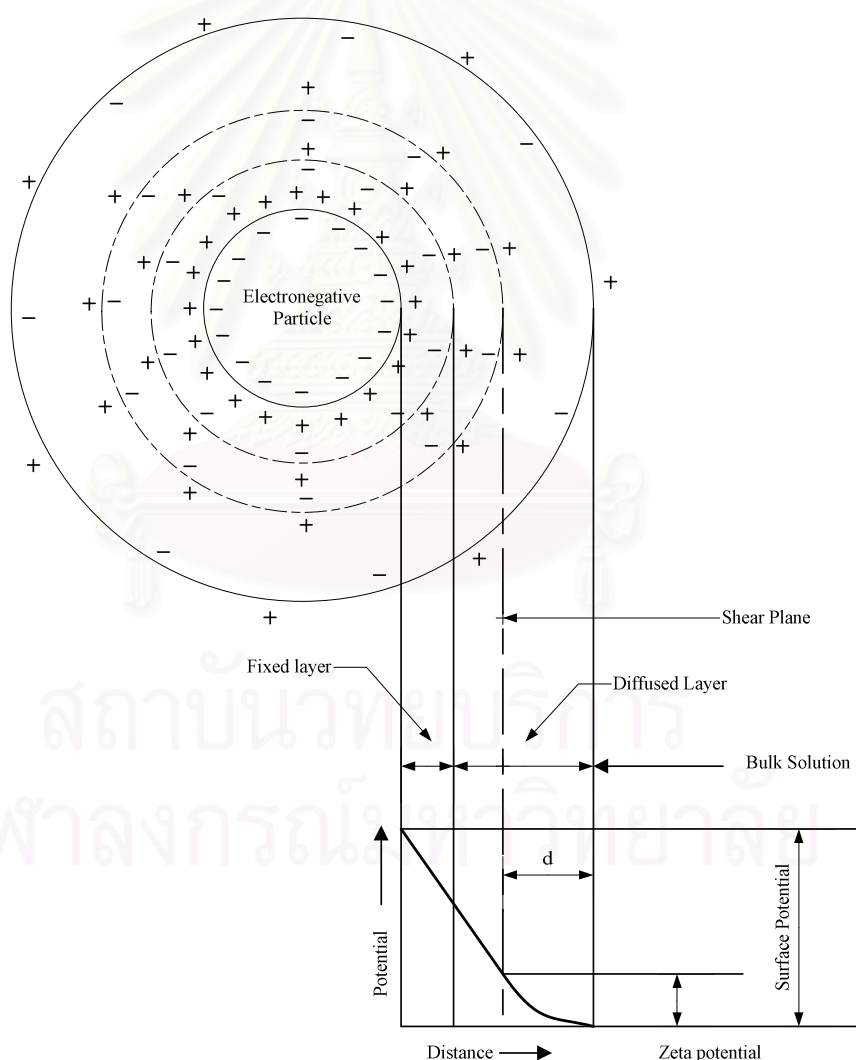


Figure II-1. A negative colloidal particle with its electrostatic field.

Thereby, there are two approaches to accomplish the destabilization of the colloidal particles:

(1) The reduction of the energetic barrier induced by the attraction/repulsion forces.

(2) The increase of the kinetic energy of the particle to overcome the previous energetic layer.

The coagulation process corresponds to the first approach which is carried out by the addition of some chemical products into the raw water in order to decrease the length of the diffusion layer of the colloidal particles. At the same time, the flocculation process is carried out by the transportation of destabilized particle to increase the collision opportunity. The obtained product of this process is called *flocs*.

1.2 Coagulation mechanisms in water production

Many studies were devoted to the description of coagulation phenomena in water production. Indeed, since the complexity of the water composition, many mechanisms can occur simultaneously and/or alternatively. In the following part, a short description of the different approaches to accomplish the coagulation was described.

1.2.1 Electrostatic coagulation

This method is accomplished by adding electrolytes to the solutions. Counterions of the added electrolyte suppress the double layer charge of the colloidal particles sufficiently enough to permit the particles contact. As the particle meets one other, Van der Waals forces or the molecular cohesive forces of attraction become dominant and give the aggregation results. The accomplishment of this approach can be measured by zeta potential value which closes to zero for the high coagulation efficiency.

1.2.2 Coagulation by chemical reaction

Colloids and coagulants may react to produce species which are not soluble or very low.

1.2.3 Adsorption/charge neutralization and Polymer bridging

The coagulant or flocculant is adsorbed on the negative surface of the colloids. The flocculant molecules are linked with the colloidal particles but they still have other free active sites for adsorption. These sites can be fixed to other sites of other colloidal particles. This mechanism is called a chemical bridging which induces a big network of coagulant and colloids.

This mechanism is very important when polymers are used as flocculant especially for anionic or non-ionic polyelectrolytes. A polymer bridging reaction is formed when two or more particles are adsorbed along its length. This bridged particle becomes intertwined with another bridged particle. At the same time, the mixing intensity must be sufficient to bring about the adsorption of the polymer onto the colloidal particle. If inadequate mixing is provided, the polymer will eventually fold back on itself and not be capable of forming polymer bridges

1.2.4 Sweep coagulation

In general, when a coagulant salt is added to water, it dissociates and the metallic ion undergoes hydrolysis and creates positively charged hydroxo-metallic ion complexes. Naturally, a coagulant is an aluminium salt such as $\text{Al}_2(\text{SO}_4)_3$, or an iron salt such as $\text{Fe}_2(\text{SO}_4)_3$. In water treatment, coagulation occurs at pH around 7 and the coagulant dosage is usually provided in appreciable excess of the amount required to produce the necessary positive hydroxo-metallic complexes. These excess complexes continue to polymerize until they form an insoluble metallic hydroxide such as $\text{Al}(\text{OH})_3$ or $\text{Fe}(\text{OH})_3$, and the solution becomes supersaturated with the hydroxide. During the formation and settling of the metallic hydroxides, the enmeshing of the negative colloids and precipitate occurs. This enmeshment type of coagulant is sometimes referred to as precipitate or sweep coagulation.

This technique, however, requires dosages of the coagulant that are inverse to the colloidal concentration due to the low opportunities of collision between the particle and coagulant when the colloidal concentration is low. Therefore, a high coagulant concentration is needed to entrap the dispersed colloidal particles in the water.

1.3 Mixing and contact time for coagulant and flocculation

For the coagulation, an intense mixing is the required parameter for dispersing the coagulant uniformly throughout the basin and for allowing an adequate contact time between the coagulant and the suspended particle. A rational approach for evaluating the mixing and design of the basin has been developed by Camp and Stein, (1943). The mixing intensity is measured by the global velocity gradient. The equation used to calculate the average velocity gradient is presented in Equation II-1.

$$G_{a,m} = \sqrt{\frac{P}{\mu V_b}} \quad \text{Equation II-1}$$

The coagulation is a very rapid phenomenon therefore; a low contact time is required. Hence, whatever the operating parameters, the average gradient velocity has to be greater than 100 s^{-1} and the mean residence time lower than 60 s. For the instantaneous mixing, the velocity gradient can reach 1000 s^{-1} as reported in Table II-1.

In flocculation, the growth of small floc sizes is performed by the adequate mixing intensity. They are contacted slowly to create the big flocs. However, floc structure may be broken if very high mixing intensity is used. The average velocity gradient has to be lower than 100 s^{-1} and the mean residence time is required to be higher than 600 s.

The recommended global velocity gradient for the coagulation and flocculation process is summarized in Table II-1

Table II-1. The recommended criteria for the coagulation and flocculation process

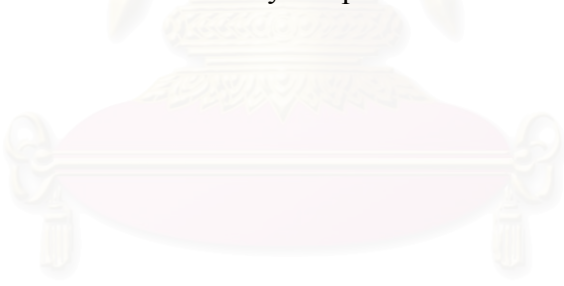
Process	Detention time, s	$G_{a,m}$ value, s^{-1}	References
Rapid mixing			
Typical rapid mixing operations in wastewater treatment	5-20	250 - 1500	Tchobanoglous, (2004).
Coagulation	-	400 – 1000	Degrémont SA., (2005).
Mixing conditions	300	200	Puprasert, (2004)
Rapid-mixing basins	20 30 40 50 or more	1000 900 790 700	Reynolds and Richards, (1995).
Slow mixing			
Typical flocculation process used in wastewater treatment	600 – 1800	20-80	Tchobanoglous, (2004).
Flocculation	-	100	Degrémont SA., (2005).
Coagulation-flocculation phase 1	1800	75	Puprasert, (2004)
Coagulation-flocculation Phase 2	600	30	

From Table II-1 the recommended values for the detention time of the rapid mixing tank range from 5 to 300 s, and the recommended velocity gradient should be within the range of 200 to 1500 s^{-1} . In the flocculation process, the recommended

contact time and velocity gradient ranges from 20 to 100 s^{-1} and 600 to 1800 s, respectively.

It could be noticed that the recommended criteria of the detention times and averaged velocity gradients in Table II-1 is valid for conventional coagulation and flocculation processes. These processes are followed by the settling which is not used for separation in this study. Therefore, these criteria could be used as the roughly guideline.

In the coagulation and flocculation processes, solid particles are destabilized and agglomerated together to form big flocs. A first step with rapid mixing is needed to neutralize the colloidal particles. A second, slow mixing is carried out to form the big floc. After floc formation, the next step at a water treatment plant is the separation process used to remove flocs formed in the water. Thereby, there are many types of separator used such as a settling tank, hydrocyclone, or floatation tank. In this study, the hydrocyclone will be used in a hybrid process due to its dominant advantages include its small footprint requirement, reliability and high separation efficiency. The following section will give the basic concepts of the hydrocyclone in order to understand why it will be use in the hybrid process.



สถาบันวิทยบริการ
จุฬาลงกรณ์มหาวิทยาลัย

Part 2 Hydrocyclone

The use of hydrocyclones is common in particle classification processes. The hydrocyclone has been widely applied in several industries; for example, it has been used in mineral processing, chemical processing, petrochemical processing, power generation, textile production, and water treatment processes. In the wastewater treatment process, it is also used in many applications, for example, in liquid classification, slurry thickening, solid washing, and the degassing of liquids. Hydrocyclones are capable for five types of separation: solid-liquid, liquid-liquid, solid-liquid-liquid, gas-solid, and gas-liquid separation. In this section, the basic theory and applications of hydrocyclones are described.

2.1 Components and operating principle of classical hydrocyclone

A classical hydrocyclone is composed of two main parts: a cylindrical part, which is connected to a conical part, and the conical part, which is placed at the bottom of the hydrocyclone, as shown in Figure II-2. Generally, a classical model is composed of three basic components: the inlet port, vortex finder (overflow), and underflow channel. The inlet port functions as the entrance for the fluid into the hydrocyclone. Through this port, the fluid is injected tangentially to create the vortex flow. Secondly, the last part of a hydrocyclone is the underflow channel, which is used to collect the liquid flow discharged through the bottom of the hydrocyclone. Finally, the vortex finder is used for the collection of the liquid solution coming from the hydrocyclone's core; it is usual placed at the top of hydrocyclone.

สถาบันวิทยบริการ
จุฬาลงกรณ์มหาวิทยาลัย

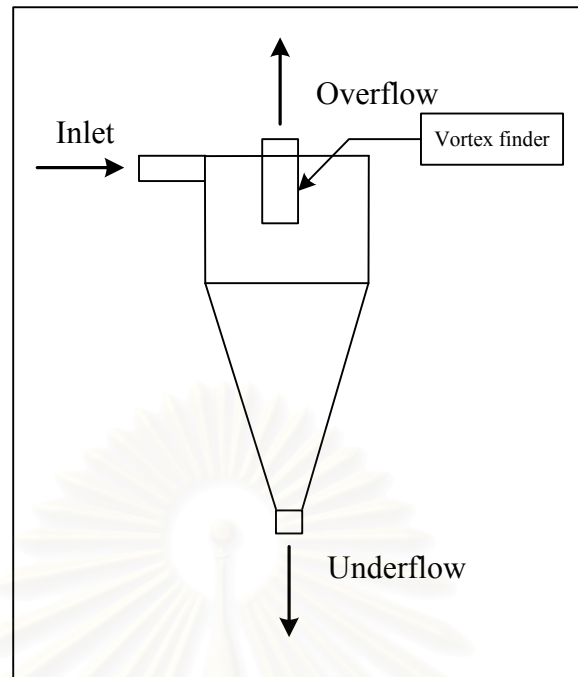


Figure II-2. Basic components of classical hydrocyclone

A hydrocyclone makes use of the static energy of a liquid (i.e., the water flow rate or the pressure of the continuous phase) to create the vortex for the separation process. In a classical hydrocyclone, the separation action is carried out by the tangential fluid flow in order to create a high tangential velocity and the high centrifugal acceleration. In classical case of solid-liquid separation, the heavy particles contained in the feed solution are forced continuously to follow the external vortex, and then they are discharged out through the underflow aperture of the hydrocyclone. At the same time, the lighter phase (normally the liquid phase mixed with some fine particles) is forced to follow the internal vortex and is removed reversely through the vortex finder at the top of the hydrocyclone. By this principle, the particles with different densities and sizes are separated. The separation of particles is operated by the principle of centrifugal acceleration. Centrifugal and drag forces are applied to the particles in the treated solution to select them into the overflow or underflow. Compared to other separation processes, the separation efficiency of the hydrocyclone is increased by centrifugal acceleration, which can be one thousand times greater than gravity acceleration.

2.2 The advantages of utilizing a hydrocyclone

The hydrocyclone has been widely used as a separator in water treatment process. Its global advantages can be summarized as follows:

A hydrocyclone is a multi-function separator used in water treatment processes; it is used generally as a liquid clarifier, a sand particle and an activated carbon recover, a dewatering mechanism, a solid classifier, a two-liquid-phase separator, and a degas liquid. The different densities or particle shaped solutions can be treated with hydrocyclones.

Hydrocyclone reactors are highly reliable and easy to install and operate because they require little maintenance, a low support structure, and no mobile parts. In addition, Schuetz et al., (2004) reported that the hydrocyclone is economical due to its ability to work at a low energy requirement compared to that of other centrifugal machines that work at a high rotational speed.

The hydrocyclone requires a small location area because of its small diameter, which makes it a suitable machine for the urban zone. In addition, the hydrocyclone also requires in low residence times. Bennett and Williams, (2004) reported that the centrifugal force in a hydrocyclone is stronger than conventional forces in a gravity separator due to the high angular velocities of the mixture. This advantage makes its separation process faster than that of a gravity separator.

Hydrocyclones can be operated with high water loading; moreover, the separation efficiency of a hydrocyclone increases as the water flow rate increases. Hydrocyclones can be utilized to classify solids since the developed high shear force inside a hydrocyclone can split any agglomerate to smaller parts.

2.3 The disadvantages of utilizing a hydrocyclone

The limitations to using hydrocyclones are summarized as follows:

It is an inflexible machine because its separation performances are directly related to the feed flow rate and the concentration of the treated solution. This fluctuation of the influent flow directly affects the velocity field and the separation efficiency of the hydrocyclone.

There are limitations to its de-watering performance or clarification power due to the solid concentration values are never greater than 50% in the underflow. Concerning cut size, (the first particle size which is only present in the underflow) is always dependent on hydrocyclone geometry. However, a multi-stage arrangement of the hydrocyclone was developed to solve this problem.

The equipment is sensitive to erosion, but a multi-stage arrangement of the hydrocyclone can be taken to reduce the effects.

Flocculation process has been studied in the hydrocyclone but at the present, the results is unsatisfactory since the created flocs are often broken up by the influence of shear force or liquid velocity gradient that acts on the floc' structure. This force produces the extremely strong impact to the collisions between particles in a hydrocyclone (Roldan-villasana and Williams, (1999)).

2.4 Basic theories of the hydrocyclone

The hydrocyclone is a static separator that uses centrifugal forces created by the water vortex within its cylindrical and conical body. In order to understand the mechanisms of the phenomena inside a hydrocyclone, some theories needed to be reviewed such as the velocity components, the liquid hydrodynamic theory, and the acting forces on the particles in a hydrocyclone. Therefore, this section summarizes the basic theories and underlines the important concepts of separation in hydrocyclones.

2.4.1 The velocity components

The velocity components of the continued liquid phase contribute to the understanding of the particle separation phenomenon that occurs within hydrocyclones. In general, the liquid velocity components in a hydrocyclone are divided into three velocity types, which are radial, axial and tangential velocity on the x-axis, y-axis, and z-axis, respectively as shown in Figure II-3.

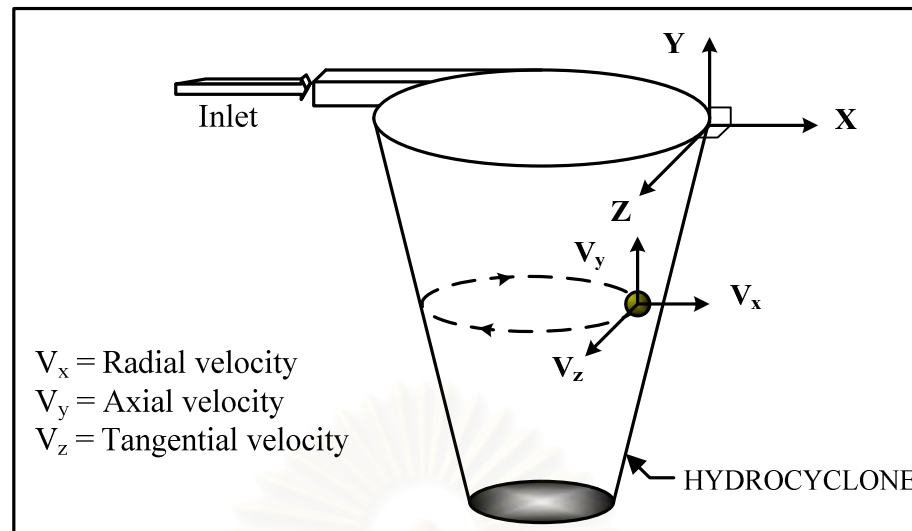


Figure II-3. Velocity directions of the three axes

2.4.1.1 The liquid tangential velocity

Tangential velocity is the most influential liquid velocity component for particle motion in a hydrocyclone; it is expressed as V_z at different radius (R) inside the hydrocyclone. Svarovsky, (1984) have provided a general equation for tangential velocity:

$$V_z R^n = K \quad \text{Equation II-2}$$

In this equation, n is an empirical constant that is usually in the range of 0.4 to 1.0, depending on the geometry of the hydrocyclone, hydrocyclone proportion degree. V_z is the tangential velocity and R is the radius of the hydrocyclone. Inside the hydrocyclone, there are two types of tangential liquid velocities. First, there is a liquid fraction called a *free vortex*; it is presented in the external vortex. It turns around the axial axis (y -axis) with a different angular velocity. The second one is called a *forced vortex*; it is presented in the internal vortex. It turns around the axial axis (y -axis) at the same angular velocity. The corresponding liquid tangential velocity variation versus the radius of the hydrocyclone for the free vortex and forced vortex is reported in Figure II-4 and expressed with Equation II-3 and Equation II-4, respectively.

$$\text{Free vortex: } V_z R^1 \approx K \quad \text{Equation II-3}$$

$$\text{Forced vortex : } V_z R^{-1} \approx K \quad \text{Equation II-4}$$

Figure II-4c presents the combination of the two vortices which is the actual tangential velocity inside a hydrocyclone.

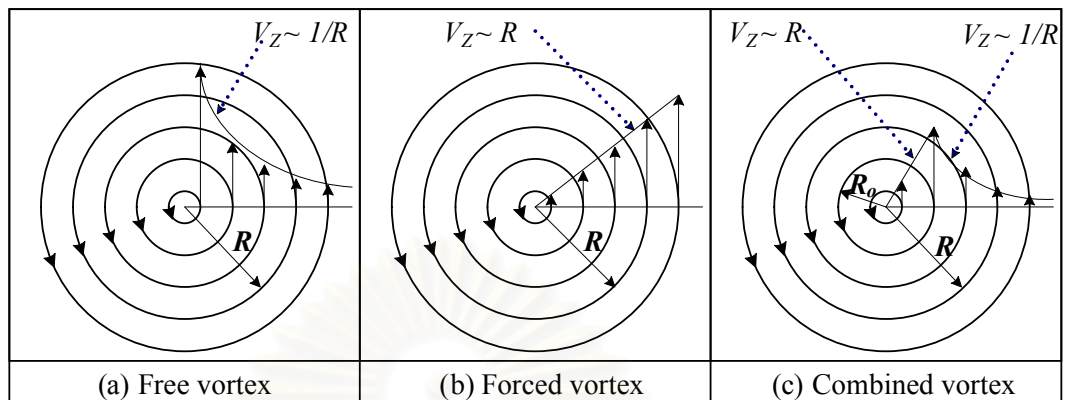


Figure II-4. Velocity profile expressions of a free vortex, forced vortex, and combined vortex in a hydrocyclone.

2.4.1.2 The liquid axial velocity

The axial velocity or the vertical velocity (in y-axis) was developed to identify the direction (upward and downward) of the flow stream in a hydrocyclone as shown in Figure II-5

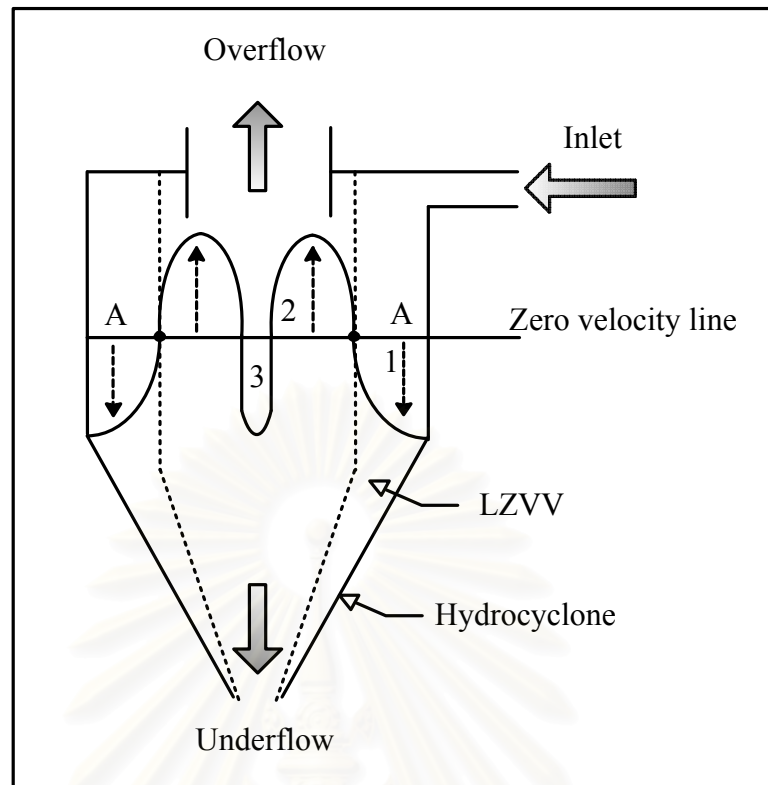


Figure II-5. Axial velocity profile in a hydrocyclone

The Locus of Zero Vertical Velocity (LZVV) contributes to specifying the vertical flow direction in a hydrocyclone. The outward velocity moves downward to the bottom of the hydrocyclone, which is the reason the internal liquid migrates to the underflow of the hydrocyclone. At the same time, the internal velocity moves upward to the top of the hydrocyclone and the internal liquid flow migrates to the overflow.

2.4.1.3 The liquid radial velocity

Figure II-6 presents the radial velocity profile in a hydrocyclone. Its function is to separate the solution in the radial direction (i.e. x-axis). The radial velocity in a hydrocyclone is the smallest of the three components and difficult to measure accurately as stated by Svarovsky, (1984), Bank and Gauvin, (1977), and Chiné and Concha, (2000). A previous experiment of Svarovsky, (1984) reported that the maximum radial velocity is located at the outward edge and decrease gradually toward the center of the hydrocyclone.

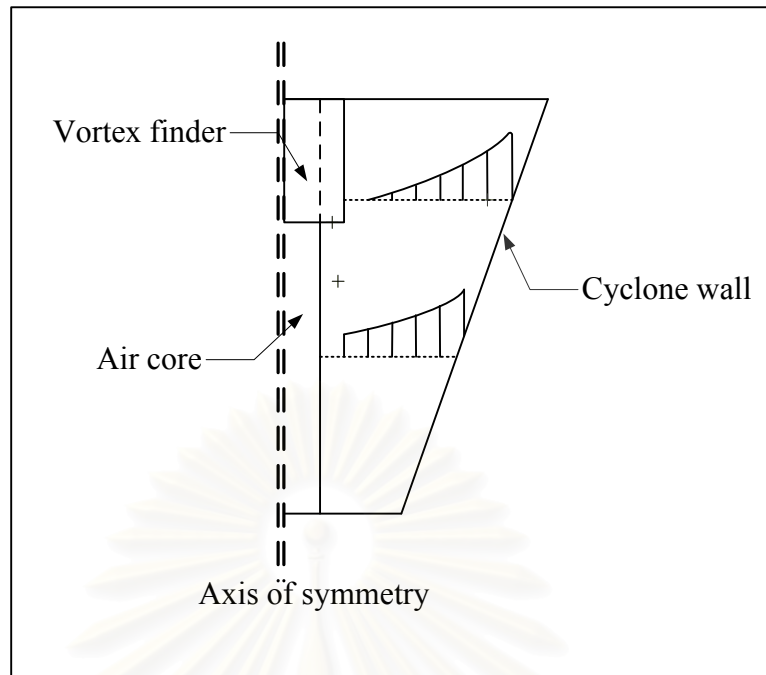


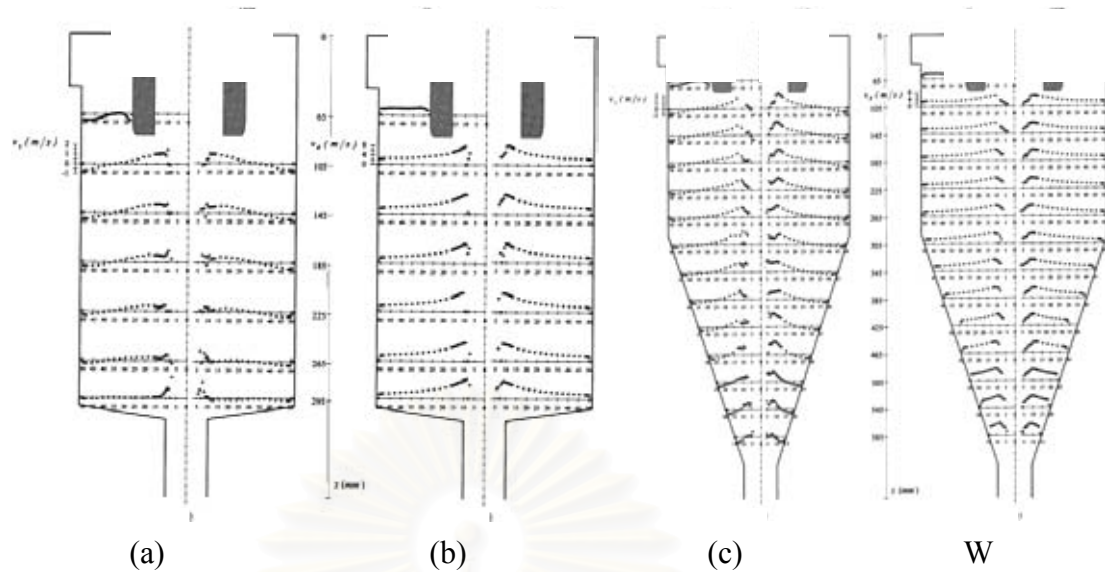
Figure II-6. Radial velocity profile in a hydrocyclone

2.4.2 The velocity profile study in the hydrocyclone

In this part presents the literature reviews of the hydrodynamics in the hydrocyclone.

2.4.2.1 Flow pattern in conical and cylindrical hydrocyclone

Chiné and Concha, (2000) studied the tangential and the axial velocity of the water flow in the 2 types of the hydrocyclone; conical and cylindrical hydrocyclone. The experiment was performed in 625 mm conical and 310 mm cylindrical hydrocyclone with the same hydrocyclone diameter, 102 mm. Water flow was injected from the top of hydrocyclone and the painted particles were used as the tracer. The laser Doppler velocity (LDV) is used to measure the velocity inside the hydrocyclone.



Note: (a) and (b): axial (v_z) and tangential (v_θ) velocity profiles in cylindrical hydrocyclone, (b) and (d): axial and tangential velocity profiles in conical hydrocyclone.

Figure II-7. Velocity profiles for cylindrical (a and b) and conical hydrocyclone (c and d)

Figure II-7 presented the experimental velocity profiles for the cylindrical and conical hydrocyclone. The results of both hydrocyclone presented that the approximately forced vortex occurred near the air core and the free vortex was found between the maximum of the tangential velocity, V_θ , and the solid wall. Regarding to the axial velocity, there are opposite axial flows separated by a surface (mantle) where the axial velocity, V_z , is zero. In addition, the experimental results prove that the flow pattern does not depend on feed pressure, since the flow changes only its magnitude, while the velocity and the turbulence profiles maintain a constant pattern. In this study stated that the radial velocity in the hydrocyclone is small.

Bergström and vomhoff, (2004) developed the new technique to measure velocity in opaque pulp fiber suspensions which had been evaluated in a cylindrical hydrocyclone. A pitometer equipped with a medical micropressure transducer was used to record the tangential velocity. A bleached softwood pulp was used with pulp suspensions for the experiments as the tracer. It was tested at four mass concentrations : 0%, 0.04%, 0.09% and 0.19%. The experimental reactor was presented in Figure II-8.

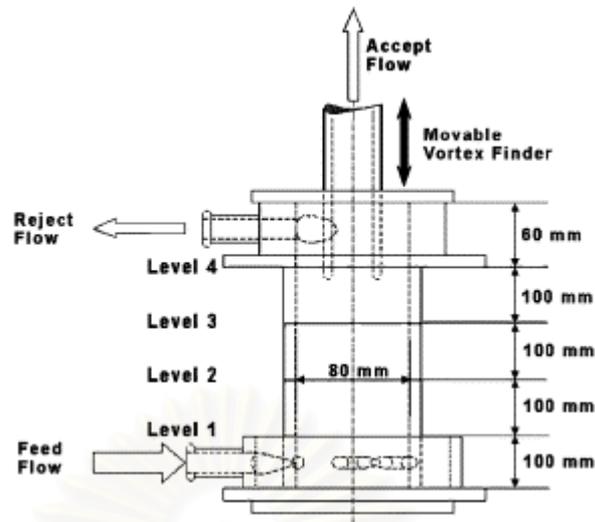


Figure II-8. Experimental hydrocyclone (sketch not proportional)

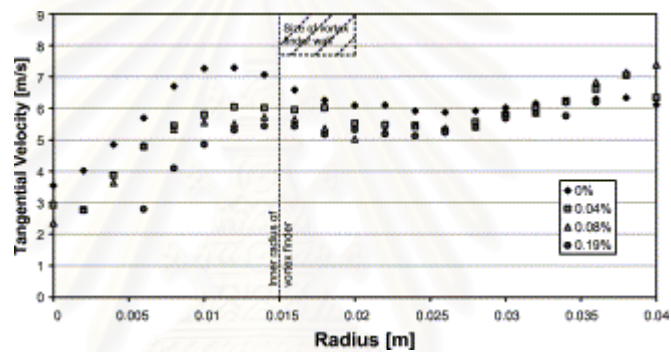


Figure II-9. Tangential velocity profiles for different concentrations, level 1 (lower part of reactor).

In Figure II-9, one can see that the feed inlet jets influence the velocity curves. For the case where fibers are present, the suspension close to the wall seems to behave as a rotating solid body, indicating the strength of the fiber network and that there are no shear forces in that particular area. All curves have high velocities close to the cyclone wall, but they start to differ towards the center. The pure water curve starts to develop a free vortex-like shape. The fiber suspensions seem to resist to be accelerated into the free vortex, resulting in lower velocities towards the center. An increased fiber concentration adds to this behavior.

2.4.3 The liquid angular velocity

In the hydrocyclone, the liquid angular velocity is defined as the ratio of the tangential velocity and the radius as expressed in Equation II-5.

$$\omega = \frac{V_z}{R} \quad \text{Equation II-5}$$

Equation II-3 and Equation II-4 give the expression of the tangential velocity versus the radius of the hydrocyclone (R): they can deduce the angular velocities corresponding to the free vortex and forced vortex as presented in Equation II-6 and Equation II-7, respectively.

$$\text{Free vortex:} \quad \omega = K \quad \text{Equation II-6}$$

$$\text{Forced vortex:} \quad \omega = \frac{K}{R^{n+1}} \quad \text{Equation II-7}$$

2.4.4 The liquid velocity gradient

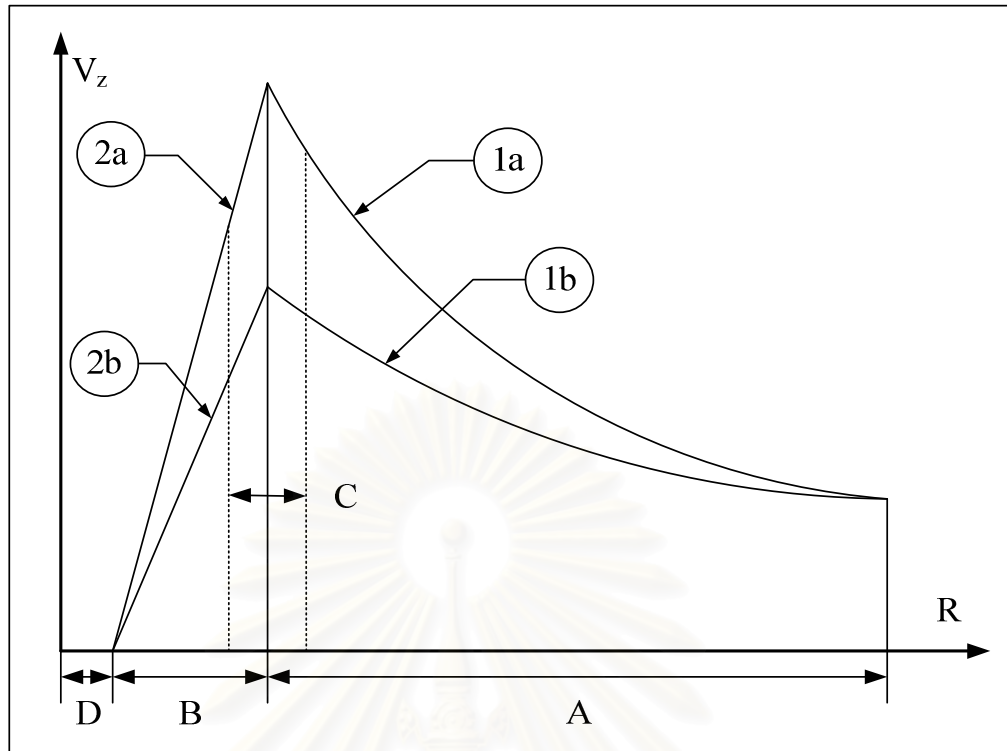
The velocity gradient is an important parameter that can explain the phenomena occurring inside a hydrocyclone such as floc breakage and floc aggregation.

The **tangential velocity gradient** is defined as the partial derivation of tangential velocity with radius (R) as presented in Equation II-8:

$$G_z = \frac{\partial V_z}{\partial R} \quad \text{Equation II-8}$$

The **angular velocity gradient** is defined as the partial derivation of angular velocity with radius (R) as presented in Equation II-9:

$$G_a = \frac{\partial \omega}{\partial R} \quad \text{Equation II-9}$$



(Note: 1a and 1b: (a) theoretical tangential velocity $V_z R = K$ and (b) real tangential velocity $V_z R^n = K$ in the external vortex. 2a and 2b: (a) theoretical and (b) real tangential velocity in the internal vortex, $V_z/R = K$ and $A =$ external vortex zone, $B =$ internal vortex zone, $C =$ transition zone, and $D =$ air core zone)

Figure II-10. The evolution of the tangential velocity in the hydrocyclone compared to the radius of the hydrocyclone.

As can be seen in Figure II-10, the tangential velocity gradient in the internal zone of the hydrocyclone is constant as present in Equation II-10 which is determined from the slope of the graph as presented in Figure II-10.

$$G = \frac{\partial V_z}{\partial R} = K = \text{constant} \quad \text{Equation II-10}$$

With regard to the same figure, the corresponding gradient of angular velocity in the internal vortex zone is equal to zero as presented in Equation II-11. It can be explained that the angular velocity is constant when compared to the radius in the internal zone of the hydrocyclone. This knowledge implies that if the particles move into this internal zone, these particles will move and swirl together at the same velocity and same distance; hence, their movement will not be broken by the shear force between the particles.

$$\frac{\partial \omega}{\partial R} = 0 \quad \text{Equation II-11}$$

Considering to the external vortex zone, the tangential and angular velocity gradients still exist, leading to an important shear stress created between neighboring particles.

Generally, a study of the flow field of a hydrocyclone in a water treatment process is determined in terms of the velocity gradient to investigate the mixing intensity of the particles inside the hydrocyclone. Puprasert, (2004) has proposed an equation to calculate the global velocity gradient (G) in a hydrocyclone as presented in Equation II-12. The main parameters are the water flow rate (Q), the cross section of the water inlet (A_i), the height of hydrocyclone (H_{hc}), the wide angle of the hydrocyclone (θ) and the radius of the hydrocyclone (r). The configurations of these parameters are illustrated in Figure II-11.

$$G = - \frac{Q \cdot \alpha \cdot n}{A_i \cdot (H_{hc} \cdot \tan \theta + r)} \quad \text{Equation II-12}$$

where n is the empirical constant of the hydrocyclone that ranges between 0.4 and 1.0. The n value for a cylindrical hydrocyclone has been recorded at 1.0 and 0.20 for a small angled hydrocyclone. The α is the ratio of the inlet velocity and average velocity in the hydrocyclone (0.11-0.92), which can be calculated using Equation II-13. However, the empirical constants (n and α) appear to be dependent on both cyclone design (such as inlet diameter and cone angle) and operating variables (such as the water flow rate and Reynolds number).

$$\alpha = 3.7 \cdot \left(\frac{D_i}{D_1} \right) \quad \text{Equation II-13}$$

where D_i is the inlet diameter of the hydrocyclone (m) and D_1 is the diameter of hydrocyclone at the mixing point (lower part of hydrocyclone) (m).

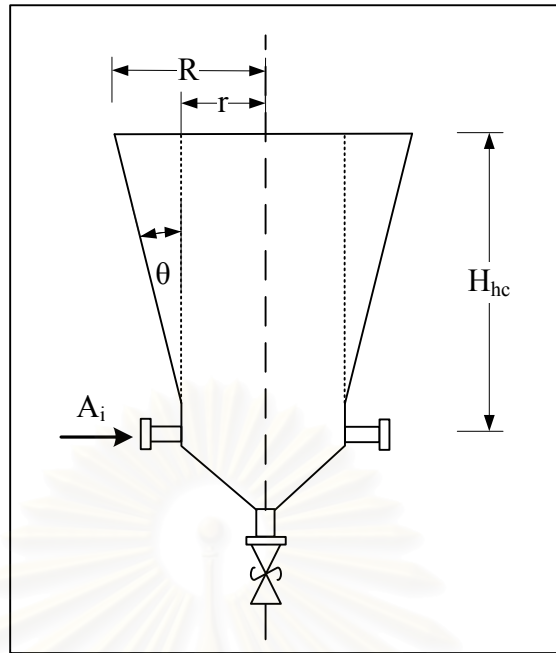


Figure II-11. The configuration of the hydrocyclone used in Puprasert, (2004) study

Relation of tangential velocity with radius (R) in Equation II-2 is used derive the differential as presented in Equation II-14:

$$\frac{\delta V_z}{\delta R} = - \frac{(V_z)(n)}{R} \quad \text{Equation II-14}$$

Bradley, (1965) deduced that the tangential velocity relates with the inlet velocity of the hydrocyclone (V_i) as presented by Equation II-15

$$V_z = \alpha (V_i) \quad \text{Equation II-15}$$

When Equation II-15 is put into Equation II-2, then the velocity gradient is

$$G = \frac{\delta V_z}{\delta R} = - \frac{\alpha \cdot V_i \cdot n}{R} = - \frac{\alpha \cdot n \cdot Q_i}{A_i (H_{hc} \tan \theta + r)} \quad \text{Equation II-16}$$

From Equation II-16, it could be interpreted that the velocity gradient increases with higher water flow rates, smaller water inlet diameter (by considering the surface area of water inlet, A_i) and smaller hydrocyclone sizes (by considering the radius of hydrocyclone, R or $H_{hc} \tan \theta + r$).

2.4.5 Particle motion into a hydrocyclone

The separation process is created in the hydrocyclone by tangential injection of the solution to the hydrocyclone. Since this process is carried out by the centrifugal force, the density of the particles has to be different from that of the water. This way, they are separated immediately by the centrifugal force, which is created by the fluid rotation in the hydrocyclone. The applied forces on the particles are detailed in the Figure II-12.

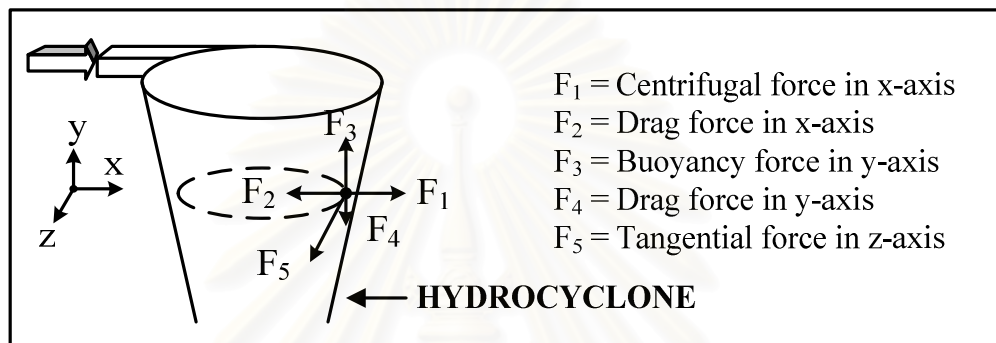


Figure II-12. Various forces applied on the particle from different axes

From Table II-2, it can be concluded that there are many forces acting on the particle motion in the hydrocyclone such as the centrifugal force, drag force, and buoyancy force. These forces are related to the different parameters such as particle size, liquid density, and viscosity of particle.

Table II-2. Expression of various forces on the different axes

Force	Expression	Equation
F ₁	Centrifugal force (on the x-axis)	$(\rho_p - \rho_m) \frac{V_z^2}{R} \frac{\pi d_p^3}{6}$
F ₂	Drag force (on the x-axis)	$\frac{1}{2} \rho_L V_x^2 \frac{\pi d_p^2}{4} C_D$
F ₃	Buoyancy force	$(\rho_p - \rho_m) g \frac{\pi d_p^3}{6}$
F ₄	Drag force (on the y-axis)	$\frac{1}{2} \rho_L V_Y^2 \frac{\pi d_p^2}{4} C_D$

The centrifugal force along the x-axis (F₁), which is proportional to particle volume, is opposed by the drag force (F₂), which according to Stokes' law is proportional to particle area. Assuming a steady state condition for one particle along the x-axis, an increase in particle diameter involves an increase in the centrifugal force that is greater than the increase in the drag force. In that case the particle is projected into the underflow via the external vortex. In an opposite situation, a decrease in particle size leads to a larger decrease in the centrifugal force than in the drag force; in this case, the particle is brought into the overflow via the internal vortex. This comment allowed understanding the cut size notion in the hydrocyclone.

2.4.6 Physico-chemical parameters

Stokes' law (Equation II-17) is the fundamental theory of fluid mechanics used to explain the liquid-solid separation phenomenon; it can be used to understand liquid-solid separation in the hydrocyclone reactor. This equation is deduced from a mass balance applied on a particle at equilibrium with particle size (d_p) and mass density (ρ_p). This equation could be applied when $Re < 10$ and the drag coefficient (C_d) could be calculated by Stokes' law coefficient ($C_d = 24/Re$)

$$V_p = \frac{g \cdot (\Delta\rho) \cdot d_p^2}{18 \cdot \mu} \quad \text{Equation II-17}$$

From Equation II-17, it was found that the terminal velocity in Stokes' law depended on various parameters that are as described as follows.

1. Acceleration due to the gravity

This is considered as the important parameter that affects the separation of solid particles from fluids such as in a settling tank. However, this acceleration can be increased in a hydrocyclone in order to increase the velocity of the particles and separation efficiency. Puprasert, (2004) reported the relation of relative centrifugal acceleration in a hydrocyclone and its tangential velocity in Equation II-18

$$\zeta = \frac{V_z^2}{R \cdot g} > 1000 \text{ time of } g, \text{ Svarovsky, (1984)} \quad \text{Equation II-18}$$

where ζ is the relative centrifugal acceleration in the hydrocyclone, V_z is the tangential velocity, and R is the radius of the hydrocyclone. From this equation, the relative centrifugal acceleration in a hydrocyclone can be increased to greater than 1000 times the gravity acceleration (g) which is performed by increasing of tangential velocity or reducing of radius of the hydrocyclone.

2. The different densities of the injected flow

This research is interested in the solid-liquid separation that occurs in a hydrocyclone. The implementation of this process takes into consideration the density of the injected solution. If the density of the two phases is equal ($\Delta\rho = \rho_p - \rho_w = 0$), the terminal settling velocity becomes zero and the separation can not take place. Therefore, different densities between the two phases is required in order to achieve a high separation efficiency.

3. The dynamic viscosity of water

It can be seen in Equation II-18, that the dynamic viscosity of water (μ) is inversely related to the terminal settling velocity. Therefore, to achieve a high separation efficiency and high terminal settling velocity, the dynamic viscosity needs to be low. In addition, the dynamic viscosity itself is affected by the surrounding environment; for example, the dynamic viscosity is lower at high temperatures.

4. The diameter of the settling particle

Regarding to Equation II-17, diameter of settling particle is a significant component to execute high terminal settling velocity due to it is squared. Therefore, increasing the diameter of the settling particle increases the separation efficiency of the hydrocyclone.

2.5 Applications of hydrocyclones in water treatment processes

In this section new applications of hydrocyclones in water treatment processes are presented. Hydrocyclones can perform five types of separation: solid-liquid, liquid-liquid, solid-liquid-liquid, gas-solid, and gas-liquid separation.

Solid-liquid separation:

Modge et al., (2004) studied the use of a hydrocarbon cyclone (Figure II-13) to treat hydrophilic oil in sand environments. The hydrocyclone in the study was capable of achieving a ternary split in a range of froth treatment process in oil sand mining and extraction. The hydrocarbon cyclones take advantage of the water-wet characteristic of oil sands in a diluted bitumen environment. In the case of purely bituminous, bitumen and fines will follow water to overflow in a hydrocyclone, but in the Athabasca oil sand deposits the sand and clay is profoundly hydrophilic and the presence of diluent alters the slurry rheology.

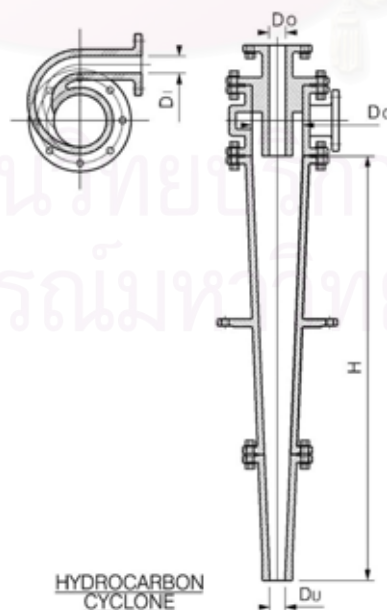
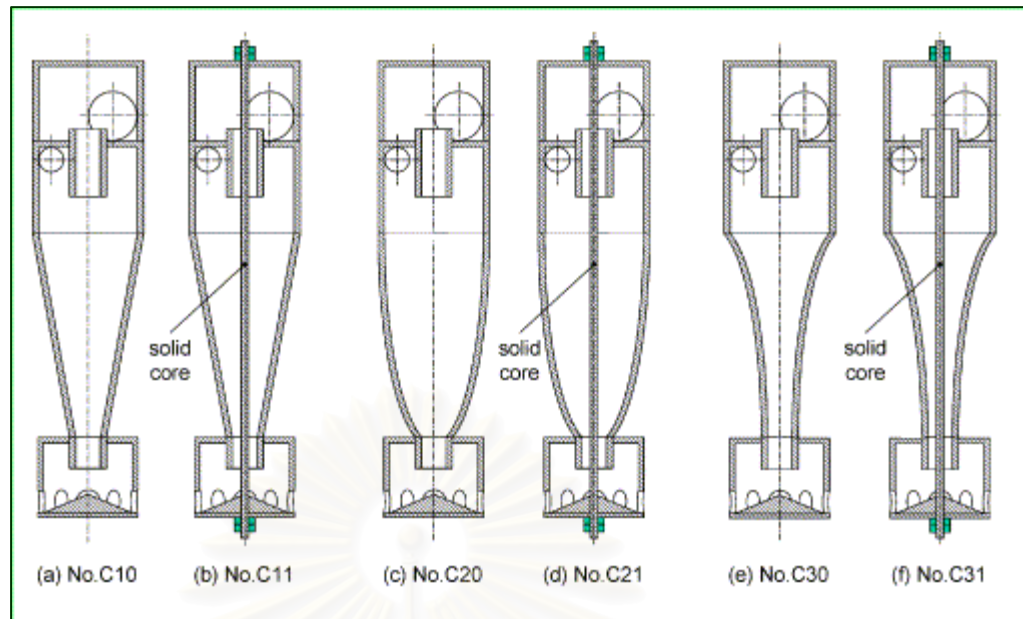


Figure II-13. The hydrocyclone used in the study of D.N. Modge et al., (2004)

Chu et al., (2004) study and understand the effect of the air core on both the flow fields and the separation performance of the hydrocyclone by replacing the air core with a solid core. A Laser Doppler Anemometer (LDA) was employed to investigate the turbulent flow field inside the hydrocyclone with and without the air core. The conventional hydrocyclone was designed according to the Rietma's optimum geometry. There are 3 shapes of the cone part; the conventional hydrocyclone, the parabola type cone and the hyperbola type cone and in the center of each types were inserted by the solid core as shown in Figure II-14. The solid core was designed at 6 mm-diameters and inserted at the center of the hydrocyclone in order to eliminate efficiently the air core. The results show that the radial and axial velocity components in the area near the entrance of the vortex finder, and the radial and axial turbulence components were all reduced by eliminating the air core, i.e. the flow field characteristic inside the hydrocyclone with solid core became more suitable for the separation process. By replacing the air core with solid core, the hydrocyclone separation performance was improved effectively. Comparing the hydrocyclone with air core and solid core, it was proved to be featured with higher total separation efficiency, larger reduced separation efficiency, smaller corrected cut size and higher separation sharpness, although the hydrocyclone cone shape changed from common type, to parabola type, and to hyperbola type. By increasing the inner space of the hydrocyclone cone, the improvement of separation performance became more remarkable.



(Note: (a) Common type hydrocyclone (No. C10); (b) new type hydrocyclone designed with a solid core (No. C11); (c) hydrocyclone with a parabola type cone (No. C20); (d) hydrocyclone with a parabola type cone and a solid core (No. C21); (e) hydrocyclone with a hyperbola type cone (No. C30); and (f) hydrocyclone with a hyperbola type cone and a solid core (No. C31)).

Figure II-14. Schematic diagram of hydrocyclones for the study of Chu et al., (2004).

Khalid et al., (2004) used the CANMET hydrocyclone to treat oily waste streams. The idea of this research was to develop a new hydrocyclone type, the CANMET hydrocyclone (as presented in Figure II-15), to treat the oily waste stream. This is an effective and economical alternative for treating these and other oily fluids that can replace traditional methods such as heating and gravitational settling.

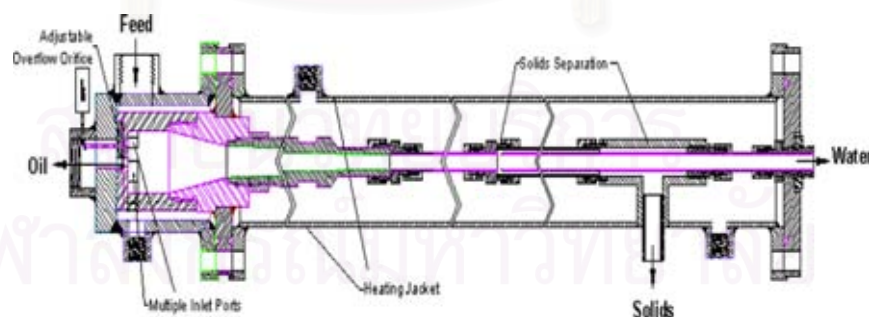


Figure II-15. Schematic of CANMET hydrocyclone

This advanced design is suitable for treating difficult-to-separate oily emulsion and recovered oil from wastewater streams. It consists of multiple inlet ports, an adjustable overflow orifice, solids separation attachments, and heating jackets.

M.P. Burt and P.R. Thomas, (2002) analyzed a hydrocyclone stock cleaning process for wasted fiber in a paper mill. The main objective of this project was to evaluate the possibility of reducing the quantity of fiber wasted at one of many hydrocyclone (centrifugal) cleaning processes in the paper mill. It was found that the application of elutriation water to both the tertiary and quaternary cleaners was essential to minimize the fiber discharged to the sewer, and the pressure of this elutriation water had dramatically reduced the fiber wastage.

R.Q. Honaker et al., (2001) studied the use of an apex water injection to improve hydrocyclone classification efficiency. Classifying cyclones is widely employed to achieve ultra fine particle size separations in industrial applications. However, inherent deficiencies include the particle density effect in multi-component suspensions and ultra fine particles short circuiting to the underflow stream due to hydraulic entrainment. A detailed in-plant test program was conducted to evaluate the benefits of tangential water injection into the apex portion of a classified cyclone for the removal or minimization of ultra fine particles.

Liquid-liquid separation:

Riviere and Garland, (1994) treated oily wastewater, composed of oil, gas, and condensate, discharged from the Elf company into the sea. A hydrocyclone (165 x 35 mm) was installed (in parallel) before the oil skimmer unit. The oily wastewater was injected into the hydrocyclone and the treated hydrocarbon from the process was conveyed to the recovery unit. They reported that they found problems despite the efficient ability of the hydrocyclone. The main causes of poor operation came from upstream conditions such as a plant shut-down and variable flow rates.

Solid-liquid-liquid:

Changirwa et al., (1999) studied a hybrid simulation for oil-solid-water separation in oil sand production. The oil-sand mixture was injected to the reactor as presented in Figure II-16, then the strong vortex separated the oil droplets and sand from the water. This hybrid process combined two individual hydrocyclones, which were used for the oil-water separation and oil-sand separation, as presented in Figure II-17. The oil-sand-water solution was fed into the hybrid hydrocyclone, and then the oil participated fully in the inner vortex and departed from the hydrocyclone through the overflow. After that, the sand-water separation was forced to take place in the

outer vortex, and it was pushed to the boundary layer before exiting through the transverse aperture; the water was moved directly to the underflow orifice.

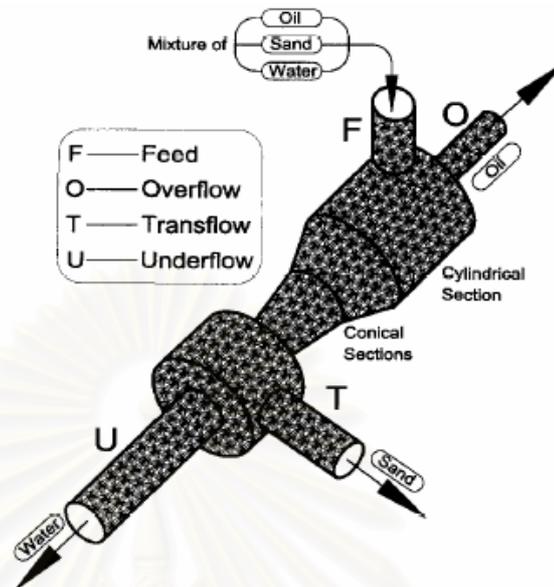


Figure II-16. Schematic diagram of a concurrent three-phase hydrocyclone

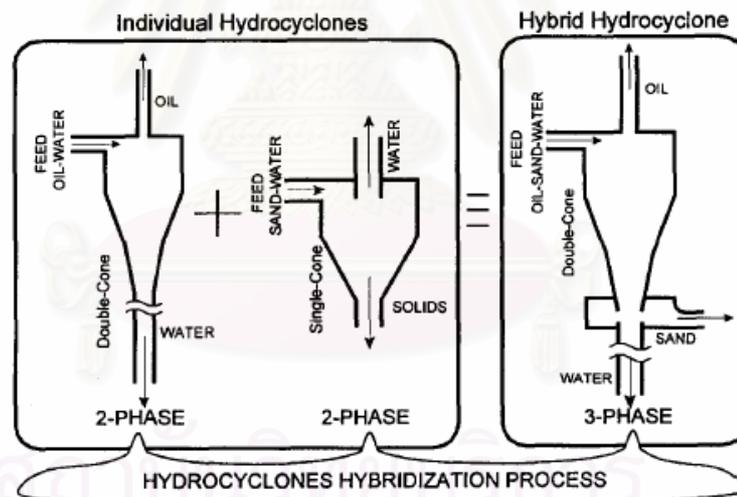


Figure II-17. Two-phase hydrocyclone hybridization process for three-phase separation

Bu Feng MA, (1993) studied three-phase hydrocyclones used for liquid-liquid-solid separation. The experiment procedure of this study integrated two types of hydrocyclones: THEW and RIETEMA, as shown in Figure II-18. The immiscible solution, which consisted of oil, water, and sand, was injected into the hydrocyclone at Port A. Then, this solution swirled inside the hydrocyclone by influence of the vortex flow; after that, the solid phase, sand, was discharged out of the under flow of

the RIETEMA hydrocyclone. In the light phase, oil and water, was moved adversely towards the THEW hydrocyclone. The main function of the THEW hydrocyclone was to separate the oil and water solutions from each other. The heavy phase in this hydrocyclone, sand solution, followed to the external vortex and was discharged out at the external flow. At the same time, the light phase which involved the oil solution followed the internal vortex and move adversely towards the RIETEMA hydrocyclone, and finally, it was discharged out at the oil outlet (port D). Furthermore, this study stated the optimum geometries of a hydrocyclone used for three-phase separation; for example, optimum inlet diameters and vortex flow diameters were provided.

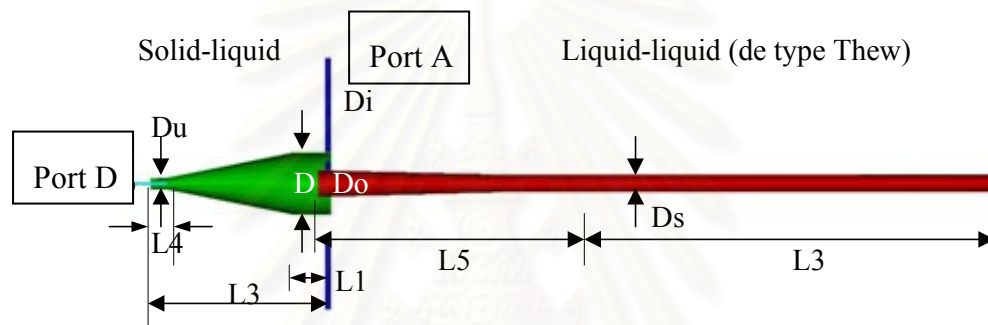


Figure II-18. The schematic diagram of the hydrocyclone used in the
Bu Feng MA study

Gas-solid separation:

Gil et al., (2002) investigated the gas-particle flow inside cyclone diplegs using pneumatic extraction. Their paper presents a detailed flow analysis of cyclone diplegs equipped with bottom gas extraction. Up to now, little experimental work has been done in relation to these devices, which are specially used for hot gas cleaning applications, such as pressurized fluidized bed combustion (PFBC).

Their experimental measurements reveal that the swirling flow penetrated deeper inside the dipleg than anticipated by literature predictions based on conventional cyclone designs. This effect was caused by the high inlet velocities of this kind of cyclone and the gas suction at the dipleg bottom.

Gas-liquid separation

Parga et al., (2002) studied the detoxification of cyanide waste solutions by oxidation with chlorine dioxide (ClO_2) in a gas sparged hydrocyclone (GSH) reactor. The GSH technology used consisted of two concentric right-vertical tubes and a conventional cyclone header at the top. Cyanide solution was fed tangentially at the top through the cyclone header to create the swirl flow beside the inner surface of the porous tube. This action allowed for an air core to form at the center of the GSH. The high velocity swirl flow passed through the sparged air to create a high concentration of small bubbles and supported the reaction between these fine bubbles of $\text{ClO}_2(\text{g})$ and the cyanide solution. Then they were transported radially to the center of the cyclone and vented into a post-treatment device. A GSH can be operated within a small area, compared to conventional air stripping devices.

The recent investigations on hydrocyclones show that different types of hydrocyclones have been proposed for different applications such as liquid-solid separation and gas-liquid-solid separation. It can be observed that new geometries of hydrocyclones are being proposed to improve the efficiency of hydrocyclone use. Moreover, it can be observed that hybrid hydrocyclones can perform as double units.

2.6 The application of coagulation and flocculation in a hydrocyclone

There have been many studies on the flocculation process in a hydrocyclone to improve its separation efficiency. Unfortunately, the aggregated flocs often are broken up; therefore, many researchers have attempted to investigate their behaviour in order to explain the occurring phenomena inside hydrocyclones.

Roldán-villasana and Williams, (1999) studied the classification and breakage of flocs in a hydrocyclone. In general, an aggregation of sub-micron particles is difficult to separate. Therefore, a coagulant or polymer was added to aggregate the colloidal particles in the hydrocyclone. It was found that, the floc that exited from the underflow aperture was broken-up or deflocculated. Therefore, the proposed solution was used in a batch vacuum filtration for the dewatering process, and a network of hydrocyclones was used to treat the overflow product. However, the use of a coagulant and flocculant to treat slurries before they are fed into the hydrocyclone

was not practical because the floc could not survive the shear force within the hydrocyclones..

Plitt and Lilge, (1967) used a 32 mm hydrocyclone and a polyacrylamide flocculant to treat 5% (w/w) clay slurry with a mean size of 5 μm . Adding flocculant reduced the solid concentration in the overflow channel by 72%, and for coarser solids (ϕ 25 μm) the solid concentration in the overflow was reduced by 50%.

Wallace et al., (1980) used six 10 mm diameter hydrocyclones configured in parallel to treat a 2% (w/w) suspension of kaolinite with a mean volume size of 0.77 μm and added a water-polymer (polyacrylamide) solution as the flocculant that increased the total efficiency of the system.

Borts et al., (1982) used 150 and 350 mm diameter hydrocyclones, and to improve the total efficiency, they added a poly-acrylamide flocculant to the slurry. A 94% removal of solids was obtained, which was higher than in the non-flocculated system (53 %). However, the characteristics of the slurry was not provided.

In conclusion, there are two possible situations that explain floc breakage: (1) the collision between particles that enhances floc agglomeration (shear-induced aggregation) and (2) the influence of the liquid velocity gradient on the floc under extremely strong impact collisions between particles and other objects such as the walls of containers or pipes and the blades of the pump or impeller.

Higashitani and Imura, (1998) reported that the break-up can be caused by two different mechanisms: (1) the rupture of floc to form two or more particles and (2) the erosion of the flow, which has a smaller effect than the rupture mechanism.

Woodfield and Bickert, (2004) investigated the separation behavior of flocculated particles in a hydrocyclone to understand the influencing mechanisms for separation. The floc structure properties, floc size distribution, and primary particle composition within all flocs were measured experimentally (i.e., the feed, overflow, and underflow of the hydrocyclone). The flocs were fed into the cyclone via a small tube (189 mm) and the effectiveness of the separation was studied in order to compare the effects of two different primary particle sizes, two different floc formation times (3 and 90 min), and two different hydrocyclone pressure drops

In addition, Williams and Roldan-Villasana, (1991) stated that the flocculated material that has been broken in high shear zones within the hydrocyclone will

reflocculate in a low shear environment during size measurement if flocculant is available.

From the experiment, it was found that the flocculant type, the changing of time for floc formation, and the changing of the operating pressure of the hydrocyclone, has no significant effect on separation efficiency. The underflow flocs were composed of a combination of fine particles and large particles; whereas, overflow flocs appeared to be made up of assemblages of fine particles only. The separation of the underflow and overflow differed, even though the floc size distribution was similar, due to the difference in floc density caused by compositional primary particle differences within the flocs. The reduced density of a floc compared to the primary particles was the main reason for the limited improvement of flocculation that could be achieved in hydrocyclone separation. Furthermore, the overflow floc size distribution was quite similar to the underflow floc size distribution.

Franks George et al., (2005) studied the resistance of aggregated flocs in a high shear force hydrocyclone, and investigate floc sizes and structures. Polymers with various molecular weights and charge densities were mixed with the tailings to determine their shear resistance in a hydrocyclone. The result showed that the application of shear resistance caused a reduction in the size of the aggregate in suspension, and the greater the shear rate, the smaller the aggregates. Furthermore, increasing the molecular weight of the flocculant produced flocs that were less susceptible to shear degradation.

Evidence from the above studies on the effects of hydrocyclones on flocs suggest that flocs are generally broken down by the shear stress present in the hydrocyclone. A low mass density difference did not improve the separation between the large and small flocs. One solution to this problem is to increase the mass density difference by injecting a gas phase during floc formation. The light floc would be immediately able to reach the quiescent area corresponding to the internal vortex.

Next, a literature investigation about micro bubble generation will define the operating conditions necessary to inject micro bubbles inside formed flocs.

Part 3 Micro bubble production

Micro bubbles are the tiny air bubbles which have been traditionally used in water treatment processes; they are especially used in the floatation process. In the floatation process, micro bubbles are produced to agglomerate and raise the solid particles to the surface level of the floatation tank by using the buoyancy force. To accomplish this, the density of the injected solution needs to be taken into consideration. In this section, the production of micro bubbles is described.

3.1.1 The available approaches that produce micro bubbles

At present, there are five approaches to creating micro bubbles:

1. Dispersed-air floatation, which uses a high-speed mechanism agitator combined with an air injection system to produce large air bubbles.
2. Dissolved-air (vacuum) floatation, which saturates the water with air at atmospheric pressure and passes it through the floatation chamber. Then, the pressure is reduced to lower than that of the atmosphere, and the supersaturated air is precipitated out of the solution as microbubbles.
3. Micro floatation, which involves the pumping of air to be dissolved in the water under a hydrostatic head. When the water flows reaches the surface, the air bubbles precipitate out of the solution.
4. Electrofloatation, which utilizes an electrical current, a direct current, or low voltage, which is charged to two plate electrodes that are sunk in the water. Due to the dissociation of the electrolytic water, the bubbles of hydrogen and oxygen are created.
5. Dissolved-air (pressure) floatation (DAF), which is performed under a higher pressure than that of the atmosphere (3-6 bars). The air is dissolved into the stream of liquid under this condition. By the immediately reduction to atmospheric pressure, the air bubbles are precipitated out of the solution in the form of fine bubbles.

Currently, the most widely used techniques in water treatment are dissolved air floatation and electrolytic floatation. In this research, dissolved-air floatation (DAF) was selected to create the micro bubbles for the hybrid process.

3.1.2 Dissolved air floatation (DAF)

The main component of dissolved-air floatation (DAF) is the saturator system, which involves a pressurized tank, a pressurized pump system, and the reducing valve. The pressurized tank is assigned to keep the saturated water that is produced by air dissolving in the water under a high pressure.

To produce the saturated water, clean water from the water supply system and high pressure air flow from the air pipe were pumped into the saturated tank. The constant high pressure in the tank was constantly regulated by a pump because the input water pressure of the water network was low and fluctuated. The detention time of this process was a few minutes (5-10 minutes) to ensure that the air dissolved in the water. In the high pressure saturator, the pressure tank was controlled by a manometer that was kept in range of 6-7 bars as reported by Tchobanoglous, G. et al. (2004).

The number for the conventional dissolved air floatation (DAF) are recommended at 0.0325 (in average) by Degrémont SA., (2005) and from Rafael Teixeira Rodrigues and Jorge Rubio, (2006) whom recommended that the air fraction is 0.025

3.1.3 New processes using microbubble injections inside flocs

Two recent papers deals with microbubble injections inside flocs

Carissimin and Rubio, (2005) described the design and basic development of a new compact in-line coiled reactor to flocculate and separate suspended particles. Three substances were fed into the FGR-reactor as presented in Figure II-19: the colloidal suspension model system ($\text{Fe}(\text{OH})_3$ at 58 mg/l), a cationic polyacrylamide (Mafloc 490 C at 5 mg/l), and the microbubbles (30-70 μm). Methylene blue was used to study the dispersion of the particles as the tracer. The studies were carried out using different FGR models (with varying length/volume ratios). The process efficiency (mainly the kinetics) was evaluated as a function of the polymer concentration, operating parameters, feed flow rate, air-to-solid ratio, and residence

time. The settling and the up-rising rates were calculated to compare the separation efficiency of the conventional floc and the aerated floc. The aerated floc was created by the introduction of microbubbles, which were produced by the DAF system. Then, the microbubbles were mixed with the $\text{Fe}(\text{OH})_3$ polymer flocs and defined as *aerated flocs*.

In addition, they described the effect of the air/solids ratio on the separation efficiency, which is presented in Equation II-19. By fixing the ratio of the injection of microbubbles at 10 % and varying the saturated pressure (i.e., 2, 3, 4, 5, and 6 atm).

$$as = \frac{R_i * Av}{FR * [sol]} * S \quad \text{Equation II-19}$$

where as = air/solid ratio (ml/mg); R_i = rate of injection of micro bubbles (l/min); Av = theoretical volume of dissolved air per liter of water, according to the Henry law (ml/l); FR = feed rate (l/min); S = saturator vessel efficiency (%).

The best results were obtained with air/solids ratios that were greater than 0.025 ml/mg. They stated that the values of the air/solids ratios were more related to the amount of air precipitated and less related to the quantity of air bubbles that actually adhered to the floating particles. The dispersion study demonstrated that when the mixing characteristic in the reactor involves a plug flow regime at the inlet feeder that is higher than 180 l/hr, the obtained corresponding velocity gradient (G) is higher than 1400 s^{-1} .

The results show that the aerated floc provided a rising rate at 112 m/hr with the length and the volume of reactor equal to 12 m and 1.8 l, respectively. Since this value was higher than the settling of the non-aerated floc (18-24 m/hr), this system can be applied to perform high rate solid-liquid separation.

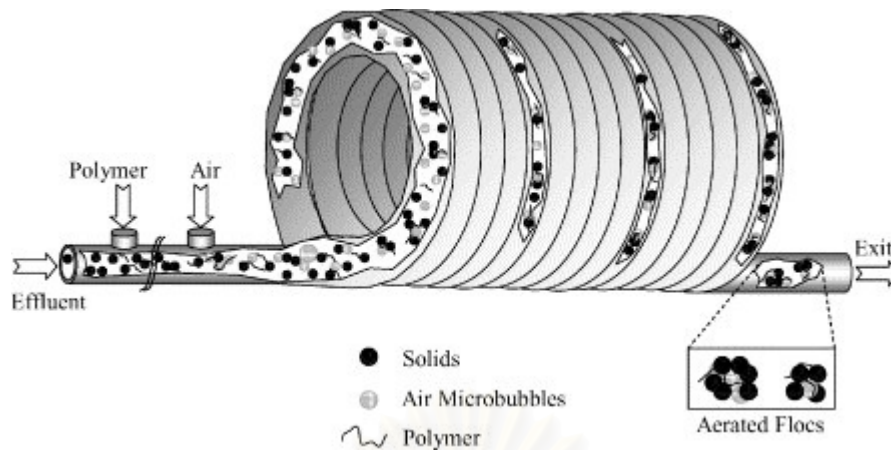


Figure II-19. Generation and growth of aerated flocs inside the FGR for the study of Carissimin and Rubio, (2005)

Rosa and Rubio, (2005). studied a new on-line flocculation system (FF) which was coupled with rapid floatation to remove the aerated flocs (i.e., flocs with entrained and entrapped bubbles) as presented in Figure II-20. These aerated flocs are formed only in the presence of high molecular weight polymers and bubbles and under high shearing (and head loss) in special “flocculators”. The excess air abandons the floatation tank (a centrifuge or a column) through the top and the flocs float after very short residence times (within seconds). The aerated flocs are large units (some millimeters in diameter) with an extremely low density. The process efficiency was found, in all cases, to be a function of the trilogy of head loss, type (and concentration) of flocculants, and air flow rate. Mechanisms involved appear to include small bubble formation and their rapid occlusion (entrapment) within flocs, the nucleation of bubbles at floc/water interfaces, polymer coiling as a result of “salting out” effects at the aqueous/air interface, and plug flow type mixing (flocculation). Successful examples of emulsified oil and solid removal from water were found; all cases were able to obtain high efficiencies (>90% removal), at high hydraulic loadings (>130 mh/1). It is believed that this kind of flocculation–floatation method appears to have a great potential in solid-liquid or liquid-liquid separation.

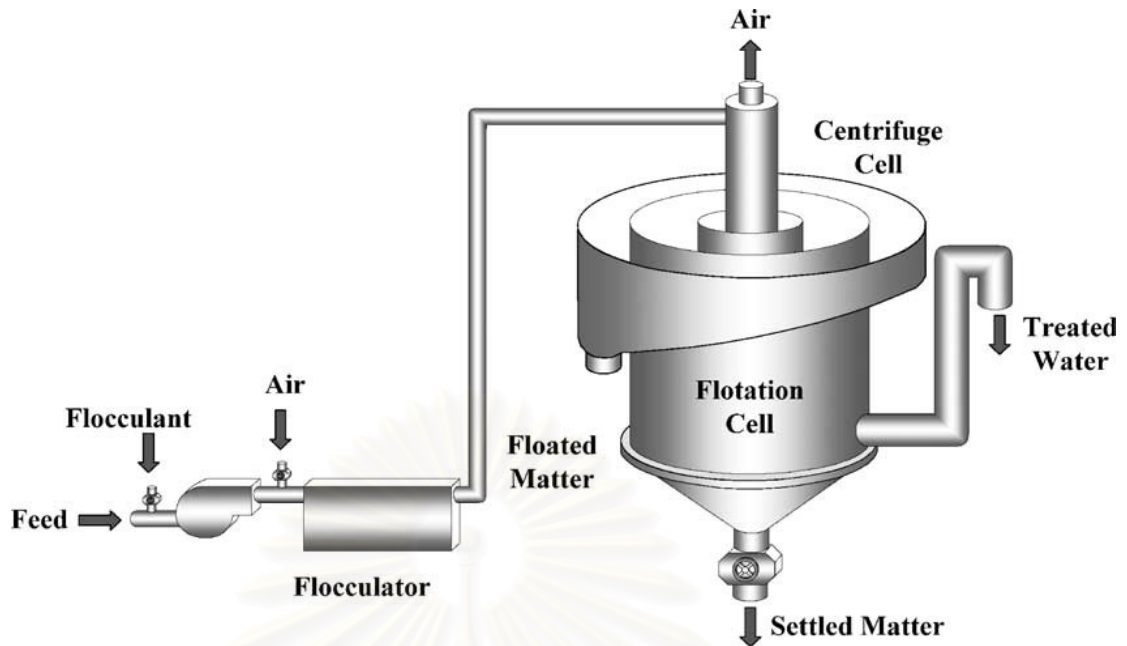


Figure II-20. The Floated Floc pilot system for the study of Rosa and Rubio, (2005)

Rodrigues and Rubio, (2003). developed a new method to measure the size of small and therefore difficult-to-characterize bubbles. Their method measured bubble size based on the bubbles captured (without movement) in combination with microscopy using digital image processing. Their results showed that the mean bubble diameters of bubbles generated by the dissolved air in water (DAF) remain constant and independent of the saturation pressure; the diameters ranged from between 33 to 37.5 μm and their size was less than 70 μm , as presented in Figure II-21 and Figure II-22. These results differ from the results of previous studies by De Rijk et al., (1994) and Rykaart and Haarhoff, (1995) in which the sizes of the bubbles generated by DAF ranged from 40-70 μm . Moreover, De Rijk et al., 1994 found that the mean size of the bubble decreased when the saturation pressure increased from 3-5 bar (350 kPa) to 6.2 bar (620 kPa).

จุฬาลงกรณ์มหาวิทยาลัย

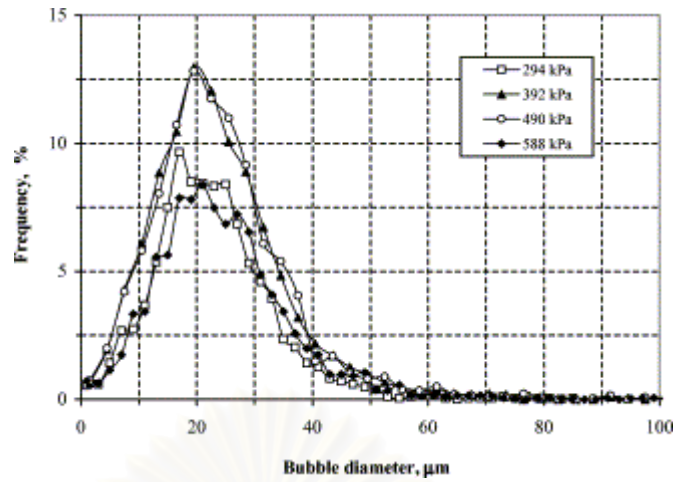


Figure II-21. Bubble size distribution (number) at different saturation pressures.

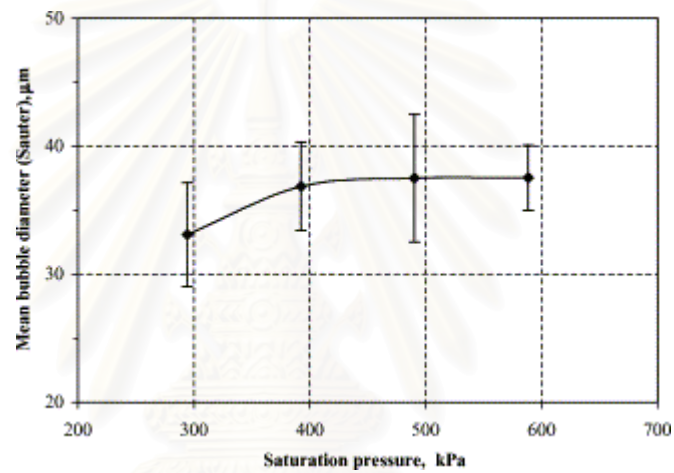


Figure II-22. Sauter mean bubble diameter at different saturation pressures (including the calculated standard deviation).

สถาบันวิทยบริการ
จุฬาลงกรณ์มหาวิทยาลัย

Part 4 Conclusion of the useful bibliography

All previous literature reviews relating to the hybrid process are summarized in this section. The principles for performing coagulation and flocculation and the main principles of hydrocyclones are included.

4.1.1 The principles of the coagulation and flocculation process

Coagulation involves the addition and rapid mixing of a coagulant, the resulting destabilization of the colloidal and fine suspended solid, and the initial aggregation at the destabilized particle. A coagulant such as the high molecular weight polymer is needed for the destabilization process. Flocculation involves slow stirring to aggregate the destabilized particle before the floc settles. The practical ways of utilizing coagulation and flocculation are through sweep coagulation and polymer bridging. To carry out these processes, specific operating conditions are required with regard to the type and dosage of the coagulant, detention time, mixing intensity, and pH.

4.1.2 The required properties for the coagulation and flocculation process

As described previously, the rapid mixing condition and slow mixing condition are required for coagulation and flocculation, respectively. Therefore, the velocity gradient, an important parameter that controls the mixing intensity in the container, is necessary for both processes. The rapid mixing at a high velocity gradient is required for contact to be made between the colloidal particle and the added coagulant since the high velocity gradient is what provides the high collision opportunities between the particles. The recommended range for the velocity gradient in a coagulation process is $100-1000\text{ s}^{-1}$.

In the flocculation process, slow mixing at a low velocity gradient is required to agglomerate the small flocs after the coagulation process, and the recommended range velocity gradient is $10-100\text{ s}^{-1}$.

4.1.3 The separation potential of the hydrocyclone

The hydrocyclone separates an immiscible solution with different densities by using the centrifugal force of the vortex flow. In a classical hydrocyclone, the mixed

solution containing heavy and light phases are injected tangentially from the top of the hydrocyclone to create the vortex flow, then the heavy phase is separated from the light phase following the external vortex, and then moves towards the bottom of hydrocyclone. Finally, it is discharged out at the underflow channel. At the same time, the light phase moves toward the top of the hydrocyclone by following the internal vortex at the core of the hydrocyclone. It is then discharged through the overflow channel at the top of the hydrocyclone. By this principle, the heavy phase and light phase in an immiscible solution can be separated in a hydrocyclone.

4.1.4 The constant angular velocity in the hydrocyclone

There are two types of tangential behaviour in the liquid phase of a hydrocyclone. One liquid fraction, called the *forced vortex*, is present in the internal vortex; it turns around the axial axis with a constant angular velocity. The second one, called the *free vortex*, is present in the external vortex; it turns around the axial axis with a different angular velocity.

The angular velocity in the internal zone of the hydrocyclone is constant, which implies that the light phase in this zone swirls continuously at the same velocity and same distance. The angular velocity is not disturbed by the strength of the shear force. The corresponding angular velocity gradient is zero, while the corresponding tangential velocity gradient is constant.

The angular velocity in the external zone of the hydrocyclone is not constant, which implies that a particle in this area will be disturbed by the strength of the shear force. The corresponding angular velocity gradient is not zero, and the corresponding tangential velocity gradient is not constant.

4.1.5 Micro bubble production

The micro bubbles in this study were produced by the principle of dissolved air floatation (DAF). This process is performed by pumping clean water and air flow into the saturated tank. In this tank, air flow is dissolved into the liquid under a high pressure (5-6 bars) to produce pressurized water (saturated water). After that, it enters the reactor through the reducing valve, where the high pressure is reduced to

atmospheric pressure. The air micro bubbles immediately precipitate out of the solution in the form of fine bubbles 30-45 μ m.



สถาบันวิทยบริการ
จุฬาลงกรณ์มหาวิทยาลัย

Part 5 Hybrid process

The summary of the hybrid process has been divided into three parts: (1) the principle and the expected phenomena of the hybrid process, (2) the controlled parameters for the hybrid process, and (3) the applications of coagulation and flocculation in hydrocyclones.

5.1 Principle and expected phenomena of the hybrid process

In the hybrid process, coagulation and flocculation are integrated in a hydrocyclone reactor, which is controlled mechanically by the vortex flow. In the hydrocyclone, the hybrid process is divided into the three parts depending on the expected mechanisms. The lower part of the hydrocyclone is the location of the coagulation process that functions under a high vortex flow with a high velocity gradient ($100-1000\text{ s}^{-1}$) to provide efficient contact between the coagulant, suspended solids, and micro air bubbles. The middle part of hydrocyclone is where the flocculation process is performed under lower mixing intensity and at a lower velocity gradient ($10-100\text{ s}^{-1}$) which aggregates the small floc. Finally, the separation process is expected to separate the aerated floc from the water; in other words, the solid particles are expected to separate from the water flow.

In a hybrid process, such as the one used in this study, a bentonite water solution, a coagulant, and micro bubbles are prepared and injected at the lower part of the hydrocyclone to perform the coagulation process. It should be noted that the water bentonite solution is injected tangentially to create the water vortex and centrifugal force in the hydrocyclone. By these forces, the three injected substances mix turbulently to create the aerated floc abundant with air micro bubbles; therefore, the floc's density is expected to be lower than the water's. In the following stage, the strength of water vortex is reduced and it plays an important role in flocculation because it aggregates the small aerated flocs together. Then, this floc is expected to move toward the core of the hydrocyclone, based on the characterization of vortex force in the hydrocyclone. The light phase is forced to follow the internal zone and swirl in the core of the hydrocyclone and at the same time, the heavy phase (water) is forced to follow the external vortex and swirl tangentially close to the wall of the

hydrocyclone. From this principle, the expected phenomena at the top part of the hydrocyclone is the swirling line of the aerated floc at the core of hydrocyclone, which is surrounded by clear water close to the wall of the hydrocyclone. Finally, the solid particles are separated from the water inside the hydrocyclone.

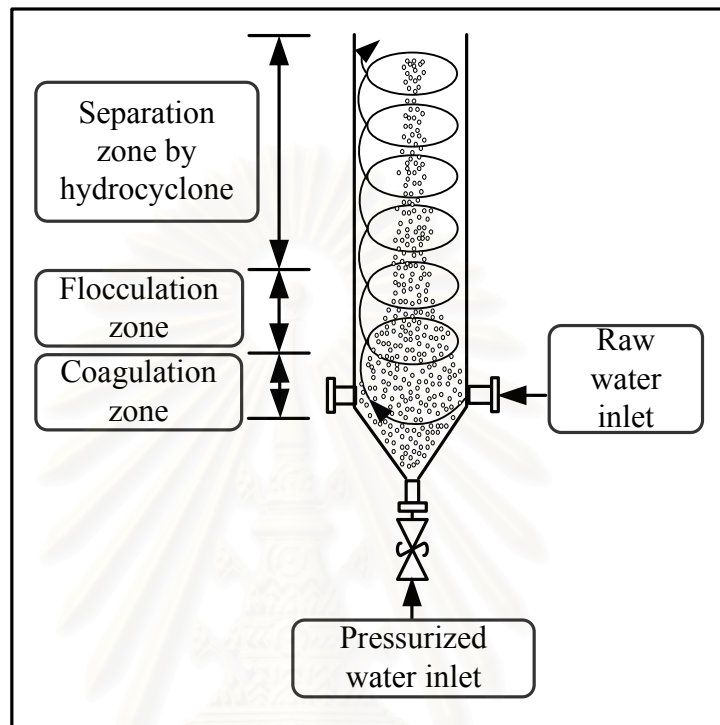


Figure II-23. The expected phenomena of the hybrid process.

The hydraulic retention time to perform the coagulation, flocculation and separation was lower than that of a classical process.

5.2 The controlled parameters for the hybrid process

The main objective of the hybrid process is to separate the solid particles from the turbid water in a hydrocyclone reactor that is driven by coagulation and flocculation. Coagulation and flocculation are performed to create the aerated flocs that contain the required high amounts of microbubbles at the lower part of the hydrocyclone. These aerated flocs must be separated from the treated water by the water vortex at the upper part of hydrocyclone. High amounts of high quantity aerated flocs are needed; consequently, the water stream direction has to be regulated suitably in order to efficiently separate the produced flocs from the water flocs inside the hydrocyclone.

In addition, the bubble coalescence phenomenon must be avoided at the lower part and at the core of the hydrocyclone. The geometry of the hydrocyclone, operating conditions, and their effects on the liquid flow stream must be considered to avoid this unwanted phenomenon. The related parameters are described in the following section.

5.2.1 Coagulant concentration

The key processes for created aerated floc are coagulation and flocculation, which bridge solid particles (i.e., bentonite in this study), air microbubbles, and a coagulant under suitable turbulent conditions. Therefore, the coagulant concentration is important parameters that need to be quantified. In preliminary test, they can be quantified by the jar test method. However, hydrodynamic conditions such as the water flow direction and turbulent conditions in a real reactor are different from those in a jar testing reactor. Therefore, future experiments should be performed in a real reactor.

5.2.2 Air fractions

The objective of this study was to create aerated floc that had a density lower than water's density. Therefore, the abundance of air micro bubbles in the hydrocyclone was an important parameter. An air fraction is defined as the ratio of the air volume and the volume of the treated water. Since the hybrid process is a new water treatment method, no air fractions have been recommended for creating aerated flocs. However, the required air fractions for conventional dissolved air floatation (DAF) are recommended at 0.0325 (in average) by Degrémont SA., (2005) and from Rafael Teixeira Rodrigues and Jorge Rubio, (2006) whom recommended that the air fraction is 0.025

5.2.3 Velocity gradient and raw water flow rate

The velocity gradient is defined as the collision frequency of particles. It is an important parameter because it is directly related to the strength of the vortex in the hydrocyclone. Vortex strength controls the hydrodynamic condition that allows for coagulation, flocculation, and separation to take place in the hybrid process. In addition, the velocity gradient can be used to indicate the strength of shear force acting on aerated floc structures that might cause floc breakup.

The velocity gradient is controlled by the water flow rate. Bradley (1965) states that increasing of the feed flow rate directly increases the shear force.

5.2.4 Water inlet diameter

This is also an important parameter because it can control the strength of the water vortex inside the hydrocyclone. Equation of Puprasert, (2004) (Equation II-12) represent how decreasing of diameter of the water inlet increases the velocity gradient. In addition, Bradley, (1965) stated that increasing the diameter of the hydrocyclone decreases the maximum shear strength of the hydrocyclone.

In summary, the inlet diameter is a parameter that can affect the floated floc formation and separation efficiency of aerated flocs because it controls the hydrodynamic condition in the hydrocyclone. Consequently, vortex flow or the hydrodynamic condition prevents coalescence bubble formation and provides better results since coalescence bubbles can block aerated floc formation and contribute to poor results. In addition, the hydrodynamic conditions in terms of the water stream direction and the strength of the water vortex also control the separation efficiency of the aerated floc from water flow. Therefore, this parameter is needed to obtain the optimum hybrid process results.

5.2.5 Geometry of the hydrocyclone

The shape and configuration of the hydrocyclone reactor are significant to the hybrid process because they control the hydrodynamic conditions inside the hydrocyclone such as the water stream direction, the hydraulic retention time of the particle inside the hydrocyclone, and the bubble coalescence phenomenon. Therefore, in this study, it was necessary to modify and test the hydrocyclone in different configurations in order to find out the best one for the hybrid process.

5.3 Application of coagulation and flocculation in the hydrocyclone

In this section, the literature review of coagulation and flocculation applications in hydrocyclones are described. The objective of this part is to present the ideas and results of previous studies that can be used as the background knowledge for this study.

Puprasert, (2004) studied the feasibility of a hybrid process which consisted of the use of a hydrocyclone, coagulation, flocculation, and floatation to treat the turbidity in synthetic water. Bentonite was mixed with tap water to represent the turbidity in natural water. A transparent column with a 50-mm reactor was used, and a cationic polymer was added as the coagulant. The research was divided into three parts, described as follows:

First a feasibility study of the hybrid process was performed. The hybrid process consisted of a hydrocyclone, coagulation-flocculation, and floatation in a continuous experiment. The raw water flow rates were varied from 100, 200, 300, and 400 l/hr, which corresponded to the velocity gradients 30, 60, 90, and 120 s^{-1} . The obtained results were not satisfactory because aerated floc was not created. Then, the researcher performed batch experiment to determine the feasibility of this hybrid process. In the batch experiment, three substances (i.e., turbid water, coagulant, and air microbubbles) were injected continuously into the hydrocyclone. The experiment was allowed to reach a steady state. Then, the experiment was stopped to observe the occurring phenomena. The results showed that just before to the experiment was stopped, the intensity of the vortex at the top of the hydrocyclone was weaker than the vortex intensity at the lower part. At the same time, the created floc inside the hydrocyclone started to agglomerate together to form a big floc and they moved toward the upper free surface area. The researcher explained that these groups of floc were forced by the water vortex to move toward the core of the hydrocyclone. Then, a floc sample was collected at the top to analyze the floc structure under a microscope. It was found that the produced floc contained many air microbubbles. This floc was defined as an *aerated floc*, and he concluded that this hybrid process could proceed if this kind of floc could be created in a hydrocyclone that maintains a vortex in its upper part.

A secondary experiment was performed to study the behavior and structure of the aerated floc. From the first experiment, some aerated floc floated up to the upper part and also agglomerated at the core of the hydrocyclone. But, at the same time, some of the floc fell down to the bottom of the hydrocyclone. Due to this, the pressurized water flow rate was studied to determine the optimum amount of air microbubbles for the aerated floc. The pressurized water flow rate was varied at 14, 21, 28 and 35 l/hr, respectively. At this maximum flow rate of 35 l/hr, all flocs floated

up to the top of the hydrocyclone and there were no flocs at the bottom of hydrocyclone, which means that aerated floc could be created effectively at 35 l/hr of pressurized water. However, this process requires much lower percentage of pressurized water than conventional dissolved air floatation (DAF) methods. Tchobanoglous, G. et al., (2004). reported that the required percentage of pressurized water in a DAF system is 30-50 % of the water inlet, but the maximum requirement in this study was only 9 percent of the water inlet.

In the hybrid process, the intensity of the mixing inside the hydrocyclone is a main controlling mechanism of the hydrocyclone. Therefore, a final experiment was carried out to find out the optimum velocity gradient intensity of the hydrocyclone. In this experiment, the strength of the velocity gradient in the hydrocyclone was controlled by the feed flow rate to create the water vortex and centrifugal force. A strong velocity gradient was expected at the lower part of hydrocyclone for the coagulation process. It was then expected to gradually reduce at the middle part for the flocculation process. Finally, at the top of the hydrocyclone, the desired separation action was to be driven by the centrifugal force and water vortex. However, the obtained results showed that the expected phenomena did not occur because while the velocity gradient was adjusted for the coagulation process at the lower part, the obtained velocity gradient at the middle part was too strong for the flocculation process. Furthermore, when the velocity gradient was reduced for the flocculation process in the middle part, the obtained velocity gradient at the lower part was too weak for the coagulation process. Lastly, the created centrifugal force at the top part of the hydrocyclone was not strong enough for the separation process.

In conclusion, the velocity gradient is a highly significant parameter that controls the hybrid process. An aerated floc was successfully developed, but the complete hybrid process requires more attention. Looking at the principles of the hybrid process (i.e., the hydrocyclone, coagulation, flocculation, and floatation) in a continuous experiment is appealing because the hybrid process requires low power consumption and produces a smaller footprint.

Siangsananun, (2006) studied the first phase of the hybrid process: coagulation and flocculation within a hydrocyclone. This study was done in a cylindrical hydrocyclone which had different inner diameters to find out preliminary information on the hybrid process. In the first experiment, different types of coagulants (FO 107,

AN 910, and AN 934) were varied at different concentrations (1.0, 2.0, 3.0, and 4.0 mg/l). This first experiment was done using the jar test method to find out the optimum dosage and type of coagulant. FO 107 gave a satisfactory result in terms of the turbidity of the supernatant. Then, 1 mg/l of FO 107 was used in the second experiment in a dis-continuous experiment. This experiment was done at different bentonite in water flow rates (150, 200, 300, 400, 500, and 550 l/hr). The bentonite concentration in the raw water was fixed at 0.5 g/l, air pressure was kept at 3.5 bars, and the inlet diameter was 0.50 cm. The observed parameters were the turbidity of the center and wall zones in the hydrocyclone, the floated floc, and the fallen floc that were observed at the end of experiment.

The result showed that, at the water flow rate of 200 l/hr to 550 l/hr, the created floc floated up to the top of the hydrocyclone, which was confirmation of successful coagulation and flocculation. However, the separation process could not be achieved, which was observed by the insignificant difference of the turbidity between the wall and center of the hydrocyclone.

The second experiment attempted to determine the optimum air quantity for the hybrid process. From the first experiment, two water flow rates, 400 and 500 l/hr, were selected to create a strong vortex at the top of the hydrocyclone. In this experiment, different pressurized waters were varied at 2.0, 2.5, 3.0, 3.5, and 4.0 bars and the pressurize water flow rate was kept constantly at 36 l/hr (maximum flow rate). The suitable air pressure was reported at 3.5-4.0 bars. However, the separation process did not occur in this experiment because the air fraction was too low (0.003-0.009).

Part 6 Mission and objectives of this Thesis

The mission of this thesis research was to create a new separation process for water treatment. This new hybrid process combined the use of coagulation and flocculation in a hydrocyclone to eliminate water turbidity.

As underlined in the literature review section, the original principle of this hybrid process is the integration of coagulation and flocculation inside a hydrocyclone reactor. The strong and low velocity gradients, which characterize the respective external and internal vortices, were employed to perform coagulation and flocculation. Pressurized water was injected simultaneously with raw water and the coagulant to initiate floc formation around microbubbles. Then, these aerated flocs, with low density were centrifuged in the internal vortex where the velocity gradient was weak. Their growth and separation were achieved in the upper part of the hydrocyclone. Puprasert, (2004) and Siangsanun, (2006) initially studied this hybrid process under static operating conditions. They underlined the sensibility of using this process to control the liquid flow, velocity gradient, and bubble coalescence.

The first objective of this thesis was to characterize the hydrodynamics of different hydrocyclones. A new experimental method was used to determine the liquid velocity and velocity gradient of the different types of hydrocyclones. A comparison of the results of the two proposed hydrocyclones is presented. The second objective of the thesis was to analyze the effects of different parameters on the separation efficiency at a steady functioning state; this was done to control the physic phenomenon and select the best operating conditions.

In a first part, floated floc production was analyzed in relationship to the hydrocyclone type in terms of its air fraction, hydrodynamic condition such as velocity gradient, coagulant concentration, and water pressurized feeding position. In a second part, one type of hydrocyclone was selected to study the separation efficiency of the new hybrid process in relationship with its operating parameters. At the end, parameters were selected that can be used in models for this hybrid process.

CHAPTER III

MATERIALS AND METHODS

Two kinds of experiments have been performed in this work. The first trial was devoted to the hydrodynamic characterization of the hydrocyclones. In this study, an original and simple method has been developed for the determination of the velocity field at four points within the zone of water. Thanks to a tracer, a comparison of the different hydrocyclone geometries was made.

In the second part, experiments on the coagulation of synthetic clay water and the flocculation within the hydrocyclone reactors were performed.

Part 1 Materials and methods for the hydrodynamic study

In the hydrodynamic study, an oil tracer solution was injected into the hydrocyclones; the tracers were injected at different positions in the hydrocyclones. A high speed camera was used for picture acquisitions of oil droplet trajectories.

1.1 Materials for the hydrodynamic study

1.1.1 Oil tracer solution

A powdery chemical product (Scharlach R, $C_{24}H_{20}N_4O$) mixed with sun flower oil was used in this experiment as the tracer. The advantage of this product is that it can only be dissolved in an oil solution. It worked as an effective tracer, but it has to be noted that the densities of the tracer solution and clean water were not significant different, 908.5 and 1000 kg/m^3 , respectively. However, this difference must be taken into account for the water velocity calculation.

The tracer solution was prepared and injected into the hydrocyclones by using a 100-ml syringe. This syringe was placed at the injection ports of the hydrocyclones during the experiments, as presented in Figure III-1

1.1.2 Hydrocyclones

The experiments were carried out in three types of glass hydrocyclones, as presented in Figure III-1: (I) a 100-cm high cylindrical hydrocyclone with different diameters (5 and 10 cm at the bottom and upper part of hydrocyclone, respectively), (II) a 130-cm high conical hydrocyclone with a 1.22° angled hydrocyclone (θ), and (III) a 100-cm high cylindrical hydrocyclone with a pressurized water wall injection port.

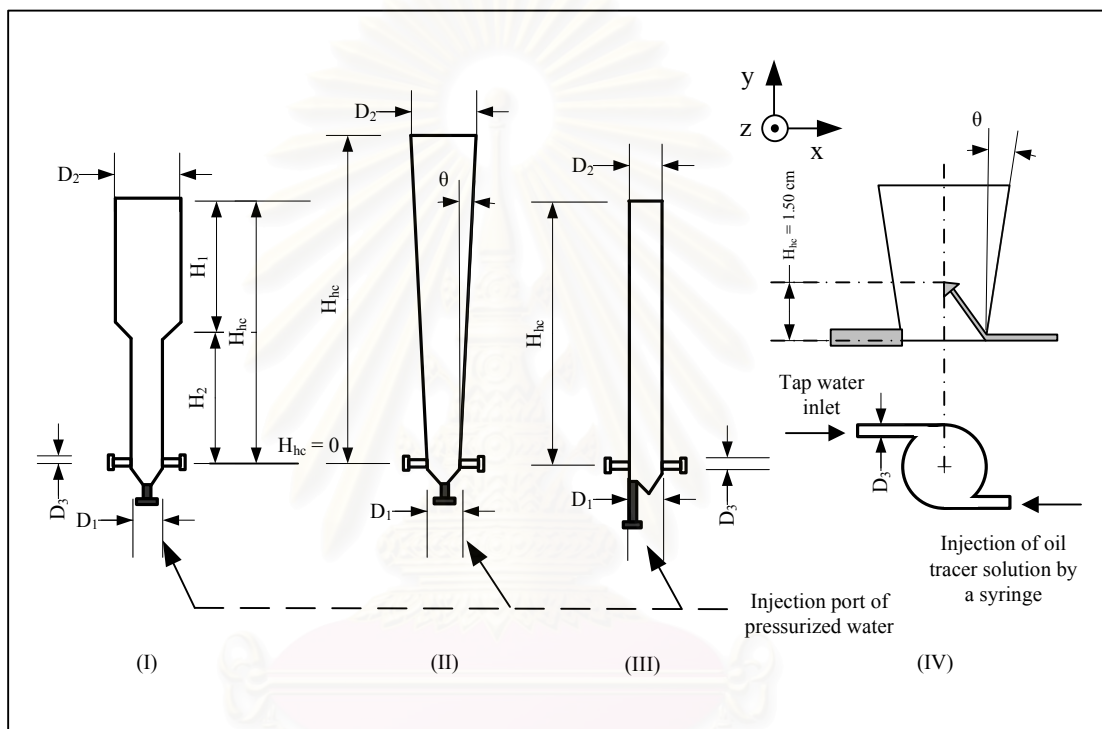


Figure III-1. The studied hydrocyclones in the hydrodynamics study

As can be seen in the diagrams of the hydrocyclones, only clean water and the oil tracer solution were injected at the lower part of each hydrocyclone at $H = 0$ and 1.5 cm (Figure III-1-IV), respectively. The water and oil tracer solution then overflowed at the top of the hydrocyclones. Table III-1 presents the main dimensions of each hydrocyclone.

Table III-1. The main dimensions of each hydrocyclone

Hydrocyclone	H _{hc} (cm)	H ₁ (cm)	H ₂ (cm)	D ₁ (cm)	D ₂ (cm)	D ₃ (cm)	θ (degree)	V _{hc} (l)
1. Different diameter cylindrical hydrocyclone	100	50	50	4.5	10	1	-	4.31
2. Conical hydrocyclone	130	-	-	4.5	10	1	1.22	7.26
3. Constant diameter cylindrical hydrocyclone with air wall injection	100	-	-	4.5	5	1	-	1.96

A simple method was developed to determine the water velocity fields inside the glass hydrocyclones. Oil droplets were injected into the vortices and then tracked using a high speed camera. Analysis of the produced images determined droplet velocities along the z-axis and y-axis, and the water velocity field was also deduced. Particle image velocimetry (PIV) and laser doppler velocimetry (LDV) were not able to be used due to the curves in the glass walls of our hydrocyclones.

1.1.3 Digital high-speed camera

A digital high-speed camera (10 bit CMOS, PCO 1200 hs) was used to record the occurring phenomena in the hydrocyclones. Generally, it is used in many scientific applications such as material testing, high speed particle image velocimetry (PIV), and hydrodynamics testing in order to capture rapidly moving phenomena.

1.2 Hydrodynamic experiment methods

The methods were divided into three parts: (1) the measurement technique, (2) the image acquisition, and (3) the calculation of the axial and tangential velocities of the water.

1.2.1.1 Injection of oil droplets in the hydrocyclones

As seen in Figure III-1, four points were assigned to the bottom part of each hydrocyclone at H_{hc} = 1.50 cm (y-axis) to study the hydrocyclone flow field. The four locations were at the center of the hydrocyclone, 1 cm from the center, 2 cm from the

center, and close to the wall of the hydrocyclone. In each experiment, three oil tracer droplets were injected continuously on the studied point. The droplet size and the droplet direction in the hydrocyclone depend upon the experimental operating conditions (i.e., the water flow rate, water inlet diameter and studied hydrodynamics positions of the hydrocyclone).

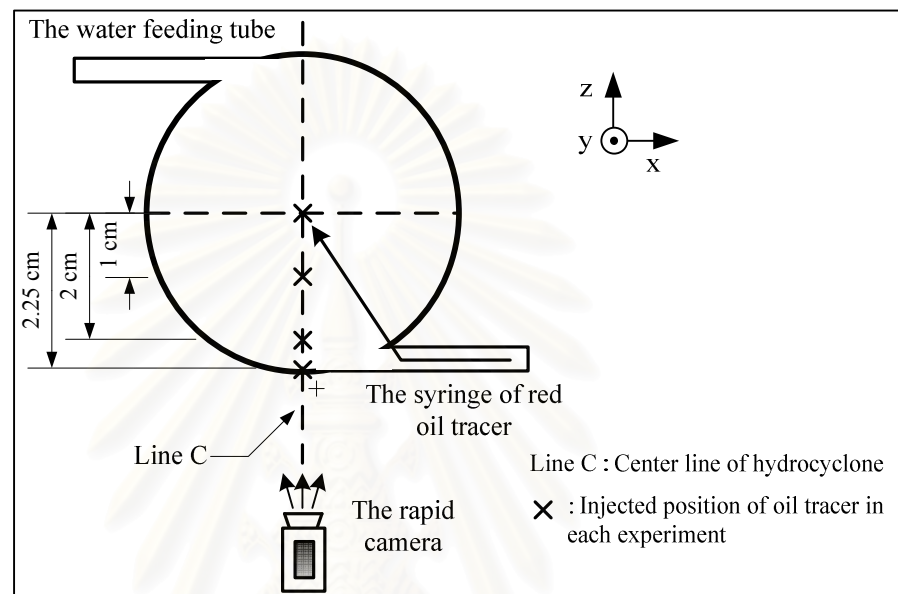


Figure III-2. The studied hydrodynamics positions in the hydrocyclones

1.2.1.2 Picture acquisition

The high speed camera was connected to the computer and placed straight on the center line (Line C in Figure III-2) in front of the hydrocyclone; the experimental procedure for this experiment is presented in Figure III-3. For each experimental run, clean water from a collection tank was fed tangentially through a tangential feeding inlet as presented in Figure III-1-IV. Then, the oil tracer solution was injected continuously into the hydrocyclone by a small syringe (1-ml) at the required position as presented in Figure III-1. The rapid camera started recording the occurring phenomena as soon as the first droplet of the trace solution left the tip of the syringe. Oil droplets moved in different directions in the hydrocyclone depending on the operating conditions. The recording process of the camera stopped automatically when the maximum recordable capacity of the camera (1428 photos) had been reached. The recorded photos were registered on the connected computer. The diameter and coordinates of each droplet on the x and y axes on the photos were

measured by using the image treatment program Visilog 5[®]. However, the measurement of the coordinates of a droplet was performed after it had left the tip of the syringe. Its trajectory was followed continuously from frame to frame until the droplet left out of the image view (see Figure III-4). Then, the coordinates of each droplet were plotted using Microsoft Excel to create the trajectory line curve. From the obtained data, the velocity field, in terms of the axial and tangential velocities and tangential velocity gradient of the water in the hydrocyclone were calculated.

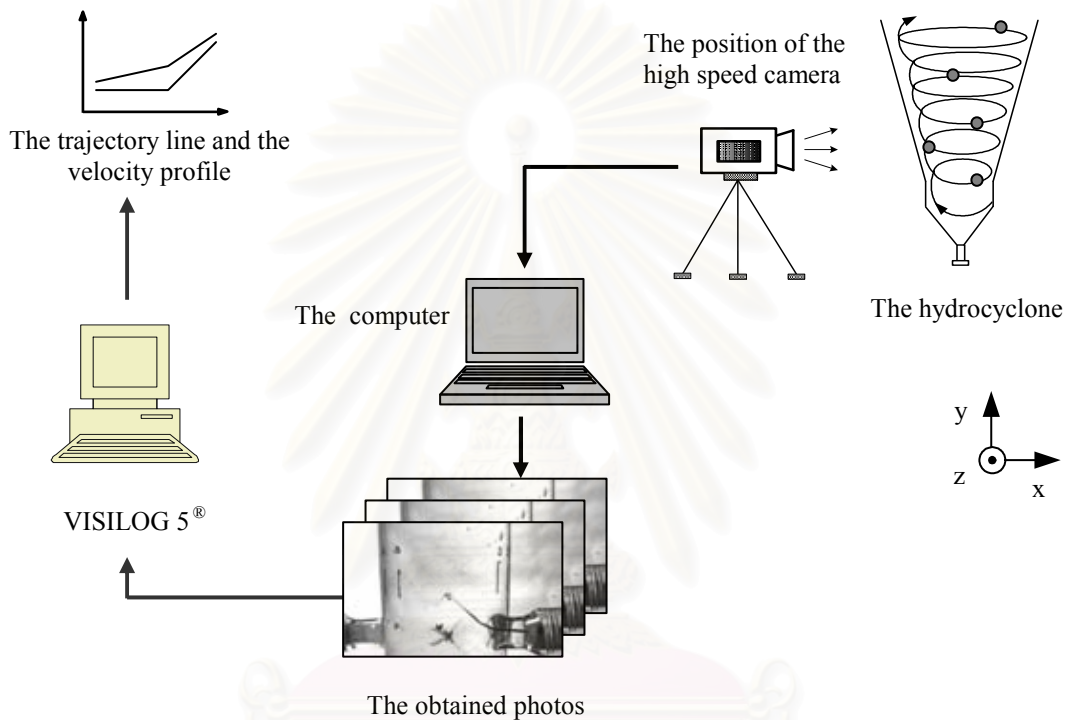


Figure III-3. The schematic diagram for the hydrodynamics experiment

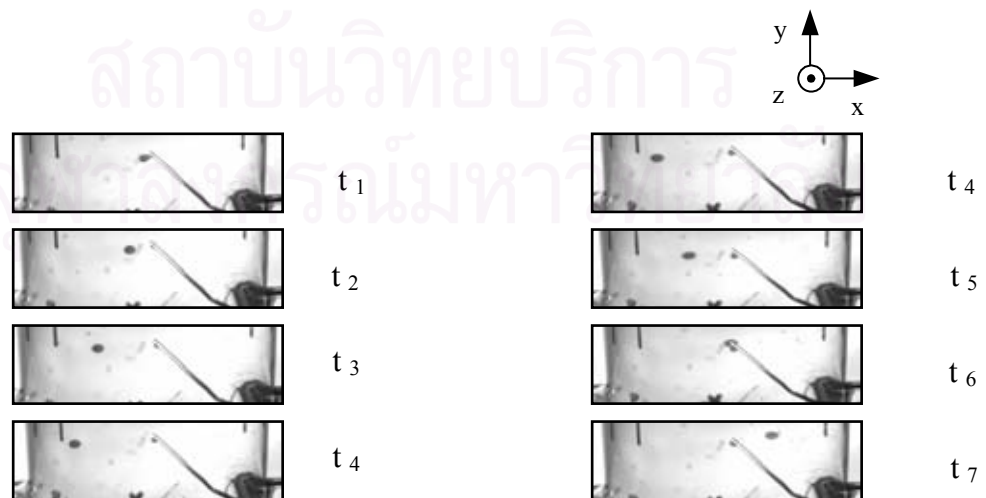


Figure III-4. The trajectory line of an oil tracer droplet at different times

1.2.1.3 Operating conditions

In all types of hydrocyclones, the experiments were carried out by using two water flow rate values (200 and 400 l/hr) with different water inlet diameters (0.30 and 0.50 cm) and different feeding positions for the oil tracer in the hydrocyclones as presented in Table III-2.

Table III-2. Operating conditions of the hydrodynamics study

Experiment	Water flow rate (l/hr)	Water inlet diameter, D_i (cm)	Velocity inlet, V_i (m/s)	Re in the water inlet	Feeding position of the oil tracer in the hydrocyclone
1	200	0.30	7.85	23550	Center
		0.50	2.83	14150	1 cm from the center
2	400	0.50	5.68	28400	2 cm from the center Close to the wall (2.25 cm from the center)

The operating conditions in this experiment were limited at the water flow rate equal to 400 l/hr and small water inlet diameter equal to 0.30 cm.

1.2.1.4 The calculation of the axial and tangential velocities of the water

In the hydrocyclone, there are three important velocities that act on the swirling flow: the tangential, axial, and radial velocities on the z, y, and x axes, respectively. The tangential velocity, which is the most important velocity in the hydrocyclone, is classified into two types that correspond to the vortex flow: a forced vortex and a free vortex. The axial velocity (or the vertical velocity) is defined as the flow stream moves in an upward or downward direction. The radial velocity in a hydrocyclone is the smallest of the three components.

At each studied position in the hydrocyclones, the coordinates of oil droplets were measured and used as the primary information to calculate the relative tangential and axial velocities of the oil droplets. Then, the data were converted to calculate the axial and tangential velocities of the water by using the terminal velocity of the droplets.

1. Oil droplet positions in the hydrocyclones

The coordinates of each droplet at different times (t_1 and t_2) on the z and y axes were measured as presented in Figure III-5. It was carried out by using the Visilog 5[®] program. The coordinates of the oil droplet were determined after it left from the tip of the syringe within zone C-C'' (as presented in Figure III-6, approximately 1 cm from line C).

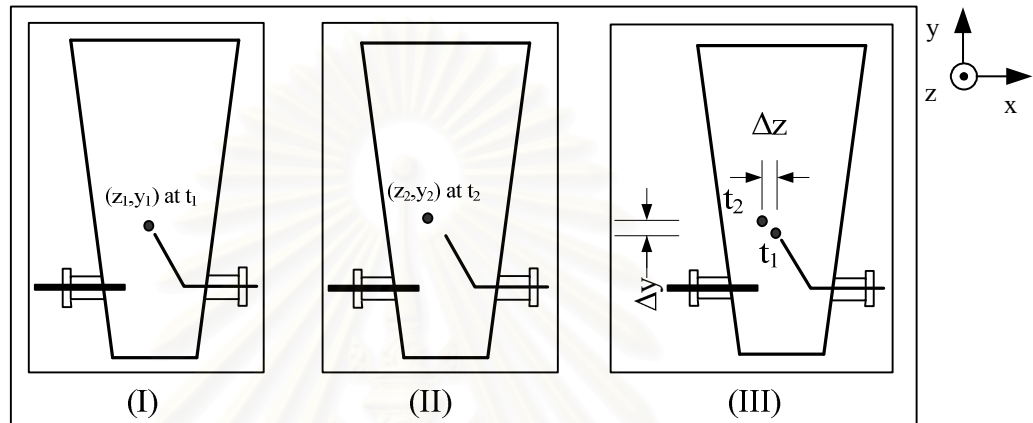


Figure III-5. Movement of the red oil droplet after leaving the tip of the syringe within the hydrocyclones at t_1 and t_2

2. The relative tangential and axial velocities of the droplets

This section presents the equations used to calculate the distances of the oil droplets while they move from t_1 to t_2 tangentially (Δz) and vertically, (Δy) in the hydrocyclones:

$$\Delta z = |z_2 - z_1| \quad \text{Equation III-1}$$

$$\Delta y = |y_2 - y_1| \quad \text{Equation III-2}$$

The relative tangential and axial velocities of each droplet were calculated by Equation III-3 and Equation III-4

$$V_{z,d} = \frac{\Delta z}{\Delta t} \quad \text{Equation III-3}$$

$$V_{y,d} = \frac{\Delta y}{\Delta t} \quad \text{Equation III-4}$$

and Δt was calculated using Equation III-5.

$$\Delta t = \left(\frac{1}{\text{Frequency of photos (fps)}} \right) * (\text{number of photos from } t_1 \text{ to } t_2) \quad \text{Equation III-5}$$

3. Selection of the suitable distance for accurate measurement

The most important parameter for accurate measurements was the selection of two nearby photos in order to obtain a very short straight line of a droplet as soon as it left the tip of the syringe, as demonstrated in Figure III-6. In this figure, the suitable distance is Δz_{ex1} , which presents the movement of the droplet from t_1 to t_2 within zone C-C'' (approximately 1 cm from the center of the hydrocyclone). This example gave an accurate measurement since it can be assumed that tangential variation Δz_{ex1} corresponds to the real length of the droplet. In contrast, if the selected distance of a droplet from two selected photos is too long, the direction of the droplet's movement may become circular as seen in the example Δz_{ex2} in Figure III-6. This example shows that the droplet's directional movement was influenced by the strength of the water vortex in the hydrocyclone, and consequently, the measured distance may be do front to the tangential point in a short range.

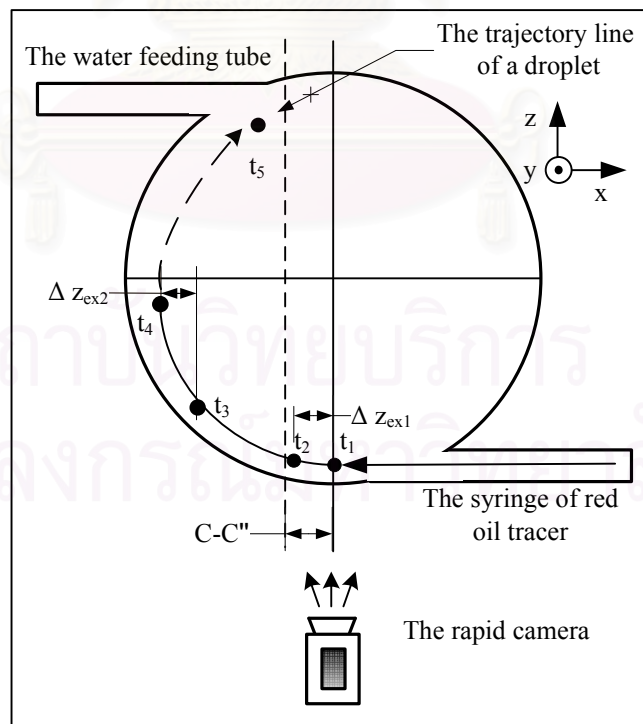


Figure III-6. Trajectory line of the droplet at different times (top view)

4. Calculation of the standard deviation

In this experimental method, the standard deviation (S D) which is a statistical function was used to calculate the statistical dispersion of the relative tangential velocities of the droplet values. For each studied point in the hydrocyclones, the relative tangential velocities of the droplets were calculated and taken into account to determine the standard deviation, which could be defined as Equation III-6:

$$\text{Standard deviation} = \sqrt{\frac{\sum_{i=1}^m (V_{zi} - \bar{V}_z)^2}{m}} \quad \text{Equation III-6}$$

5. Tangential velocity of water

The tangential velocity of water was defined under the assumption that the oil droplets leave instantaneously from the syringe tip and move in balance with the water stream in the hydrocyclone. In terms of tangential direction, there was no external acceleration acting upon the droplet. Therefore, it could be deduced that the relative tangential droplet velocity was equal to the tangential velocity of the water.

6. The axial velocity of water

In the experiment, the red oil droplets were injected to the water stream in the hydrocyclone as the tracer to determine the axial velocity of the water (not for the oil droplet velocity). This calculation was based on the relative velocity of the droplet and the terminal velocity of the droplet due to the different densities of the two liquid phases (oil and water) and the size of the droplet. The calculation of the axial velocity of the water ($V_{y,w}$) was defined as presented in Equation III-7,

$$V_{y,d} = V_{y,w} - V_d \quad \text{Equation III-7}$$

In Equation III-7, the relative axial velocity of the droplet, $V_{y,d}$, was calculated by the experiment (see section 2). The terminal velocity of droplet, V_d , could be calculated by using the Equation III-8 and the required parameter of this equation was the drag coefficient, C_d , which was expressed in the function of Reynolds number, Re , as can be seen in Equation III-9 and Equation III-10. These proposed drag coefficient equations have been validated for a liquid droplet with a Reynolds number greater than 1 or the turbulent flow (Cliff, Grace and Weber, 1978). Therefore, it needed firstly to calculate the Reynolds number (Re), which helps to identify the flow

regimes, laminar, and turbulent flow. In this equation, it could be seen that the Re relates directly to an unknown relative velocity (V_d); a practical way of calculating the terminal velocity is the trial and error method. A number was substituted for this unknown relative velocity in Equation III-8 and then the trial and error process was employed until the final terminal velocity in the equation was constant. The results of these calculations are presented in Table 1 of appendix A.

$$V_d = \sqrt{\frac{4 \cdot \Delta\rho \cdot d_d \cdot g}{3 \cdot C_d \cdot \rho_w}} \quad \text{Equation III-8}$$

$$C_d = \frac{24}{Re} \cdot (1 + 0.15 \cdot Re^{0.687}) \quad \text{for } 1 < Re < 800 \quad \text{Equation III-9}$$

$$C_d \approx 0.45 \quad \text{for } 800 < Re < 3.7 \times 10^5 \quad \text{Equation III-10}$$

$$Re = \frac{d_d \cdot \rho_w \cdot V_d}{\mu_w} \quad \text{Equation III-11}$$

1.2.1.5 The tangential velocity gradient

A hydrocyclone uses the static energy of liquid (i.e., the water flow rate or pressure of the continuous phase) to create a vortex for the separation process. The created vortex is divided into two zones, the internal and external vortices. The tangential velocity gradient is higher in the external vortex than in the internal vortex. In addition, the tangential velocity gradient is a hydrodynamics parameter used to evaluate the shear force acting upon the water flow and the aerated floc. Moreover, it is also applied to observe the intensity of the collisions between particles in the hydrocyclone, which is necessary to evaluate the performance of the coagulation and flocculation processes.

In this study, there are 4 methods to calculate the velocity gradient. First, the velocity gradient was measured from the experiment. Second, it was calculated from the differential of the tangential velocity. Third, it was calculated based on the intensity in the mixing tank. Fourth, it was calculated from a modification of Bradley's equation.

1. The tangential velocity gradient

In this experiment, the tangential velocity gradient was measured to determine the magnitude of the shear force at the different zones inside the hydrocyclones. The tangential velocity gradient was calculated by measuring the tangential velocity of the fluid spatially (from point to point) as presented in Equation III-12

$$G_{z,\text{exp}} = \frac{\delta V_z}{\delta R} = \frac{V_{z2} - V_{z1}}{R_2 - R_1} \quad \text{Equation III-12}$$

where δV_z is the difference of the tangential velocity between two positions and δR is difference of the radius between two positions.

2. The velocity gradient calculated from the tangential velocity correlation

From experimental results, a correlation was proposed to predict the tangential velocity gradient versus the radius of the hydrocyclone (R) which was developed from Equation II-2:

$$V_z R^n = K \quad \text{Equation II-2}$$

This relation is derived to obtain the predicted tangential velocity gradient as presented in Equation III-13

$$G_z = \frac{\delta V_z}{\delta R} = \frac{\delta(K.R^n)}{\delta R} = n.K.R^{n-1} \quad \text{Equation III-13}$$

3. The velocity gradient based on the principle of the mixing tank

In the water treatment process, the average velocity gradient is calculated with Equation III-14; it is used to quantify and verify the mixing performance of the agitator in the mixing tank, it can be also applied to calculate the average velocity gradient in the hydrocyclone.

$$G_{a,m} = \sqrt{\frac{P}{\mu_w \cdot V_{hc}}} \quad \text{Equation III-14}$$

4. The average velocity gradient calculation by a modification of Bradley's equation

Bradley (1965) proposed an equation to investigate the average velocity gradient in a hydrocyclone. In this equation, the average velocity gradient in the hydrocyclone can be calculated depending on the empirical constants (i.e., n and α) related to the geometry of the hydrocyclone where:

Bradley (1965) estimated that the tangential velocity (V_z) relates to the inlet velocity of the hydrocyclone (V_i) as presented in Equation II-15

$$V_z = \alpha (V_i) \quad \text{Equation II-15}$$

From the velocity correlations, the velocity gradient can be calculated as Equation III-15,

$$G_{g,b} = \frac{\delta V}{\delta R} = -K.R^{n-1} = n.V_z \cdot \frac{R^{n-1}}{R^n} = \frac{n.V_z}{R} = \frac{n.\alpha.Q_i}{R.A_i} \quad \text{Equation III-15}$$

where n is the empirical constant issue from the velocity's correlations and α is the ratio of the tangential velocity (V_z) with the inlet velocity (V_i).

Part 2 Materials and methods of the hybrid process study

2.1 Materials of the hybrid process study

The hybrid process experiments focused on the coagulation of synthetic clay particles. Air injections were made by dissolved air floatation (DAF) and aerated flocs were created inside the hydrocyclones.

2.1.1 Pilot experiment description

In this study, the hybrid process was divided into four parts: (1) the pressurized system to produce the air micro bubbles, which was installed on the left-hand side; (2) the glass hydrocyclone reactor, which was installed at the center of the pilot; (3) the raw water preparation, which was on the right side; and (4) the coagulant feeding system, as presented in Figure III-7

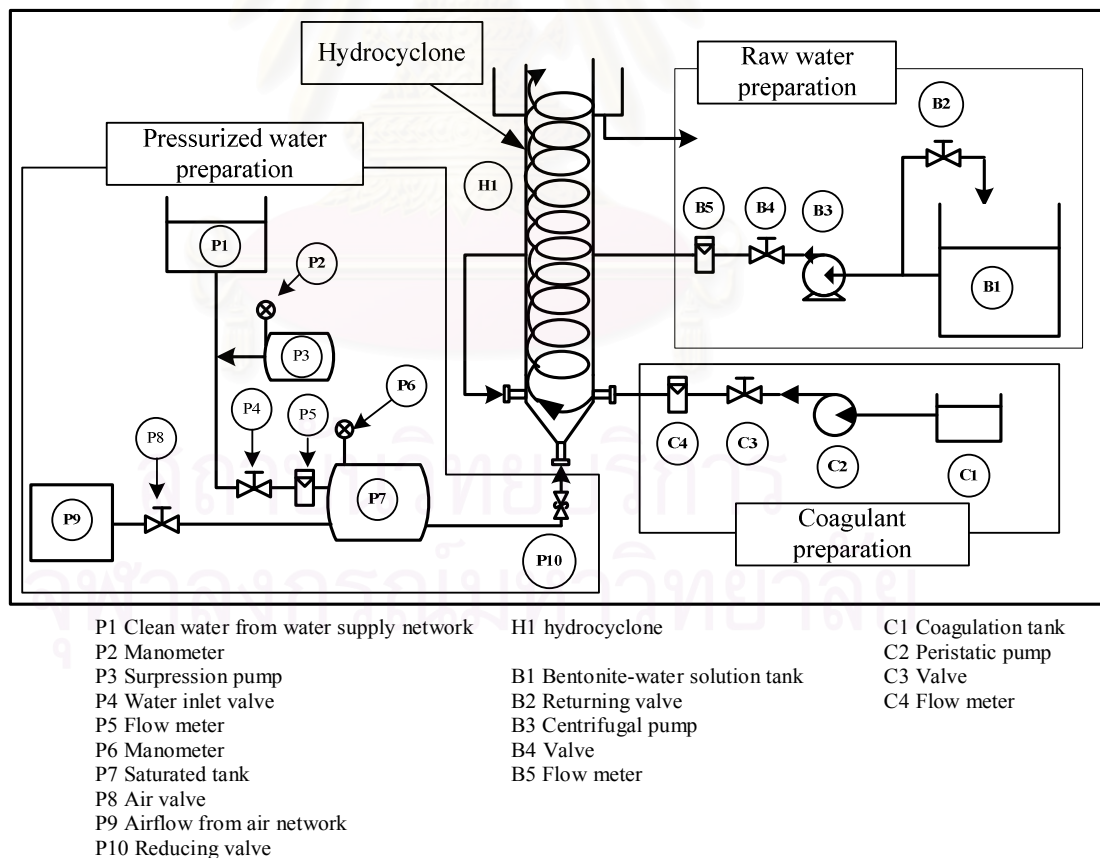


Figure III-7. Schematic diagram of the pilot hybrid process



Figure III-8. Photo of the pilot hybrid apparatus

2.1.2 Preparation of raw water

The raw water was prepared by mixing the bentonite powder with tap water. The bentonite powder was mixed with the tap water in a 50-l mixing tank for 12 hours (minimum) to assure that the bentonite powder was suspended entirely in the solution. Then, it was conveyed to the bentonite 200-l tank and it was diluted with tap water to obtain a concentration equal to 0.5 g/l.

2.1.3 Hydrocyclone

Four types of glass hydrocyclones were used to carry out the hybrid process experiments. They are presented in Figure III-9 and Figure III-10. The first three (HC1, HC2, and HC3) were also used in the hydrodynamics characterization study and a fourth one was added to further study the effects of the pressurized water injection position.

HC 1: A 100-cm high cylindrical hydrocyclone with different diameters (5 and 10 cm at the lower and upper part of hydrocyclone, respectively). The volume of this reactor was 4.31 l.

HC 2: A 130-cm high conical hydrocyclone with a 1.22° wide angle of hydrocyclone (θ). The volume of this reactor was 7.26 l.

HC 3: A 100-cm high cylindrical hydrocyclone with a wall injection port for pressurized water. The volume of this reactor was 1.96 l.

HC 4: A 100-cm high cylindrical hydrocyclone with a bottom injection port for pressurized water in the center of hydrocyclone. The volume of this reactor was 1.96 l, as well.

In this hybrid process experiment, it could be noticed that the main geometry of the HC 3 and the HC 4 was the same but the different point was the air injection position at the bottom of hydrocyclone. The air injection position of the HC 3 is close the wall of the hydrocyclone but the forth one was placed at the center of hydrocyclone.

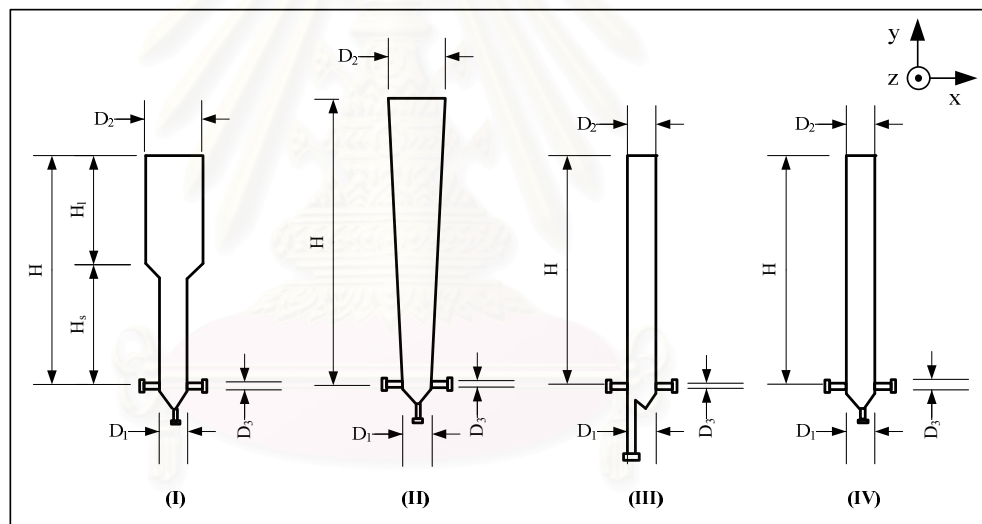


Figure III-9. The studied hydrocyclones in the hybrid process.

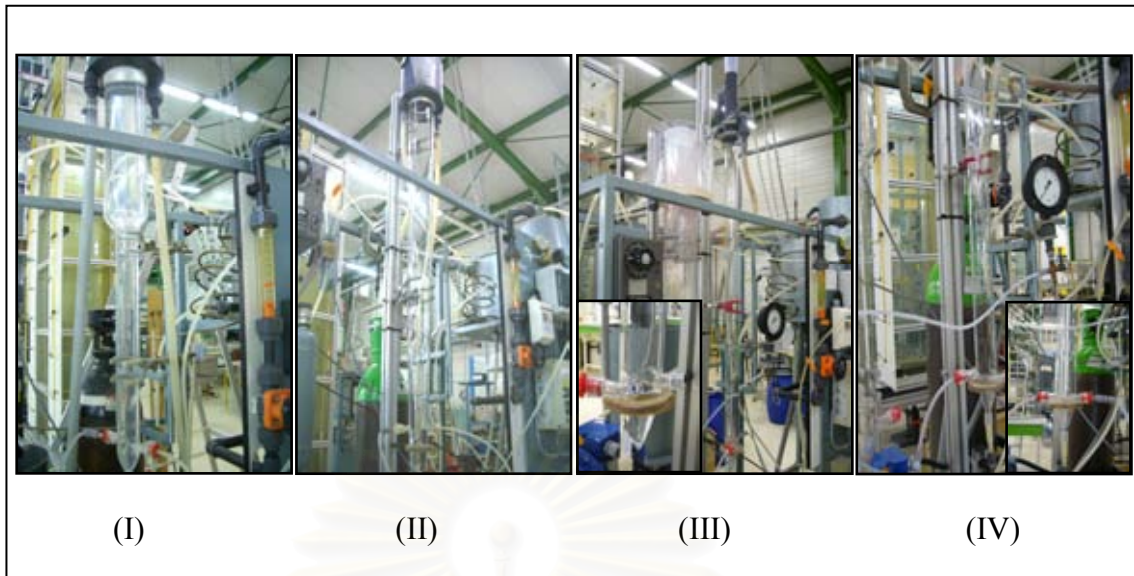


Figure III-10. Photos of the hydrocyclones for the hybrid process experiments.

2.1.4 Raw water inlet diameter.

Plastic tubes were used in this study for the raw water inlets, which were varied at 0.30 and 0.50 cm in diameter. During the experiment, the raw water was pumped through these tubes, which were placed at the left channel of the hydrocyclones in order to create the water vortices inside the reactors.

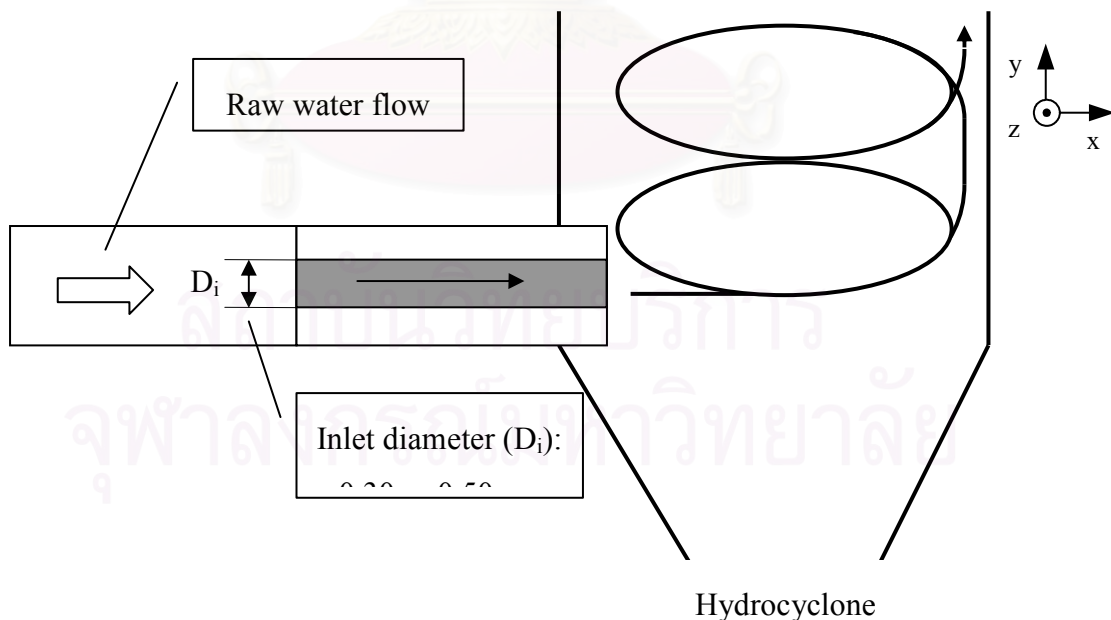


Figure III-11. Raw water inlet diameter.

2.1.5 Coagulant

The white powder polymer FO 107 was used in this study as the polymer to bridge the bentonite particles and micro bubbles. This coagulant was selected based on the study of Siangsanun, (2006). The characteristics of this coagulant with a low cationic charge polymer, 2 mm mesh size, 1 hour dissolution time and 1 day stability of the solution.

For each experiment the solution was prepared by the mixing the polymer powder with clean water. The coagulant concentrations in the hydrocyclones were varied at 1.0, 2.0, 3.0, and 4.0 mg/l.

2.1.6 Pressurized water preparation.

The pressurized water was prepared by means of a dissolved air floatation (DAF) system that produced air micro bubbles; this system was installed on the left-hand side of the pilot system as presented in Figure III-7. This system consisted primarily of the pressurized tank, the pressure regulating pump (surpression pump), the air inlet, and the clean water inlet as illustrated in Figure III-12.

In order to produce the microbubbles, clean water from the water supply system was poured in through a valve (P4) into the saturated tank. In addition, the water pressure of the network water supply was quite low and fluctuated therefore the pressure regulating pump (P3) was used to pump the water supply into the saturated tank in order to increase and maintain the high pressure in the saturated tank. After that, the air stream from the air network (P9) was entered through the valve (P8) into the tank. To ensure an adequate amount of air dissolved in the saturated tank, the detention time was kept at 8-10 minutes. After the pressurized water had been prepared, the reducing valve (P10) at the bottom of hydrocyclone was opened to create the micro air bubbles in the hydrocyclone. During this step, the supersaturated air was precipitated out from the pressurized water and fine air micro bubbles were produced (30-45 μ m in diameter).



Figure III-12. Photos of the pressurized water system

2.1.7 Experimental description

As seen in the presented pilot system in Figure III-7 the water bentonite solution, coagulant, and pressurized water were prepared to perform the experiment. To start the experiment, the bentonite suspension in the 200-l collection tank was pumped into the hydrocyclone continuously under a constant flow rate, which could be regulated using the by-pass system (see valve (B2 and B4)). The raw water suspension was injected tangentially to each hydrocyclone to create the vortex flow in the hydrocyclone

With regard to the coagulant feeding system, the coagulant solution in the feeding tank (C1) was pumped into each hydrocyclone at the required dosage by using a Peristaltic pump (C2). The coagulant injection port was placed at the right side of each hydrocyclone.

In this step, the raw water, coagulant and pressurized water were mixed together under the influence of the vortex flow in the hydrocyclones. At the lower part of the hydrocyclones, strong mixing conditions were observed and they became reduced in the upper part of hydrocyclones. In this experiment, all substances were injected at the lower part of the hydrocyclones; they mixed together inside the hydrocyclones and exited through the tops of the hydrocyclones.

2.1.8 Experimental feeding procedure

In this part, the start-up method of raw water is described. To start the experiment, the raw water was mixed with other materials which were coagulant and air micro bubbles through two methods.

2.1.8.1 Rapid start-up (Method 1)

In this method, the raw water, coagulant, and air micro bubbles were fed constantly into the hydrocyclone at the same time. The raw water rate was kept constantly at the required water flow rate until the end of experiment, for 10 minutes.

2.1.8.2 Progressive start-up (Method 2)

In this method, the raw water, coagulant and air micro bubbles are fed constantly into a hydrocyclone. The injection of the raw water is progressively made in order to prevent big air bubbles from forming inside the hydrocyclone. If the required water flow rate was 200 l/hr, the water flow rate would be firstly fed at 100 l/hr for 3 minutes; secondly, it would be increased to 150 l/hr for 3 minutes and 175 l/hr for 3 minutes, respectively. Finally the water flow rate would be kept constantly at 200 l/hr for 10 minutes and then shut off. The observations were made regarding the different parameters such as suspended solid. In this method, the coagulant dosage and the pressurized water flow rate were adjusted proportionally based on the tested water flow rates.

2.2 Calculation methods for the hybrid process

2.2.1 Calculation of air fractions

Since one objective of the hybrid process is to create aerated flocs abundant in microbubbles, the fraction of the air volume and treated water volume is an important factor because it indicates the air sufficiency in the system. This is a parameter for controlling the hybrid process. The air and treated water fraction can be calculated by Equation III-16:

$$\text{Fraction of air and treated water} = \frac{\text{Air volume (l)}}{\text{Treated water volume (l)}} \quad \text{Equation III-16}$$

where air volume is the dissolved air volume at the required pressure which is calculated by using Henry's law. The treated water volume is the summation of the raw water volume and pressurized water volume.

Henry's law was used in this study to calculate the dissolved air in water, which is a function of the type of gas and the partial pressure of the gas that came in the contact with the water. The relationship between the mole fractions of the gas in the atmosphere above the water and the mole fraction of the gas in the water is given by the following form of Henry's law as expressed in Equation III-17.

$$p_g = \left(\frac{H}{P_T}\right) \cdot x_g \quad \text{Equation III-17}$$

x_g was the mole fraction of gas in water, mole gas/ mole water as expressed in Equation III-18,

$$x_g = \frac{\text{mole of gas } (n_g)}{\text{mole of gas } (n_g) + \text{mole of water } (n_w)} \quad \text{Equation III-18}$$

An example of an air fraction and treated water calculation in this study is reported in the appendix B.

2.3 Operating conditions

2.3.1 Summarized operating conditions in the hybrid process study

In order to study the hybrid process different parameters were modified:, namely water inlet diameter, the raw water flow rate (the bentonite suspension flow rate), the air fraction, and the coagulant concentration. The ranges of values are given in Table III-3.

Table III-3. The operating conditions and experimental values in this study

Studied parameter	Experimental value
Raw water flow rate	Rapid start-up: 100, 150, 200, 300, and 400 l/hr Progressive start-up: 100-150-175-200 l/hr
Raw water inlet diameter	0.30 and 0.50 cm.
Air fraction	0.0082, 0.010, 0.124, 0.0153
Coagulant concentration in the hydrocyclone	1.0, 2.0, 3.0, 4.0 mg/l
Bentonite concentration in raw water	0.0, 0.50 g/l

Velocity inlet and the detention time of all types of hydrocyclones were calculated for each raw water flow rate as presented in Table III-4

Table III-4. The velocity inlet and detention time for each operating condition

Raw water flow rate (l/hr)	Inlet diameter (cm)	Velocity inlet (m/s)	Pressure in the tube (bar)	Re	Detention time (min.)			
					HC 1	HC 2	HC 3	HC 4
100	0.30	3.93	0.55	11,795	2.59	4.36	1.18	1.18
	0.50	1.42	0.07	7,077				
150	0.30	5.90	0.60	17,693	1.73	2.90	0.78	0.78
	0.50	2.12	0.07	10,616				
175	0.30	6.88	0.70	20,642	1.48	2.49	0.67	0.67
	0.50	2.48	0.07	12,385				
200	0.30	7.86	0.70	23,590	1.30	2.18	0.59	0.59
	0.50	2.83	0.07	14,154				
250	0.30	9.83	-	29,488	1.04	1.74	0.47	0.47
	0.50	3.54	0.07	17,693				
300	0.30	11.80	-	35,386	0.86	1.45	0.39	0.39
	0.50	4.25	0.07	21,231				
400	0.30	15.73	-	47,181	0.65	1.09	0.29	0.29
	0.50	5.66	0.07	28,309				

Remark: Volume of HC1, HC2, HC3, and HC4 are 4.31, 7.26, 1.96, and 1.96 l, respectively

2.3.2 Observed parameters for the hybrid process study

The observed parameters in this experiment were divided into two types: during the experiment and 10 minutes after the experiment was stopped as presented in Table III-5.

Table III-5. The observed parameter and observation methods used in this study

During the experiment	
Parameter	Observation method
The bubbles coalescence	Observation by visualization and recorded by a digital camera.
The separation line in the core of hydrocyclone	
The strength of water vortex	
The turbulent condition in the hydrocyclone	
Turbidity (NTU)	Turbidity meter
Suspended solid (mg/l)	Dried at 103-105°C (Sartorius, MA 45, MA 145)
10 minutes after the experiment was stopped	
Height of the floated and fallen floc	Measurement of the thickness
Visual characteristic of floc (dense or loose floc)	Observed by visualisation

The duration of one experiment was limited by the capacity of the bentonite tank. However, the different phenomena such as bubble formation, and microfloc formation, occurred very quickly in the hydrocyclone and the steady state condition can be obtained after 8-10 minutes (on average).

During the experiment, many observations were made visually and by a digital camera. In addition, turbidity and suspended solid measurements were made. Two water samplings at the center and close to the wall of the hydrocyclones were taken

from the top of the hydrocyclones using a long syringe. The turbidity meter and Sartorius (MA 45, MA 145) were used to analyze the turbidity and suspended solid, respectively. In this case, the separation efficiency of the hybrid process could be calculated by using Equation III-19 and Equation III-20.

$\text{separation efficiency by ss (\%)} = \frac{SS_{\text{center}} - SS_{\text{wall}}}{SS_{\text{center}}} * 100$	Equation III-19
$\text{separation efficiency by turbidity (\%)} = \frac{T_{\text{center}} - T_{\text{wall}}}{T_{\text{center}}} * 100$	Equation III-20

At the end of the experiment, the raw water and coagulant flows were stopped and flocs were allowed to float or settled depending on their density. After 10 minutes, the measurements of the heights of the floating and settled floc were made in order to know if the flocs contained bubbles or not.

CHAPTER IV

EXPERIMENTAL RESULTS

The hybrid process is a new water treatment method that integrates a conventional coagulation and flocculation, air microbubbles injection, and a hydrocyclone for floc separation. In this experiment, different hydrocyclone geometries were developed to reach the previously specified objectives. The experiments were done in the hydrocyclone to find out the optimum operating conditions such as raw water flow rate (bentonite suspension flow rate), flow rate and pressure of pressurized water, and coagulant concentration. In order to carry out the hybrid process, it was necessary to characterize the hydrodynamics for each type of hydrocyclone reactor. Due to the direction of water stream was an important parameter to perform the hybrid process such as in the coagulation zone where the microbubbles are injected. In addition, the velocity field of the water stream, the velocity gradient value at the mixing point of the injected substances was investigated in this study. The results of the hydrodynamic conditions were used to understand the performance of the hybrid process in terms of its aerated floc production and separation efficiency. Finally, the hydrodynamic characterization data were used to design a suitable configuration for this hybrid reactor.

The experimental results were divided into two parts: (1) the hydrodynamic characterization study and (2) the hybrid process study.

สถาบันวิทยบริการ
จุฬาลงกรณ์มหาวิทยาลัย

Part 1 The hydrodynamic characterization study

The use of oil droplet injection in a hydrocyclone to study the hydrodynamics in the transparent reactor is a new method; therefore, it was necessary to verify the accuracy and precision of this method.

1.1 Validation of the oil droplet tracer method

To validate the method, three oil droplets were injected into a hydrocyclone. A tracer and a high speed camera were used to observe the occurring phenomena inside the hydrocyclone as presented in Figure IV-1.

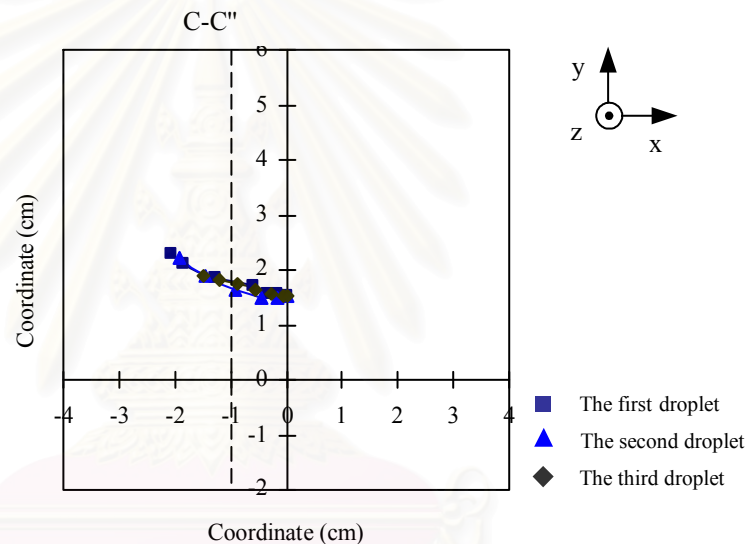


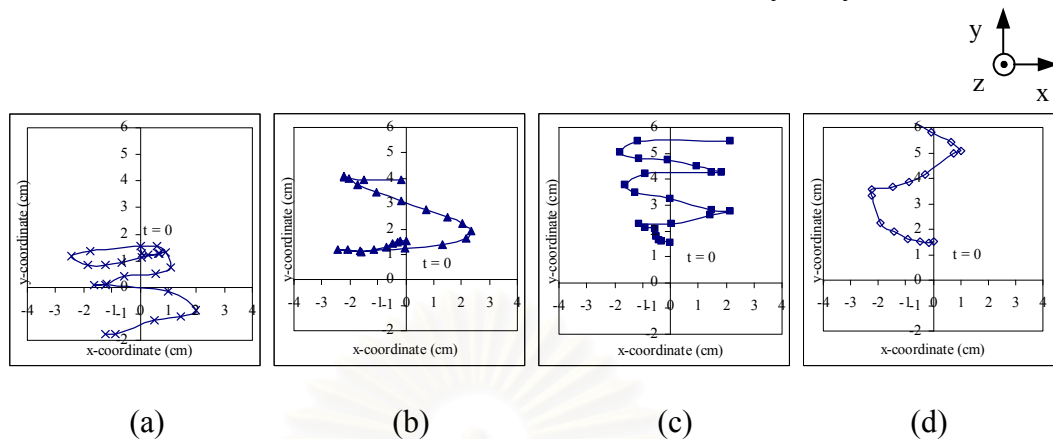
Figure IV-1. The trajectory lines of the oil tracer droplets at different times.

Figure IV-1 presents three trajectory lines of the oil droplets from the time they left from the tip of the syringe. From this figure, it can be seen that the three injected droplets moved in the same direction inside the C-C'' zone ($-1 < x < 0$ cm); this indicated that the measured coordinates of this experiment were of good accuracy. Therefore, this experiment proved that the velocity profile calculations in this study are reliable.

1.2 The trajectory line of the oil droplets

The different trajectory lines from the cylindrical hydrocyclone HC3 is presented as an example in Figure IV-2. The different trajectories correspond to the

different positions of droplet injection: at the center point of hydrocyclone, 1 cm from the center, 2 cm from the center, and close to the wall of the hydrocyclone.



(Note: the locations of the oil droplet injections were (a) at center of the hydrocyclone, (b) at 1 cm from the center of the hydrocyclone, (c) at 2 cm from the center of the hydrocyclone, and (d) close to the wall of the hydrocyclone.)

Figure IV-2. Trajectory lines of the droplets of HC3 at a water flow rate of 200 l/hr and water inlet diameter of 0.50 cm.

It can be seen in Figure IV-2 that the droplet trajectory lines at a low water flow rate, 200 l/hr, swirled everywhere inside the hydrocyclone. At the center of the hydrocyclone, the droplet moved downward directly to the lower part of hydrocyclone; on the other hand, the droplets move upward to the upper part when they were injected 2 cm from the center and close to the wall of the hydrocyclone.

The trajectory line trends of the other hydrocyclones are summarized in the following tables. An arrow oriented in the upward direction indicates an upward flow stream, while an arrow oriented in a downward direction indicate a downward flow stream.

From Table IV-1, the same trend of variations can be observed for all configurations, except at the wall of HC1, where a upward flow stream was observed in the external zone of the hydrocyclone (2 cm). The ratios of the upward flow area and the downward flow area were the same for the HC2 and HC3 configurations, but this ratio was higher for HC1, which had two different diameters at the upper and lower part, as presented in Table IV-1. This design, therefore, could prevent downward flow in the internal zone of hydrocyclone.

From Table IV-1 and Table IV-2 it can be observed that an increase of the flow rate does not modify the direction of the flow stream inside the hydrocyclone. The same conclusion can be made for all hydrocyclone configurations except at 2 cm from the center in HC1 for the water flow rate equal to 200 l/hr, where a downward flow stream was observed.

Table IV-1. Axial direction of the flow streams of each hydrocyclone at a water flow rate of 200 l/hr and water inlet diameter of 0.50 cm

Hydrocyclone	Feeding position of the oil tracer in the hydrocyclone			
	Center	1 cm	2 cm	Wall
HC 1	↓	↓	↑	↑
HC 2	↓	↓	↓	↑
HC 3	↓	↓	↓	↑

Table IV-2. Axial Direction of flow stream of each hydrocyclone at a water flow rate of 400 l/hr and water inlet diameter of 0.50 cm

Hydrocyclone	Feeding position of the oil tracer in the hydrocyclone			
	Center	1 cm	2 cm	Wall
HC 1	↓	↓	↓	↑
HC 2	↓	↓	↓	↑
HC 3	↓	↓	↓	↑

Increasing the velocity of the feed water by decreasing the water inlet diameter, only modified the ratio of the up flow to down flow in HC2 (Table IV-3)

Table IV-3. Axial direction of the flow streams of each hydrocyclone at a water flow rate of 200 l/hr and water inlet diameter of 0.30 cm

Hydrocyclone	Feeding position of the oil tracer in the hydrocyclone			
	Center	1 cm	2 cm	Wall
HC 1	↓	↓	↓	↑
HC 2	↓	↓	↑	↑
HC 3	↓	↓	↓	↑

1.2.1 Conclusions of the trajectory line for the hybrid process

The useful conclusions of the trajectory line study are as follows:

The investigation method used to follow the trajectory lines of the injected oil droplets in zone C-C" is reliable. From the experiment, it can be seen that the trajectory line was repeatable.

Regardless of the type of hydrocyclone and the flow rate used, the direction of the water flow stream in the hydrocyclone was upward at the wall zone and downward at the center point.

The ratios of the upward flow area and the downward flow area were the same for conical and cylindrical configurations, but this ratio was higher for HC1, which had two different diameters at the lower and upper parts of hydrocyclone. This design, therefore, could be used to prevent downward flow in a hydrocyclone.

The obtained information in this section can be used to explain the observed phenomenon such as the coalescence of big air bubbles at the lower part of the hydrocyclone. Moreover, it can be used to modify the hybrid process system; for example, it could be used to accurate the position of the pressurized air injection port at the bottom of the hydrocyclone.

1.3 The velocity profiles inside the hydrocyclones

In this section, the velocity profiles of three types of hydrocyclones (i.e., the different diameter cylindrical hydrocyclone, HC1; conical hydrocyclone, HC2; and constant diameter cylindrical hydrocyclone, HC3) are presented. For each hydrocyclone, the velocity profile is given in relation to the studied parameters: (1) the water flow rate and (2) the water inlet diameter.

1.3.1 The different diameter cylindrical hydrocyclone, HC1

This cylindrical hydrocyclone had different diameters: 5 cm at the lower part and 10 cm at the upper part. The details of its configuration were provided in Chapter III.

The tangential and axial velocity profiles of water in the hydrocyclone were presented (in z-axis and y-axis) as functions of the droplet feeding positions in the hydrocyclones.

1.3.1.1 Effects of the water flow rate

To present the effects of water flow rate on the velocity profiles in HC1, experiments were performed at two water flow rates: 200 and 400 l/hr. The water inlet diameter was kept constantly at 0.50 cm. The experimental results of the tangential and axial velocity profiles of water flow in the hydrocyclones are presented in Figure IV-3.

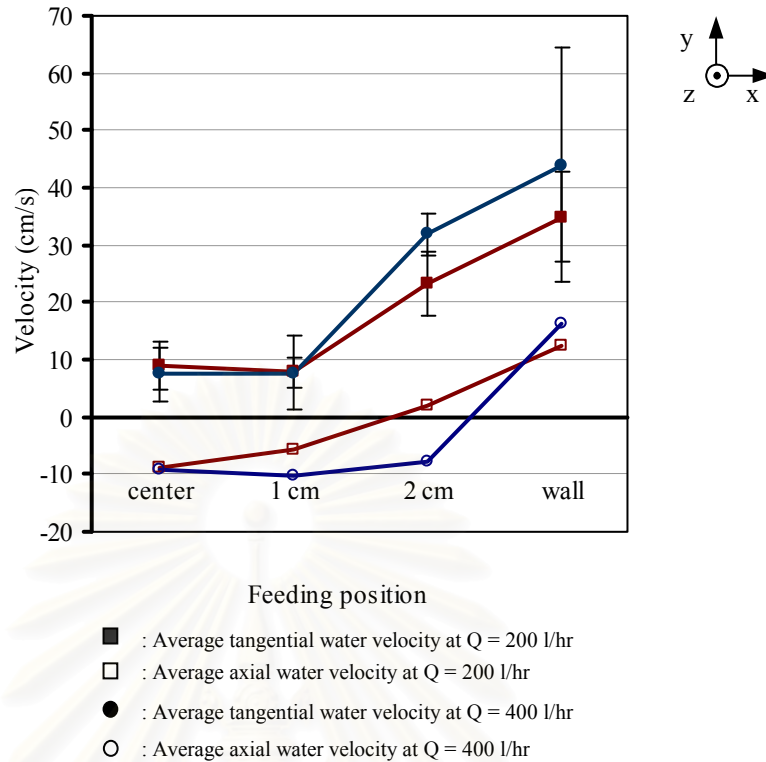


Figure IV-3. Tangential and axial water velocity at different studied points in HC1, which was operated with a constant inlet diameter (0.50 cm) and at different water flow rates (200 and 400 l/hr)

In Figure IV-3, the same tangential velocity profile can be observed: the tangential velocity of the water flow of both operating conditions increased when the droplets were injected farther away from the center of the hydrocyclone. The tangential velocity of the water flow at the wall zone was higher than that of the center of the hydrocyclone.

The average tangential velocities of water in the internal zone ($0 \leq x \leq 1$ cm) under both operating condition were constant at 8 cm/s. At the wall of the hydrocyclone in the external zone ($2 \leq x \leq 2.25$ cm), the tangential velocity of high water flow rate, 400 l/hr, was greater than the tangential velocity of low water flow rate, 200 l/hr, at 44 and 35 cm/s, respectively.

Regarding the same figure, variations of axial velocity were the same at both water flow rates. The axial velocity (in absolute value) in the internal zone ($0 < x < 1$) was lower than the axial velocity in the wall zone (-8 cm/s at the center and 14 cm/s in the external zone).

In addition, the axial velocity value of the high water flow rate was the same as the axial velocity values of the low water flow rates when taken at the center and at the wall. These values differed from the axial velocity value observed in the intermediate zone.

In conclusion, it can be noted that these experimental results are in good agreement with the literature: (1) the axial velocity is in the same range as the tangential one in the center zone, (2) the tangential velocity is the highest at the wall zone, and (3) an increase of the tangential feed water flow rate allows an increase in the tangential velocity at the wall zone.

1.3.1.2 Effects of the water inlet diameter

The objective of this part is to present the effects of the water inlet diameter on the velocity profiles in the HC1 hydrocyclone. The experiments were operated at a constant water flow rate of 200 l/hr, and the water inlet diameters were varied at 0.30 and 0.50 cm. The experimental results of the tangential and axial velocity profiles of water flow in the hydrocyclone HC1 are presented in Figure IV-4.

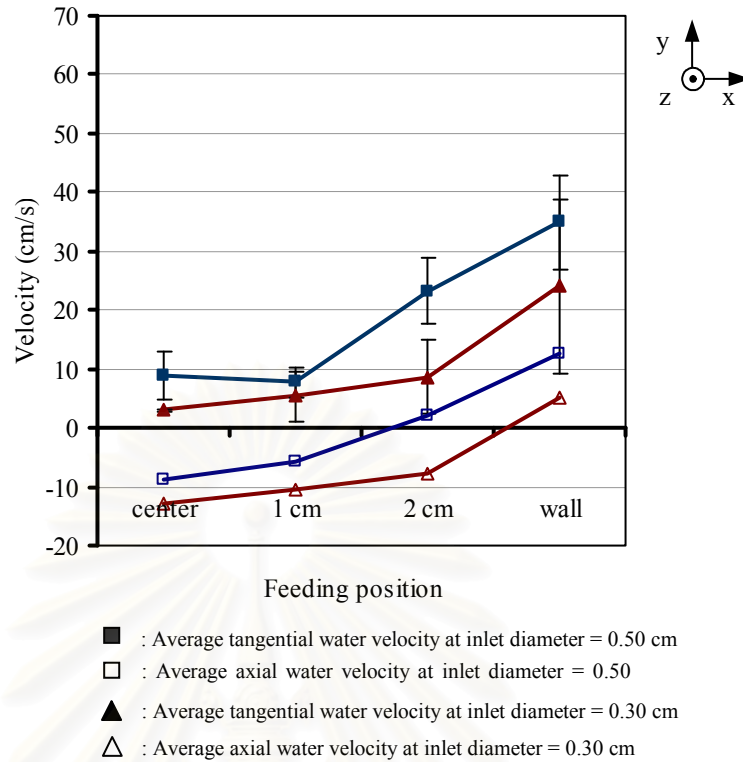


Figure IV-4. Tangential and axial water velocity at different studied points in the HC1, which was operated at a constant water flow rate (200 l/hr) and with different inlet diameters (0.30 and 0.50 cm)

As can be seen in Figure IV-4, the tangential velocity increased from the center to the wall zone at both water inlet diameters. For example, in the internal zone ($0 < x < 1$ cm) the value was about 5 cm/s, and it increased by a factor 6 at the wall.

In addition, the tangential velocities for the larger 0.50 cm water inlet were higher than the tangential velocities of smaller 0.30 cm water inlet; for example, at the wall zone, the tangential velocities of the large and small water inlets were 35 and 24 cm/s, respectively.

As seen in Figure IV-4, the variations of axial velocity were the same regardless of the water inlet diameter. The axial velocity values were negative in the internal zone (denoting downward motion); whereas, the axial velocities at the wall zone were positive (denoting upward motion). Their progression from the internal zone ($0 < x < 1$) to the external zone ($2 < x < 2.5$) were the same.

With regard to the effects of the water inlet diameter in the HC1 hydrocyclone, the axial velocities of the smaller one, 0.30 cm, were higher than the axial velocities of the larger one, 0.50 cm, except at the wall zone.

In conclusion, the highest values of the tangential velocity in the HC1 hydrocyclone were obtained at a water flow rate equal to 400 l/hr and an inlet diameter equal to 0.5 cm.

1.3.2 Conical hydrocyclone HC2

This hydrocyclone had a conical shape (as presented clearly in Chapter III) to remove the zone where the diameter changes (as in the HC1), increase the retention time of the particles in the hydrocyclone and maintain a strong vortex in the upper part.

The tangential and axial velocity profiles of water in the hydrocyclone were presented (on the z-axis and y-axis) as a function of the droplet feeding positions in the hydrocyclone.

1.3.2.1 Effects of the water flow rate

The objective of this part was also to present the effects of water flow rate on the velocity profiles in the conical hydrocyclone HC2. Some experiments were performed at water flow rates equal to 200 and 400 l/hr and the water inlet diameter was maintained constantly at 0.50 cm. The results of the tangential and axial velocity profiles of water flow in the hydrocyclone are presented in Figure IV-5

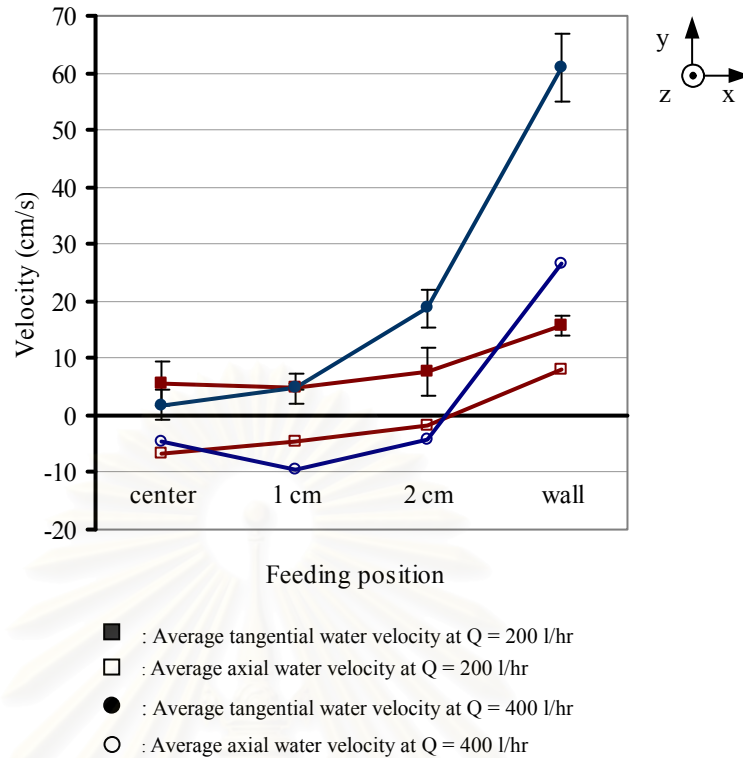


Figure IV-5. Tangential and axial water velocity at different studied points in HC2, which was operated with a constant inlet diameter (0.50 cm) and at different water flow rates (200 and 400 l/hr)

It can be observed that the tangential velocity increased as a function of the feeding position: the velocity was the highest at the wall zone.

Moreover, the tangential velocities in the internal zone ($0 \leq x \leq 1$ cm) for both water flow rates were quite constant at 7 cm/s. In contrast, the tangential velocities of the different water flow rates were dramatically different at the hydrocyclone wall ($x = 2.25$ cm): the velocity of 61 cm/s for the high water flow rate (400 l/hr) was four times higher than that of the low water flow rate (200 l/hr).

As far as axial velocity was concerned, it was quite similar at both water flow rates in the internal zone ($0 < x < 2$ cm). In contrast, in the external zone ($2 < x < 2.5$ cm), the axial velocity decreased from 26 cm/s at the high water flow rate to 8 cm/s at the low water flow rate.

1.3.2.2 Effects of the water inlet diameter

The objective of this part was to present the effects of the water inlet diameter on the velocity profiles in HC2. The experiments were operated at a constant water flow rate of 200 l/hr, and the water inlet diameters were varied at 0.30 and 0.50 cm. The results of tangential and axial velocity profiles of water flow in the hydrocyclone were presented in Figure IV-6.

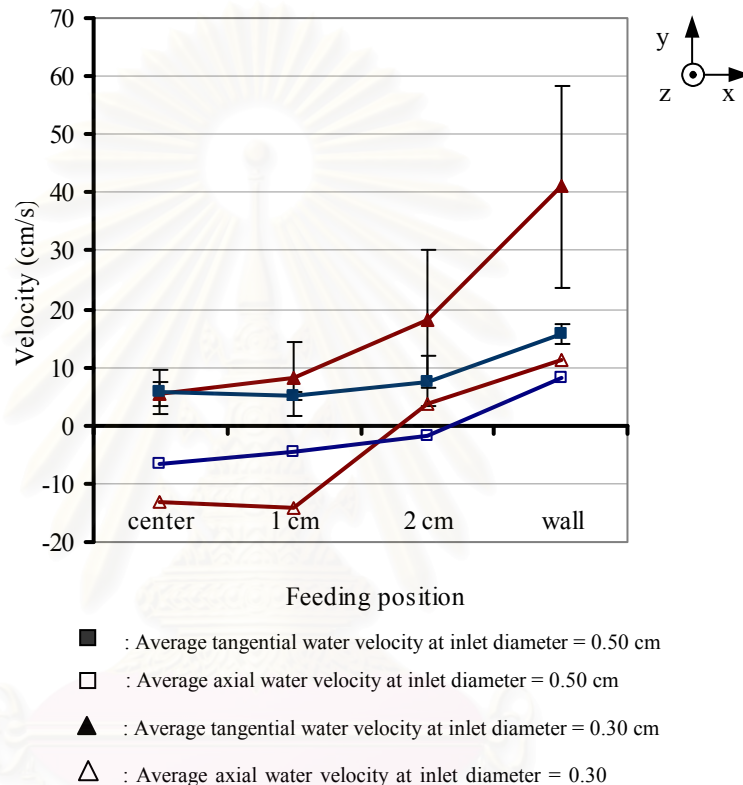


Figure IV-6. Tangential and axial water velocity at different studied points in HC2, which was operated at a constant water flow rate (200 l/hr) with different inlet diameters (0.30 and 0.50 cm)

As can be seen in Figure IV-6, the average tangential velocities of both water inlet diameters increased when the droplets were injected far away from the center of the hydrocyclone.

For both operating conditions, the tangential velocities in the internal zone ($0 \leq x \leq 1$ cm) were fairly constant at 6 cm/s. However, in the external zone ($1 \leq x \leq 2.5$ cm), the tangential velocities were notably different: the tangential velocity measured with the small water inlet was 41 cm/s and that of the big water inlet was 16 cm/s.

In the internal zone ($0 < x < 1.0$ cm), the axial velocity obtained with the larger inlet diameter, 0.50 cm, was lower (in absolute value) than the velocity obtained with the smaller inlet diameter. In contrast, in the wall zone, the inlet diameter had no significant impact on axial velocity (mean value 10 cm/s).

In conclusion, the highest tangential velocity values in the conical hydrocyclone were obtained at a water flow rate equal to 400 l/hr and with an inlet diameter equal to 0.5 cm.

1.3.3 Constant diameter cylindrical hydrocyclone HC3

This hydrocyclone had a 5 cm-diameter cylindrical shape throughout as presented clearly in the materials and methods chapter. It was designed to maintain the vortex force in the upper part of the hydrocyclone while upholding the advantages of a cylindrical hydrocyclone for the hybrid process.

The tangential and axial velocity profiles of water in the hydrocyclone were presented (on the z-axis and y-axis) as a function of the droplet feeding positions in the hydrocyclone.

1.3.3.1 Effects of the water flow rate

The experiments were performed at the water flow rates of 200 and 400 l/hr and using a constant water inlet diameter of 0.50 cm. The tangential and axial velocity profiles of the water flow in the hydrocyclone are presented in Figure IV-7.

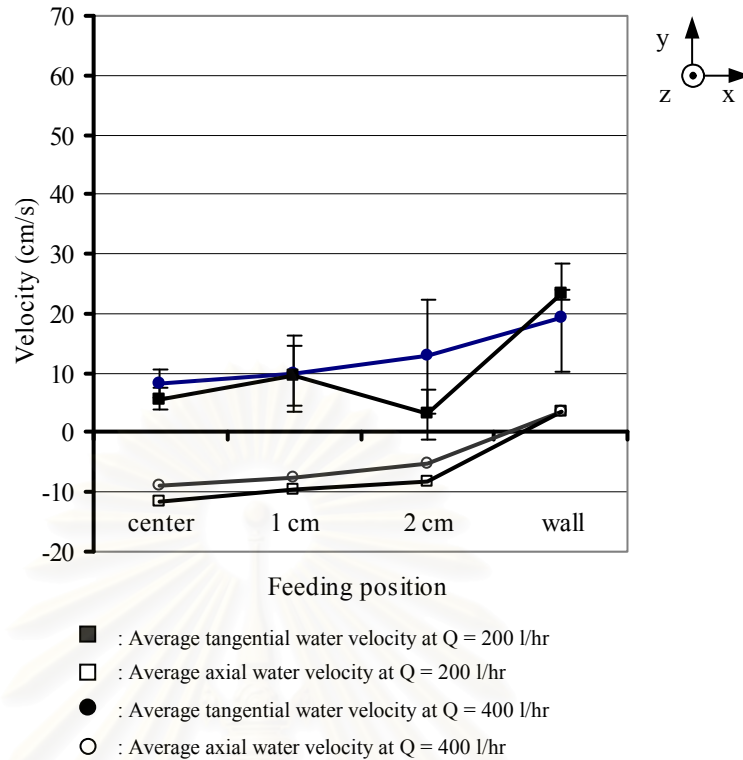


Figure IV-7. Tangential and axial water velocity at the studied points in HC3, which was operated with a constant inlet diameter (0.50 cm) and at different water flow rates (200 and 400 l/hr)

As in the others hydrocyclones, it can be seen in Figure IV-7 that the tangential velocity at the wall zone was higher than that of the center zone, except at 2 cm. The tangential velocities were the same at both water flow rates. In the internal zone of the hydrocyclone ($0 < x < 1$ cm) the velocity was roughly averaged to be 8 cm/s. At the wall of hydrocyclone, it increased slowly to 21 cm/s.

With regard to axial velocity, there was no difference between the two tested water flow rates.

1.3.3.2 Effects of the inlet diameter

The objective of this part was to determine the effects of the water inlet diameter on the velocity profiles in the HC3 hydrocyclone. The experiments were performed at a constant water flow rate equal to 200 l/hr, and the water inlet diameters were varied at 0.30 and 0.50 cm. The tangential and axial velocity profiles of the water flow in the hydrocyclone are presented in Figure IV-8.

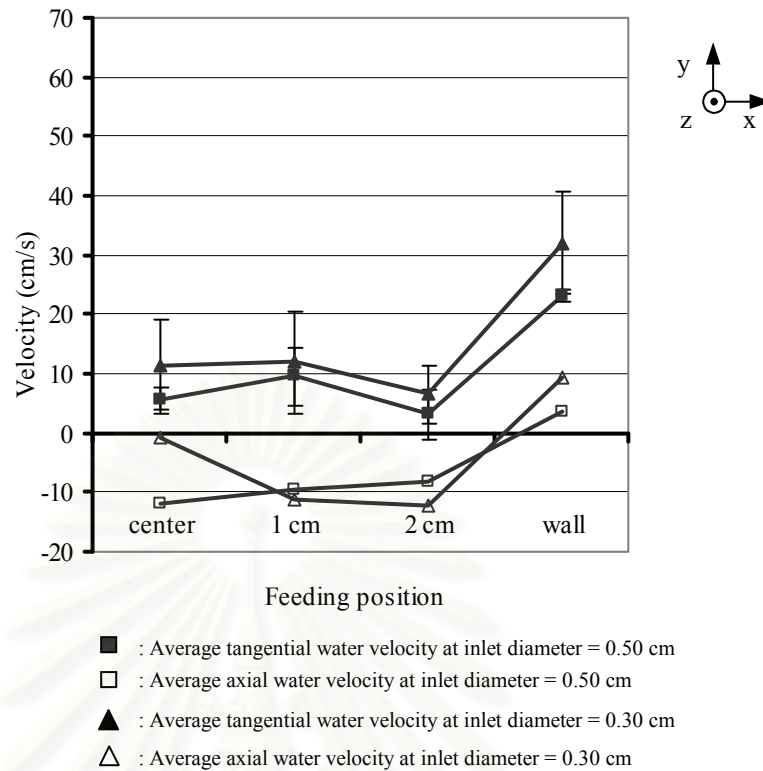


Figure IV-8. Tangential and axial water velocity at different studied points in HC3, which was operated at a constant water flow rate (200 l/hr) and with different inlet diameters (0.30 and 0.50 cm).

Regardless of the water inlet diameters, it was observed in Figure IV-8 that the tangential velocity variations along the x axis were the same. Tangential velocity increases gradually from the center (8 cm/s) to the wall of the hydrocyclone (27 cm/s).

The axial water velocity was always found to be negative in the center of the hydrocyclone ($0 < x < 2$ cm) and positive at the wall. Its average value at the center was -8 cm/s (where it moved in a downward direction), and it increased to 6 cm/s at the wall of hydrocyclone (where it moved in an upward direction).

In conclusion, the highest tangential velocity values in HC3 were obtained at a water flow rate equal to 200 l/hr and with an inlet diameter equal to 0.3 cm.

1.4 Comparison of tangential velocity for the different hydrocyclones: HC1, HC2, and HC3

In this part, a comparison of the tangential velocity under the different operating conditions is presented for the different hydrocyclones.

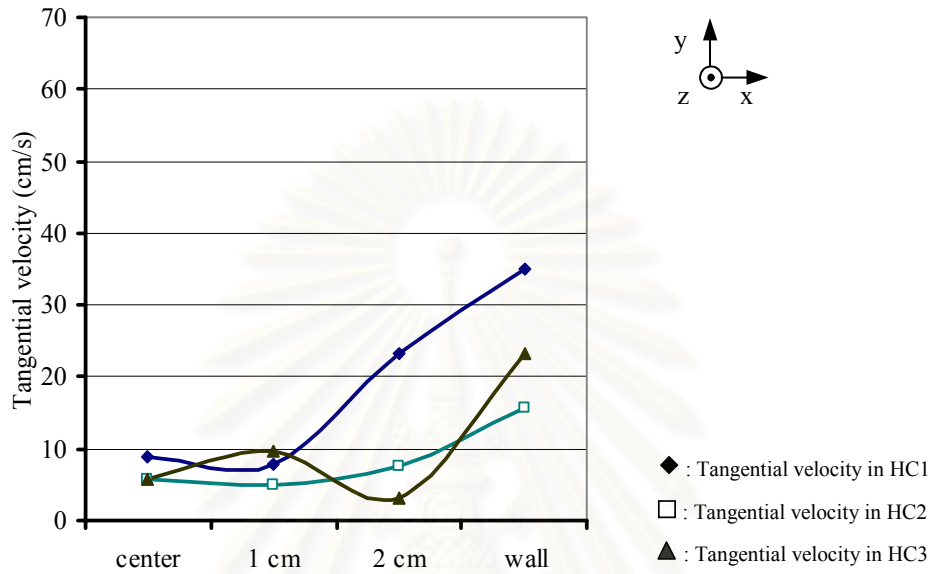


Figure IV-9. The tangential velocities values obtained for the three hydrocyclones (HC1, HC2, and HC3) with an inlet injection diameter of 0.5 cm and a water flow rate of 200 l/hr.

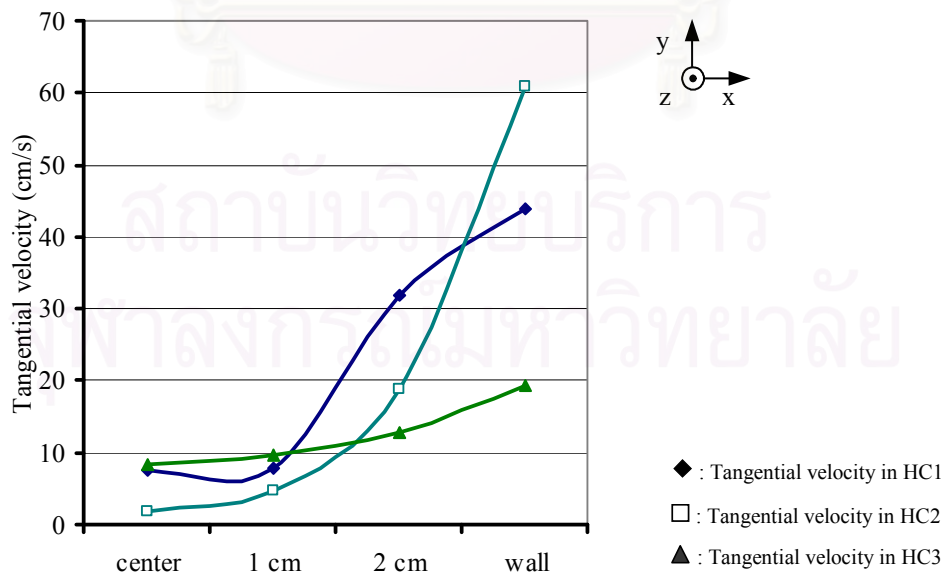


Figure IV-10. Tangential water velocity at the studied points in HC1, HC2, and HC3 at a water flow rate of 400 l/hr and an inlet diameter of 0.50 cm.

It can be observed from the Figure IV-9 and Figure IV-10 that under all operating conditions, the tangential velocity in the internal zone was not affected much by the hydrocyclone type.

The highest tangential velocity was observed in HC1 within the wall zone at the low water flow rate. In addition, this value was two times higher than the tangential velocity in HC2 at the same location and under the same conditions.

At the highest water flow rate, 400 l/hr, the tangential velocity at the wall zone of HC2 was higher than that of HC3 and HC1.

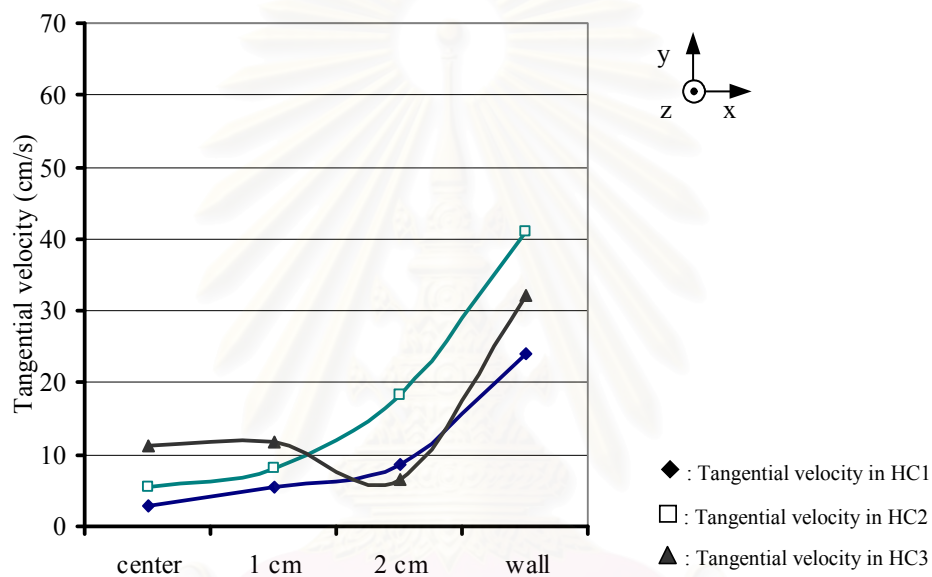


Figure IV-11. The tangential velocity values of the three hydrocyclones (HC1, HC2, and HC3), which were operated at a water flow rate equal to 200 l/hr and with a water inlet diameter equal to 0.30 cm.

สถาบันวิทยบริการ
จุฬาลงกรณ์มหาวิทยาลัย

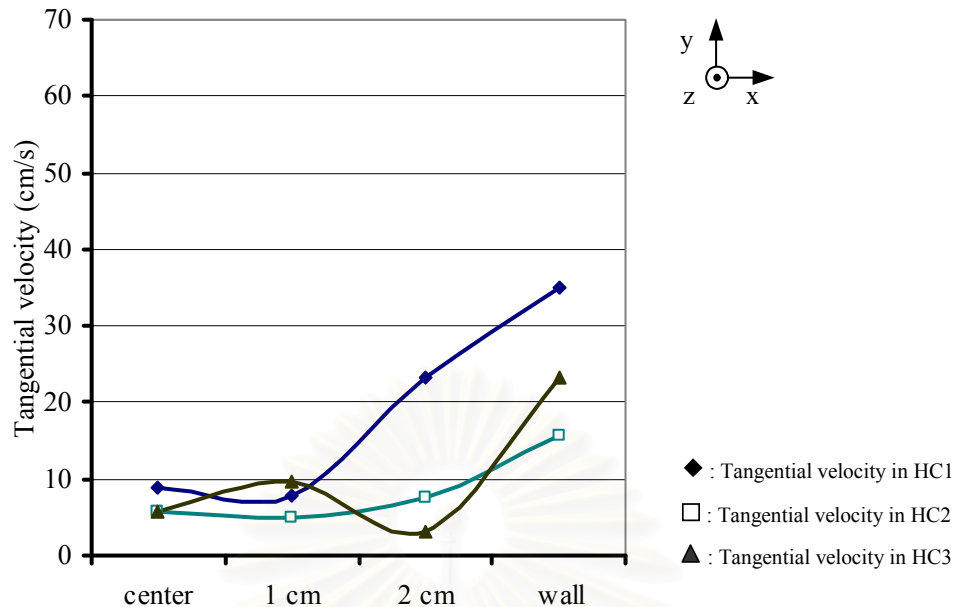


Figure IV-12. Tangential water velocity at the studied points in HC1, HC2, and HC3, which were operated with an inlet diameter equal to 0.50 cm and at a water flow rate equal to 200 l/hr

It can be observed from Figure IV-11 and Figure IV-12 that the internal zone was slightly influenced by the hydrocyclone's geometry when the smaller water inlet diameter (0.30 cm) was used. The velocity was highest in HC3. On the other hand, when the larger inlet diameter (0.50 cm) was used, there was no significant difference in the results among the different hydrocyclones.

The highest velocities were observed in HC2 at the wall zone when the small inlet diameter was used. When the inlet diameter was increased, the highest values were observed in hydrocyclone HC1.

In addition, the comparison between HC1 and HC3 highlights the influence of the modification of the diameter at half height in HC1: this parameter had no significant effect on the tangential velocity values at the internal zone and near the wall.

1.5 Prediction of tangential velocity (V_z) versus the radius (R)

In the previous part, the experimental evolutions of tangential velocity have been described; now experimental correlations will be proposed for each hydrocyclone in order to predict tangential velocity (V_z) versus the radius (R).

Due to the different flow streams in the hybrid process, the water flow rate was comparatively much lower than the flow rate in a classical hydrocyclone. Therefore, the classical relation proposed by Bradley to model the tangential water velocity versus the radius (R) could not be used. In Bradley's equation, the tangential water velocity in the external vortex decreases when the radius increases. In this study, the tangential velocity increased as the radius increased. A relation in power was tested to describe the experimental evolution observed between tangential velocity and the radius:

$$V_z = K.R^n$$

The values of K and n are deduced from the following linearization:

$$\text{LN}(V_z) = \text{LN}(K) + n \cdot \text{LN}(R)$$

Where n is the slope of the straight line, LN, (K) is the constant value obtained when radius of hydrocyclone (R) equals zero.

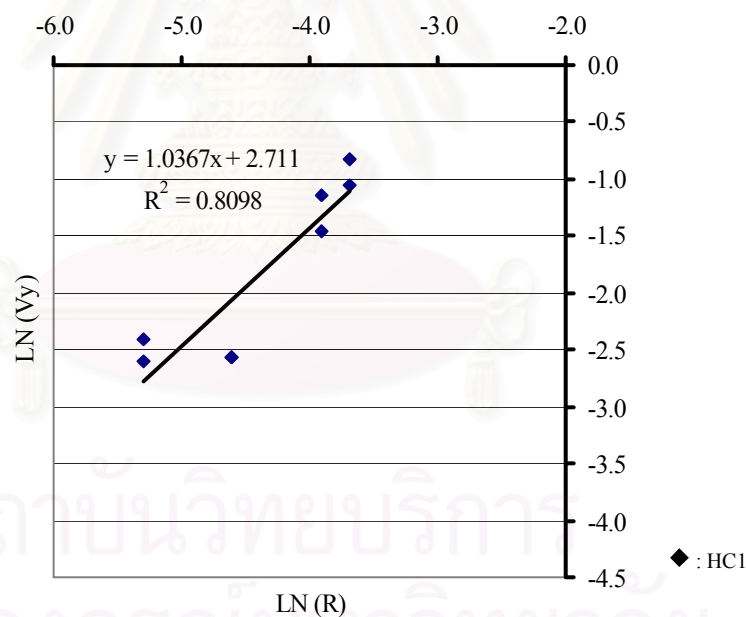


Figure IV-13. Linear regression used to determine the relation between the tangential velocity, V_z , and the radius, R , for HC1 with an inlet diameter of 0.50 cm

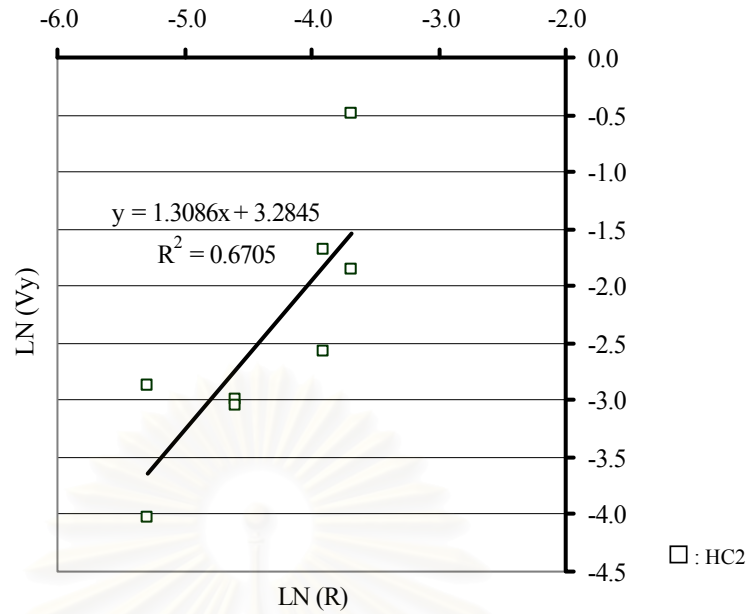


Figure IV-14. Linear regression used to determine the relation between the tangential velocity, V_z , and the radius, R , for HC2 with an inlet diameter of 0.50 cm

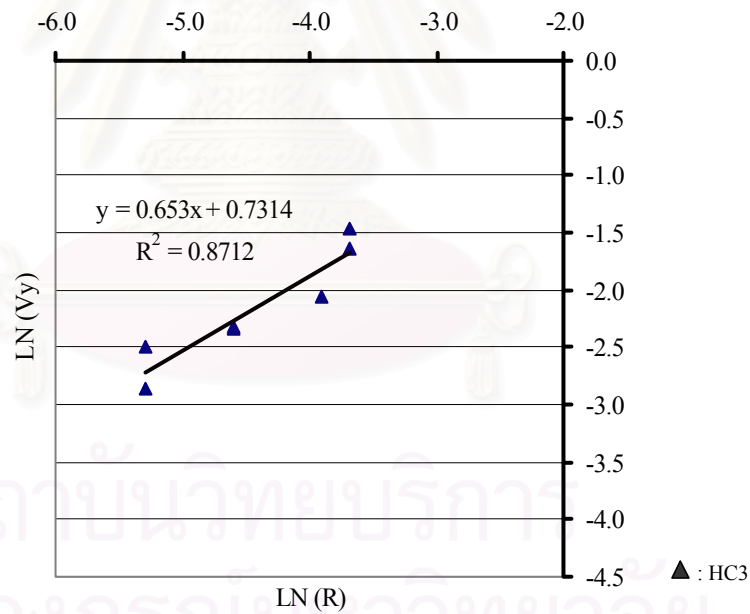


Figure IV-15. Linear regression used to determine the relation between the tangential velocity, V_z , and the radius, R , for HC3 with a constant inlet diameter of 0.50 cm.

Figure IV-13 to Figure IV-15 reports the linear regression that was used to determine the relation between the tangential velocity, V_z , and the radius, R , for HC1, HC2, and HC3, respectively, with a constant inlet diameter of 0.50 cm.

The resulting relations are presented in Table IV-4. They were used to predict the velocity gradients in each hydrocyclone in the following part.

Table IV-4. Relations between the tangential velocity, V_z , and the radius, R , with a constant inlet diameter of 0.50 cm

Type of hydrocyclone	n	K	Correlations
HC1	1.0	15	$V_z = 15.R$
HC2	1.3	26	$V_z = 26.R^{1.3}$
HC3	0.6	2	$V_z = 2.R^{0.6}$

1.6 Discussion and conclusions on the velocity field for the hybrid process

In all hydrocyclone types, the tangential velocities at the wall zone were higher than those measured at the center, particularly in the conical hydrocyclone. These results are similar to the velocity profiles presented by Jonas and Hannes, (2004). They used a pitometer to characterize flows inside a cylindrical hydrocyclone with three tangential inlet holes of 10 mm in diameter. In addition, Jonas et al., (2007) studied the measurement of tangential velocity flow in a 65 mm down flow conical hydrocyclone using the same method. The results of both studies show that the tangential velocity increased from the center to the wall of the hydrocyclone, which concurs with the results of this study.

In the different diameter cylindrical hydrocyclone, HC1, and conical hydrocyclone, HC2, the tangential velocities at the high water flow rate, 400 l/hr, were significantly higher than those produced at low water flow rate, 200 l/hr. However, in the constant cylindrical hydrocyclone, HC3, they did not differ significantly. Considering that the change of the water flow rate from 200 l/hr to 400 l/hr involves an increase of the kinetic energy by a factor 4, the tangential velocity in HC3 increased when the inlet diameter was reduced.

The highest tangential velocities were observed in the conical hydrocyclone, HC2, within the wall zone at the high flow rate (400 l/hr). This result shows that the conical configuration of HC2 is the best configuration to induce high tangential velocities; this means it generates a good external vortex.

In the internal zone of the hydrocyclone, the hydrocyclone configuration had no significant influence on the axial velocity.

Finally, the experimental results have demonstrated that there are two ways to increase the tangential velocity in different cylindrical and conical hydrocyclones: to reduce the water inlet diameter or to increase the water flow rate.

1.7 Tangential velocity gradient

In this section, the experimental tangential velocity gradients were calculated from the experimental tangential velocity using Equation III-12 presented in the previous chapter. Results are given for all types of hydrocyclones as a function of the positions inside the hydrocyclone (x-axis) (i.e., at the center, 1 cm from the center, 2 cm from the center, and at the wall of hydrocyclone).

1.7.1 Different diameter cylindrical hydrocyclone HC1

The results are provided in two sections: (1) the effects of water flow rate and (2) the effects of the water inlet diameter.

1.7.1.1 Effects of the water flow rate

The experiments were operated with a constant water inlet diameter of 0.50 cm, while the water flow rates were varied at 200 and 400 l/hr. The obtained results are presented in Figure IV-16.

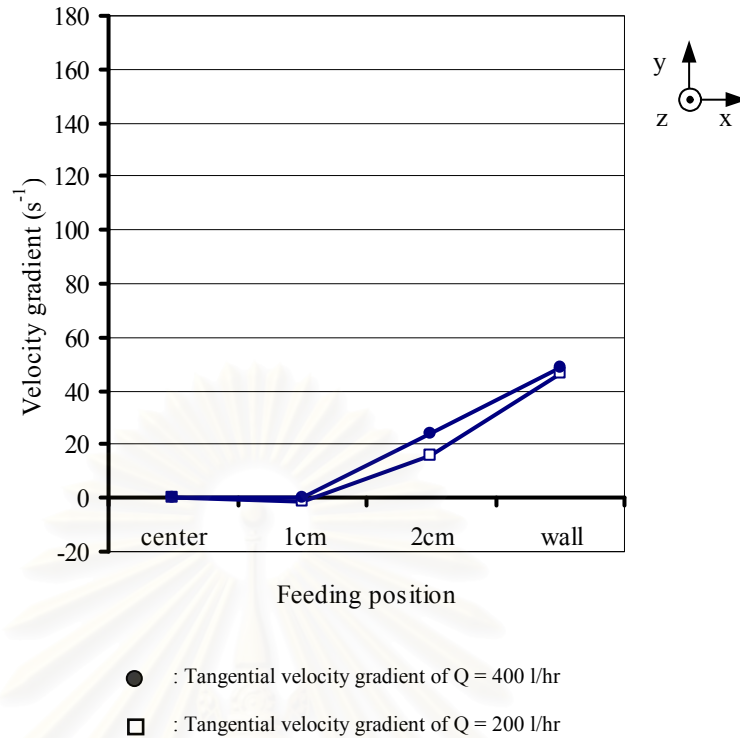


Figure IV-16. Average tangential velocity gradients in HC1 at different flow rates, 200 and 400 l/hr, and with a constant inlet diameter (0.5 cm).

As can be seen in Figure IV-16, the tangential velocity gradient in the internal zone ($0 \leq x \leq 1$ cm) was equal to zero at both the water flow rates. This gradient increased to 48 s^{-1} close to the wall of the hydrocyclone. This result indicated that the external shear force was stronger than the internal shear and the velocity gradient was not significantly affected by the water flow rates.

1.7.1.2 Effects of the water inlet diameter

The experiments were performed at a constant water flow rate of 200 l/hr and the water inlet diameters were varied at 0.30 and 0.50 cm. The obtained results are presented in Figure IV-17.

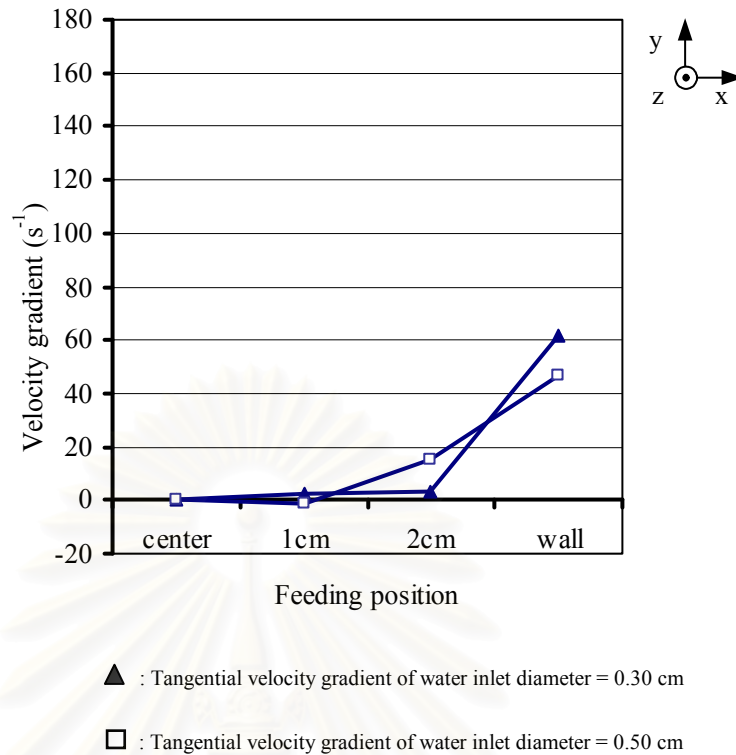


Figure IV-17. Average tangential velocity gradients in HC1, which was operated using different inlet diameters (0.3 and 0.5 cm) and at a constant flow rate of 200 l/hr.

As seen in Figure IV-17, the tangential velocity gradient at the wall zone of the hydrocyclone was greater than the gradient at the center of the hydrocyclone. This observation emphasizes that the shear force in the external zone was greater than the shear force in the internal zone. In this figure, the average tangential velocity gradient in the internal zone equaled to zero and it increased to 55 s^{-1} (by average) at the wall zone of hydrocyclone.

In HC1, the velocity gradient was not significantly affected by the water inlet diameter. Similar to the effect of the water flow rate, a modification of the tangential velocity induced by the reduction of the inlet section did not significantly affect the tangential velocity gradient.

These results are surprising because the tangential velocity in HC1 is in power one versus the radius as presented in Table IV-4. In fact, in this case, the tangential velocity gradient, which is equal to the variation of V_z with (R) , should have been constant.

Moreover, twice the water flow produced twice the tangential velocity at all radiuses, so the corresponding gradient should increase when the flow rate increases.

The relation proposed to predict the tangential velocity gradient variation versus (R) is an average relation, which could not accurately describe the velocity variations necessary to calculate the velocity gradient with good accuracy. Moreover the standard deviation associated to each tangential velocity led to a very important error in the velocity gradient value. So, these values should be taken into account as qualitative values and not as quantitative values.

1.7.2 Conical hydrocyclone HC2

In the conical hydrocyclone, the results of the velocity gradients were divided into two sections which were (1) the effect of water flow rate and (2) the effect of the water inlet diameter.

1.7.2.1 Effects of the water flow rate

The experiments were operated using a constant water inlet diameter of 0.50 cm, and the water flow rates were varied at 200 and 400 l/hr. The obtained results are presented in Figure IV-18 .

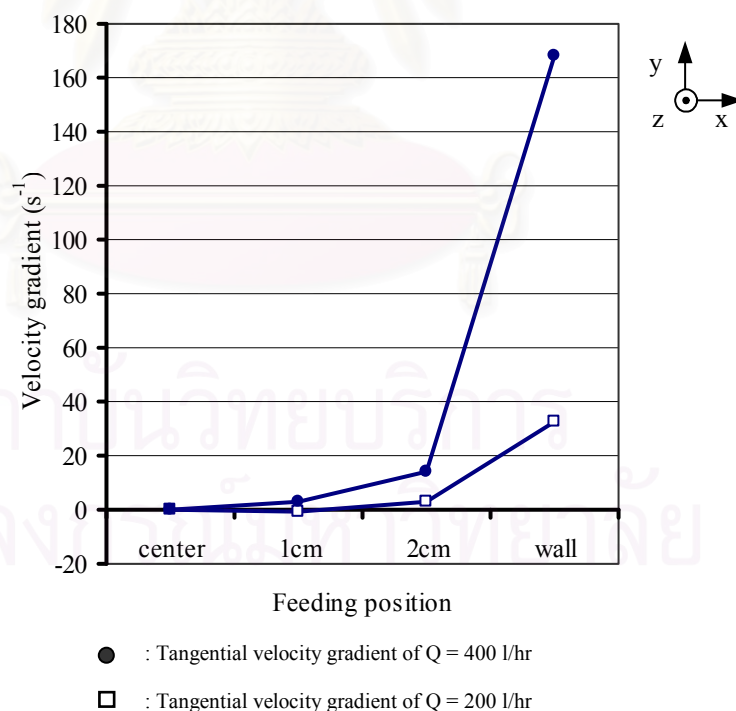


Figure IV-18. Average tangential velocity gradients in HC2, which was operated at different flow rates, 200 and 400 l/hr, with a constant inlet diameter (0.50 cm).

As can be seen in Figure IV-18, tangential velocity gradients are strongly influenced by the water flow rate, particularly at the wall zone of the hydrocyclone.

In the internal zone, the tangential velocity gradient values from both operating conditions nearly pointed to zero. In the external zone, however, they were markedly different at 164 and 32 s^{-1} for the water flow rates of 400 and 200 l/hr, respectively. From this result, it could be concluded for HC2 that the velocity gradient of the high water flow rate was stronger than velocity gradient of the low water flow rate, as was expected theoretically.

For HC2 the tangential velocity is in power 1.3 versus the radius, the tangential velocity gradient should increase with (R) as it is observed in Figure IV-18.

1.7.2.2 Effects of the inlet diameter

The experiments were operated at a constant water flow rate of 200 l/hr and the water inlet diameters were varied at 0.30 and 0.50 cm. The obtained results are presented in Figure IV-19.

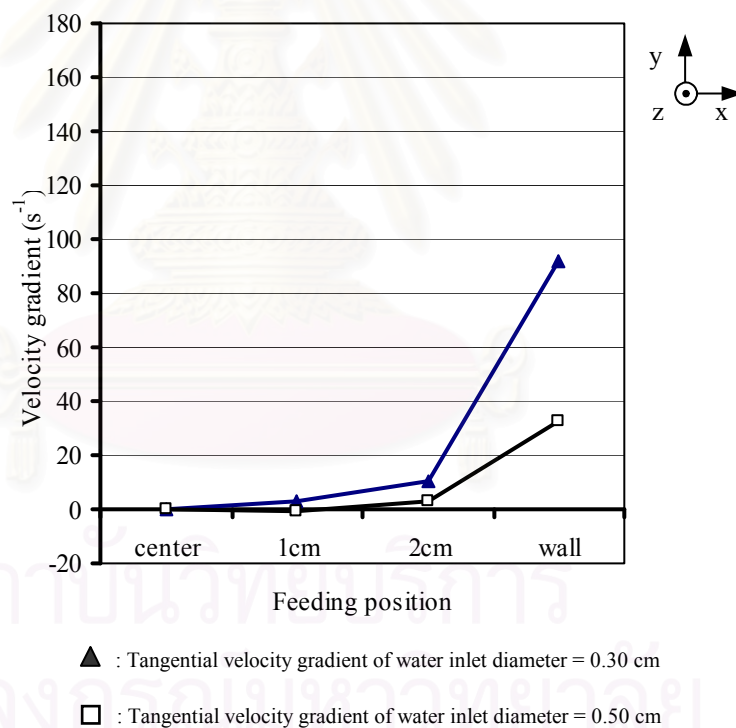


Figure IV-19. Average tangential velocity gradients in HC2, which was operated with different inlet diameters (0.30 to 0.50 cm) and at a constant flow rate of 200 l/hr.

As seen in Figure IV-19, the tangential velocity gradient increased at the wall zone of the hydrocyclone, this means that the shear force in the external zone was greater than the shear force in the internal zone. The average tangential velocity

gradients in the internal zone at both water inlet diameters were equal to zero, but these values increased up 32 s^{-1} and 92 s^{-1} at the wall of hydrocyclone.

However, in this hydrocyclone, the tangential velocity gradient of the smaller water inlet was significantly greater than the tangential velocity gradient of the larger water inlet. This indicated that the small water inlet was able to create a stronger shear force in the conical hydrocyclone. This observation was also made in HC2 by the corresponding variation of the tangential velocity versus radius which was in power of 1.3.

1.7.3 Constant diameter cylindrical hydrocyclone, HC3

The results for this 5 cm-constant diameter cylindrical hydrocyclone were divided into two sections: (1) the effects of water flow rate and (2) the effects of the water inlet diameter.

1.7.3.1 Effects of the water flow rate

The experiments were operated at a constant water inlet diameter of 0.50 cm and the water flow rates were varied at 200 and 400 l/hr. The obtained results are presented in Figure IV-20.

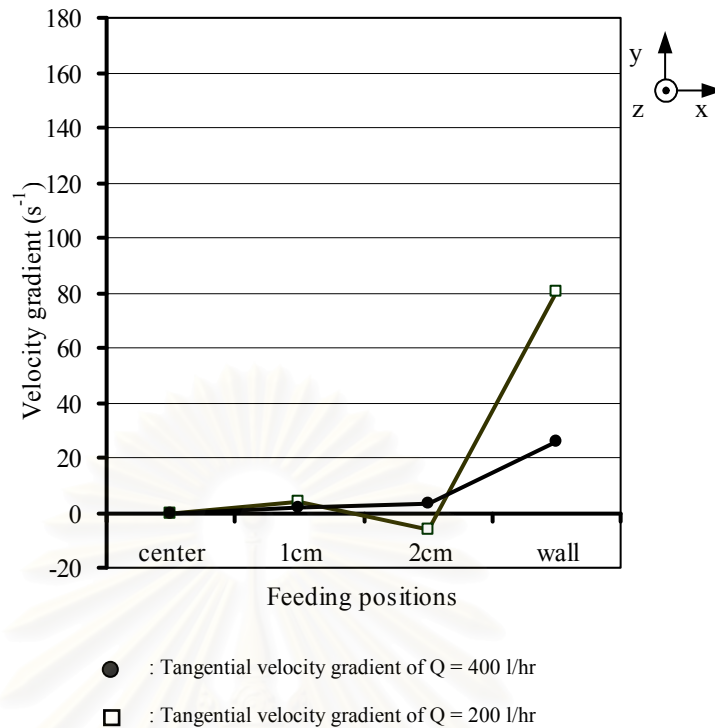


Figure IV-20. Average tangential velocity gradients in HC3, which was operated at different flow rates, 200 and 400 l/hr, and with a constant inlet diameter, 0.50 cm.

It can be observed that at both flow rates, the velocity gradient was equal to zero except at the wall zone of the hydrocyclone. In this zone, the velocity gradient was more significant. If the relation reported in Table IV-4 for the prediction of tangential velocity in HC3 were applied (a power 0.6 relation), the corresponding velocity gradient should have decreased with the radius. However, the calculated velocity gradients reported in Figure IV-20 show the contrary. The average correlation of tangential velocity to comment the Figure IV-21, must be used with caution. In fact the relation proposed to predict the tangential velocity gradient variation versus radius (R) is an average relation which cannot perfectly describe the velocity variations necessary to calculate the velocity gradient with good accuracy.

Moreover, the standard deviation associated to each tangential velocity leads to an error in the velocity gradient value. Therefore, these values should be taken into account as qualitative values and not as quantitative values.

1.7.3.2 Effects of the inlet diameter

The experiments were operated at a constant water flow rate of 200 l/hr and the water inlet diameters were varied at 0.30 and 0.50 cm. The obtained results are presented in Figure IV-21.

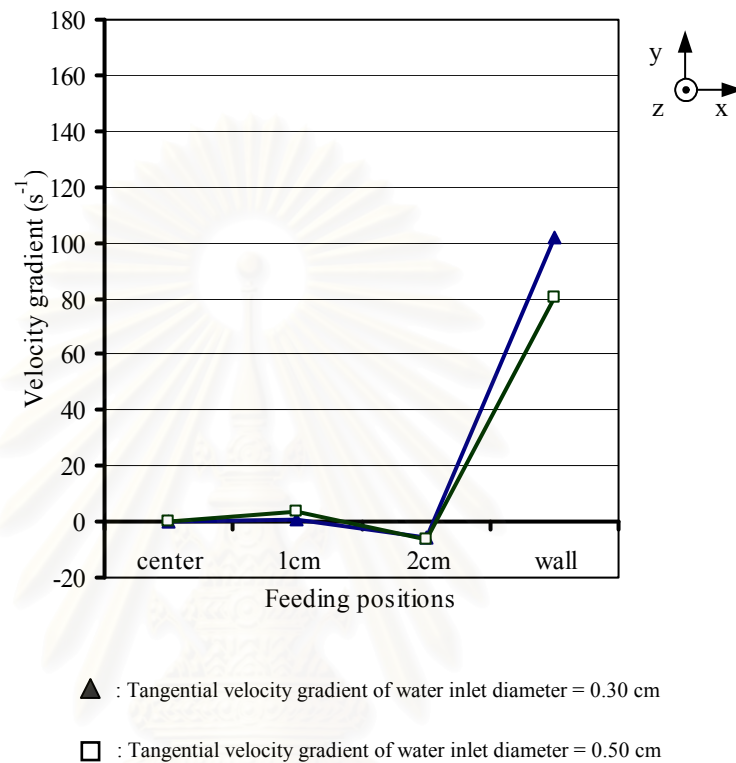


Figure IV-21. Average tangential velocity gradients in HC3 at two water inlet diameters, 0.30 and 0.50 cm.

From Figure IV-21, it can be seen that the tangential velocity gradient increased at the wall zone of the hydrocyclone. This showed that the shear force in the external zone was greater than the shear force in the internal zone. The average tangential velocity gradients in the internal zone when both water inlets were used were equal to zero, and these values increased to 80 s⁻¹ or 100 s⁻¹ at the wall zone of hydrocyclone.

However, in this hydrocyclone, the tangential velocity gradient of the smaller water inlet was greater than the tangential velocity gradient of the larger water inlet. This indicated that the small water inlet was able to create a stronger shear force in this cylindrical hydrocyclone.

1.7.4 Comparison of the different hydrocyclone configurations

Like for the experimental results for tangential and axial velocity, it is interesting to compare the experimental tangential velocity gradient values of the different hydrocyclones. The following graphs in Figure IV-22 to Figure IV-24 give the velocity gradients under the different operating conditions:

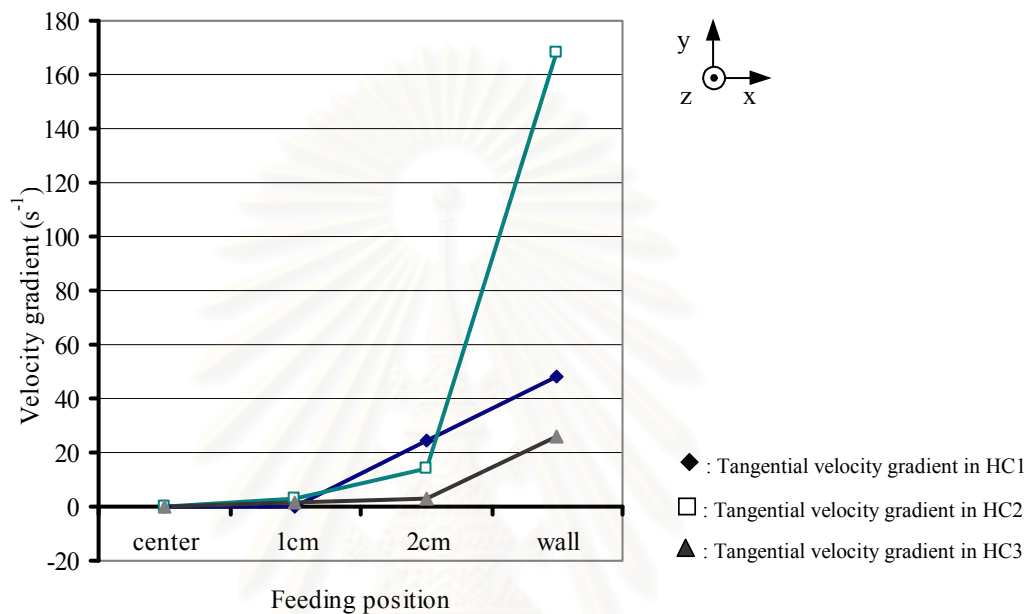


Figure IV-22. Average tangential velocity gradients for HC1, HC2, and HC3 at a constant inlet diameter of 0.50 cm and a constant liquid flow of 400 l/hr.

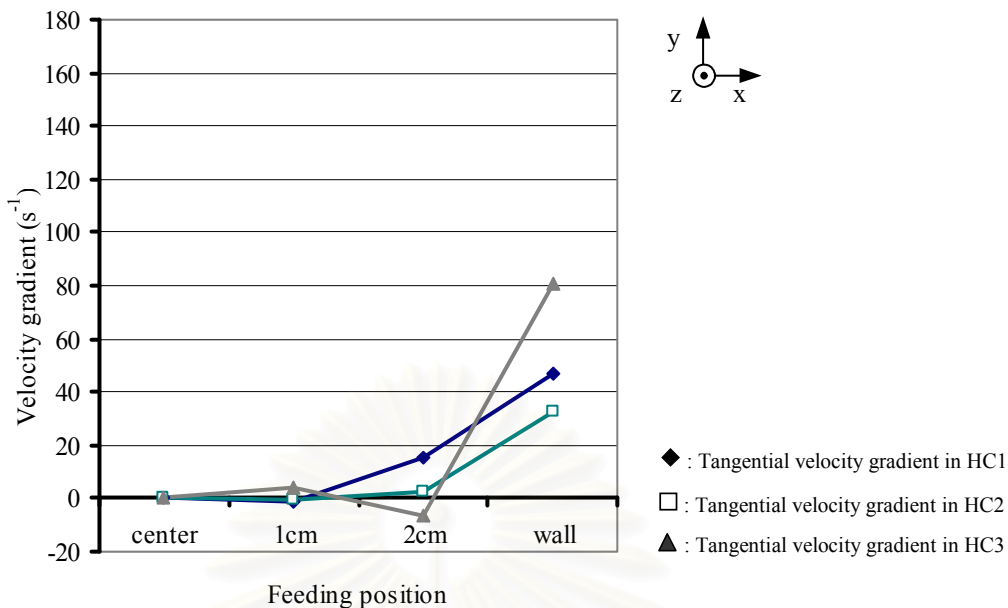


Figure IV-23. Average tangential velocity gradients for HC1, HC2, and HC3 at a constant inlet diameter of 0.50 cm for a constant water flow of 200 l/hr.

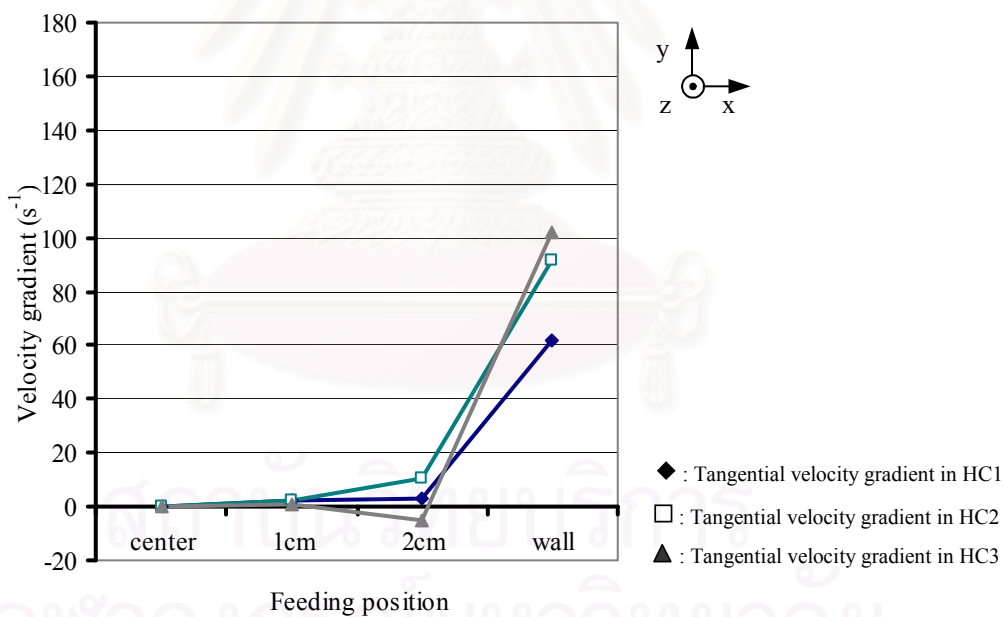


Figure IV-24. Average tangential velocity gradients for HC1, HC2, and HC3 at a constant inlet diameter of 0.30 cm and a constant water flow of 200 l/hr.

At the high water flow rate (400 l/hr), the velocity gradient was different from zero in the external circular section (between 2 cm and the wall). At the wall, the highest value was observed in the conical hydrocyclone, HC2

At the low water flow rate (200 l/hr), the velocity gradient was different from zero at the wall of the hydrocyclone. Furthermore, at both inlet diameters, the trends were the same: the velocity gradient was highest in HC3, followed by HC1, and finally HC2.

HC2, which was the biggest hydrocyclone, needed a higher flow rate to achieve a stable vortex. Moreover the standard deviation associated with each tangential velocity led to an error in the velocity gradient value. So these values should be taken into account as qualitative values and not as quantitative values. Nevertheless, it can be assumed that regardless of the operating conditions, the tangential velocity gradient is greater in the wall zone than in the internal zone of hydrocyclone.

1.7.5 Tangential velocity gradient modeling

In this section the previous results will be discussed with others expressions of velocity gradients that have been presented in the previous chapter.

Table IV-5. The average calculated and predicted velocity gradients at the constant water inlet diameter of 0.5 cm.

Velocity gradient, G, (s ⁻¹)	Q _i = 200 l/hr			Q _i = 400 l/hr		
	HC1	HC2	HC3	HC1	HC2	HC3
G experimental, (s ⁻¹)	48	32	80	48	164	27
G correlation, (s ⁻¹)	15	11	5	15	11	5
G Bradley modify, (s ⁻¹)	47	61	28	93	121	56
G power, (s ⁻¹)	213	164	315	397	306	588

The following comments can be made:

- The experimental gradient was in the range of the gradient calculated from Bradley modification. In contrast, the values coming from the mean gradient for dissipating energy were 10 times higher than the experimental ones. The gradient calculated from the tangential velocity correlations underestimated the actual value.

- The influence of the flow rate can be observed in the calculated gradient from Bradley modification which was contrary to the experimental observations.

- With this comparison of the different gradient values, it appears difficult to use the existing models for G calculation; the complexity of the hydrocyclones in this study and the empirical parameters of the existing correlation made it difficult to use them to determine the velocity gradient with good accuracy.

1.7.6 Experimental velocity gradient conclusions

As expected from the literature, the experimental results demonstrate that the tangential velocity gradient at the internal zone is lower than that of the external zone of a hydrocyclone, regardless of hydrocyclone type. The mixing intensity of the external zone is also higher than that of the internal zone.

The effects of the water flow rate and the water inlet diameter depend on the hydrocyclone's configuration. The influence was more significant for conical and cylindrical hydrocyclones: when the flow rate increased or the inlet diameter decreased, the velocity gradient increased at the hydrocyclone wall zone. Finally the highest value was observed in HC2 at a flow rate equal to 400 l/hr and an inlet diameter equal to 0.50 cm.

1.8 Hydrodynamic characterization study

A very simple method was developed in this study to compare the hydrodynamics in the different hydrocyclone configurations. This method was used to quantify the direction of the flow in the center area of the hydrocyclone, the value of tangential and axial velocities as a function of the radial position in the hydrocyclone, and the tangential velocity gradient near the wall of the hydrocyclone.

All these characterizations were made in the cross sections of the hydrocyclones corresponding to the location of the main inflow ports in the hydrocyclone (i.e., where the coagulant and raw water was injected). Microbubbles were created at a few centimeters lower than the main inflow ports in the hydrocyclone either in the internal zone or near the wall.

The following requirements are necessary for the hybrid process to be successful:

- A high velocity gradient in the area where contact between the coagulant and particles occurs, i.e. near the wall of the hydrocyclone.
- An absence of downward flow at the center of the hydrocyclone, which induces an accumulation of bubbles in the area and in so doing causes them to coalesce. The results of axial direction of water in hydrocyclone were presented in Table IV-1 to Table IV-3.
- Optimal tangential velocity which relate to the centrifugal force in the hydrocyclone as presented in Table I-2 which is needed to create a strong vortex. In addition, this important velocity may increase the accumulation of bubbles in the vortex center before they come in contact with the microflocs.

These different points will be discussed relating with the performance of the hybrid process in the following section.

Part 2 The hybrid process study

In this section, the experimental results of the hybrid process study are presented. The experiments were performed in four types of hydrocyclones to find out the optimum operating conditions for the hybrid process. The different experimental parameters such as the shape and geometry of the hydrocyclones, raw water flow rates, and raw water inlet diameters were tested. The experimental results of the hybrid process study were divided into three sections:

The main objectives of hybrid process

- (1) The main objectives of the hybrid process
- (2) The effects of the important parameters on floating floc production
- (3) The effects of the important parameters on separation efficiency

2.1 The main objective of the hybrid process

The main objective of the hybrid process was to separate the solid particles from water; this was described clearly in Chapter II: Bibliography (see Figure II-23). Coagulation and flocculation processes were integrated in hydrocyclone reactors and controlled by the strength of the vortex flow. These processes were performed in the lower part of the hydrocyclones at a high turbulent flow. In the upper part, the separation was expected to occur in the core and upper parts of the hydrocyclones.

The hybrid process requires the production of aerated flocs which contained the abundant air microbubbles in the structures. The advantage of these flocs is that their densities are lower than that of water. Therefore, they are deduced to the core of a hydrocyclone by vortex from the upper part of the hydrocyclone. Following this, the solid particles are separated from the raw water and the turbidity is then removed.

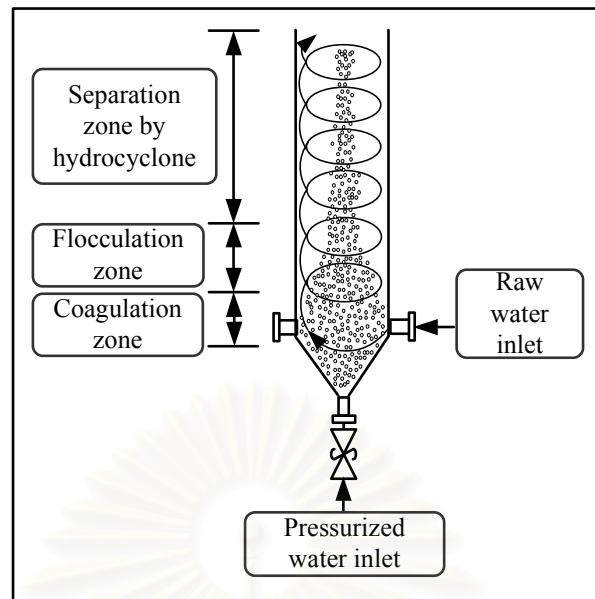


Figure II-23. The expected phenomena of the hybrid process.

Two parameters were used to indicate the working status of the hybrid process: (1) the percentage of floating flocs and (2) separation efficiency.

1. The percentage of the floating and settled flocs

This parameter was used to indicate the success of the coagulation and flocculation processes. To calculate it, the height of the floating floc was divided by height summation of the floating and settled flocs.

The continuous experiment ended by halting all flow rates. There were two desired results with regard to the flocs in the reactor:

- a. A high amount of light flocs, abundant of microbubbles, floating at the top of the reactor as presented in Figure IV-25 and Figure IV-26.
- b. A low amount of heavy flocs, without air bubbles in their structures, at the bottom of the hydrocyclone.



Figure IV-25. The photos of the floating floc at the top of hydrocyclone

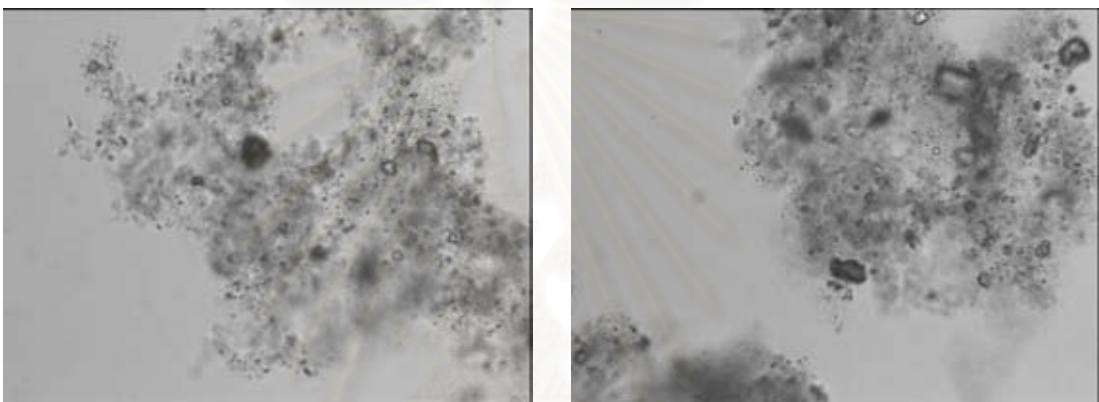


Figure IV-26. The photos of the microbubbles inside the floating flocs which taken by the microscope.

2. The separation efficiency

The separation efficiency percentage was determined by the measurements of the difference of suspended solid concentration and turbidity at the center and wall zones of each reactor during the continuous experiment. It was used to indicate the success of the entire processes: coagulation, flocculation, and separation in the hybrid process reactor. These results correlated to the separation line observation (an apparent line of flocs) in the core-upper part of the hydrocyclone as presented in the Figure IV-27.



Figure IV-27. Separation lines in the hydrocyclone (HC3)

Therefore, the experimental targets of this experiment were to find out the optimal operating conditions for a high percentage of floating floc and high separation efficiency percentage. In order to achieve these results, many parameters needed to be optimized such as the air fraction in the hydrocyclone, the coagulant concentration, the raw water flow rate, and the water inlet diameter.

2.2 The effects of important parameters on floating floc production

In this part, the effluence parameters on the floating floc production were divided into four parts which were (1) the hydrodynamics (2) the air fraction (3) the coagulant concentration (4) the position of pressurized water injection. The experimental results of these parameters were described.

2.2.1 Influence of hydrodynamics on the floating floc production.

In this section, the hydrodynamics results from the previous part were used to explain the production of floating floc and the observed phenomena in the hybrid process reactor such as the coalesced bubbles.

The coalescence of micro air bubbles was observed at the lower part of hydrocyclone during the experiment of hybrid process. The characterization and mechanisms of bubble coalescence were described.

Bubble coalescence

Regarding the hybrid process objective, the production of aerated flocs is very important to the hybrid process because they contain an abundance of microbubbles in

their structures. During the experiment, microbubbles were injected into the hydrocyclone at the bottom, and they were expected to combine with the bentonite particles and coagulant under high turbulent conditions to form aerated floc.

However, a coalescence of air bubbles was found at the lower part under some operating conditions during the continuous experiment; the injected microbubbles coalesced to form big air bubbles. The aerated floc could not be created because the injected microbubbles did not enter the floc structures. These results were unsatisfactory for the hybrid process.

Table IV-6 gives the experimental results of the conical hydrocyclone HC2 and cylindrical hydrocyclone HC3 that provide a better picture on the influence of hydrocyclone hydrodynamics on bubble coalescence. In these experiments, the raw water flow rate was maintained at 400 l/hr, the air fraction was 0.0045, the raw water inlet diameter was 0.50 cm, and the coagulant concentration was 1.0 mg/l. Both the coalescence observations and percentages of floating flocs are presented in the table along with conclusions from the hydrodynamic characterization study.

Table IV-6. Production of floating floc and hydrodynamic result for HC2 and HC3.

(Note: The operating condition: $Q = 400$ l/hr, $D_i = 0.50$ cm, $C_c = 1.0$ mg/l, $P_t = 3.5$ bars, and $Q_p = 40$ l/hr)

Parameters	HC2	HC3
Coalesced bubbles	Yes	Yes, a little bit
Coalesced bubbles size (d_a)	3-5 mm	2-3 mm
Axial water direction	Same direction (Downward)	
Tangential velocity and tangential velocity gradient	HC2 > HC3 (see Figure IV-10 and Figure IV-22)	
Percentage of floating floc	0	22 %

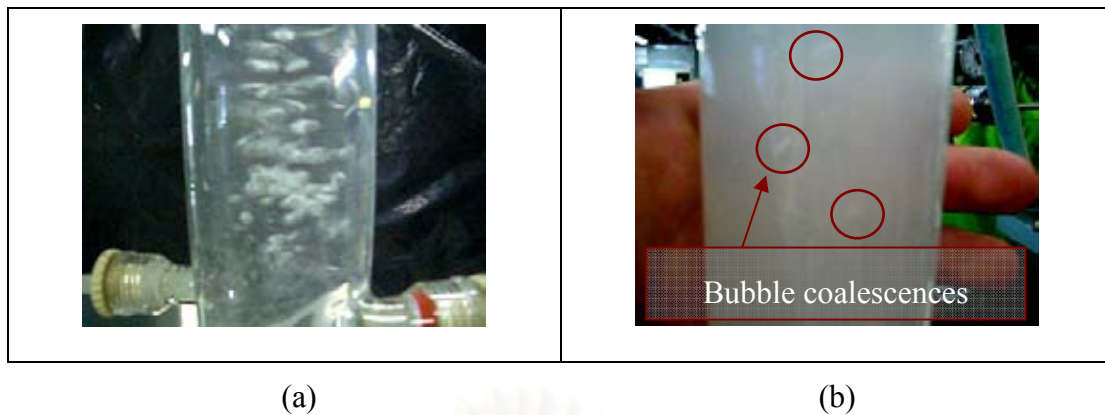


Figure IV-28. The coalescence of bubbles in (a) HC2 and (b) HC3

From Table IV-6 and

Figure IV-28, it can be seen that coalesced bubbles were observed in all hydrocyclones; however, it can be seen that the amount and sizes of coalesced bubbles in HC2 were higher and bigger than those of HC3. These results could be explained by the higher tangential velocity in HC2, which induced the injected microbubbles to the center of the hydrocyclone where bubble coalescence consequently occurred. This directly affected the percentages of floating floc in HC2 and HC3, which were 0 and 22 %, respectively, as injected microbubbles were not used to create the aerated floc in HC2.

2.2.2 The effects of axial velocity on bubble coalescence

This section presents the experimental results that show the effects of axial velocity on the examined parameters of observed bubble coalescence and the percentage of floating floc. This study was performed in all hydrocyclone geometries by using two raw water inlet diameters, 0.30 and 0.50 cm.

2.2.2.1 The experimental results of HC1

A summary of the experimental results of HC1 used with raw water flow rates of 200 to 400 l/hr are presented in Table IV-7. The coagulant concentration was 1.0 mg/l and the total pressure was maintained at 3.5 bars. Since the velocity gradient remained the same under these conditions, the influence of axial velocity can be discussed.

Table IV-7. A comparison of the hydrodynamics results of the different raw water inlet diameters for HC1.

(Note: The operating condition: $Q = 200-400$ l/hr, $C_c = 1.0$ mg/l, $P_1 = 3.5$ bars, and $Q_p = 36$ l/hr)

Parameter	Raw water inlet diameter (cm)	
	0.50	0.30
Percentage of floating floc (%)	$\neq 0$	0
Bubbles coalescences	No coalescence	Yes
Axial velocity at the center of hydrocyclone	Downward direction, $ V_{0.50} < V_{0.30} $	
Velocity gradient	Identical values	

From Table IV-7, it could be observed that coalesced bubbles occurred when the small raw water inlet, 0.30 cm, was used. Moreover, the axial velocities at the center of the hydrocyclone produced a downward flow (negative value), and the axial velocity value when the small inlet diameter, 0.30 cm, was used was higher than that of the big inlet diameter, 0.50 cm (see Figure IV-4). These results show that a high axial velocity may decrease the opportunity for microbubbles to rise and increase the coalescence of microbubbles in the center of a hydrocyclone. Therefore, this result gave an unsatisfactory floating floc percentage.

2.2.2.2 The experimental results of HC2

1. In this section, the experimental results of HC2 are presented; the experiment was performed using the same operating conditions as in section 2.2.2.1.

Table IV-8. A comparison of the hydrodynamics results of the different raw water inlet diameters for HC2.

(Note: The operating condition: $Q = 200-400$ l/hr, $C_c = 1.0$ mg/l, $P_t = 3.5$ bars, and $Q_p = 36$ l/hr)

Parameter	Raw water inlet diameter (cm)	
	0.50	0.30
Percentage of floating floc	Yes, a little bit	No, not at all
Coalescence of bubbles	No, except at $Q = 300$ and 400 l/hr	Yes, for all raw water flow rates
Axial velocity at the center of the hydrocyclone	Downward direction, $ V_{0.50} < V_{0.30} $	
Tangential velocity gradient	$G_{0.30} > G_{0.50}$	

From Table IV-8, it could be seen that bubble coalescence was observed when the small inlet diameter, 0.30 cm, was used; whereas, bubble coalescence was only observed at the high raw water flow rate of 400 l/hr when the big inlet diameter, 0.50 cm, was used. When the 0.30 cm of water inlet was used, the downward axial velocity at the center of the hydrocyclone and the high velocity gradient induced the bubbles to coalesce. Therefore, the floating flocs were not observed when the small inlet diameter, 0.30, was used.

From these results, it could be concluded that use of the small water inlet, 0.30 cm, with HC2 is not suitable for the hybrid process.

2.2.2.3 The experimental results of HC2 and HC3

1. The objective of this part was to compare the influence of hydrodynamics on the production of floating floc. This experiment was performed in the HC2 and HC3 at water flow rates of 200 to 400 l/hr. The coagulant concentration

was 1.0 mg/l, total pressure was maintained at 3.5 bars, and the water inlet diameter was 0.50 cm. The experimental results are presented in Table IV-9.

Table IV-9. The hydrodynamic experimental results for HC2 and HC3.

(Note: The operating condition: $Q = 200\text{-}400$ l/hr, $C_c = 1.0$ mg/l, $P_t = 3.5$ bars, $D_i = 0.50$ cm, and $Q_p = 36$ l/hr)

Parameter	Hydrocyclone type	
	HC2	HC3
Percentage of floating floc	Yes, a little bit	Yes, 51 %
Coalescence of bubbles	Yes, at $Q = 300$ and 400 l/hr	No
Axial velocity at the center of the hydrocyclone	Downward direction	Downward direction
Tangential velocity gradient	$G_{HC2} > G_{HC3}$	

From Table IV-9, it could be seen that the floating floc percentage in HC3 was higher than that of HC2. In addition, the coalescence of bubbles was found in HC2 at the high water flow rates of 300 and 400 l/hr. It could be explained that the high velocity gradient in HC2 induced the formation of coalesced bubbles in the hydrocyclone. Since bubble coalescence was not observed in HC3, it is a more suitable reactor for the hybrid process.

2.2.3 Influence of the air fraction on the production of floating floc

The raw water, coagulant, and microbubbles were injected into the hydrocyclones to create aerated flocs, which were induced to the center of the hydrocyclones by vortex flow for the separation process. Therefore, the air fraction in a hydrocyclone, which is the ratio of the air volume and treated water volume (i.e., the raw water flow rate and pressurized water flow rate), was an important parameter for the hybrid process.

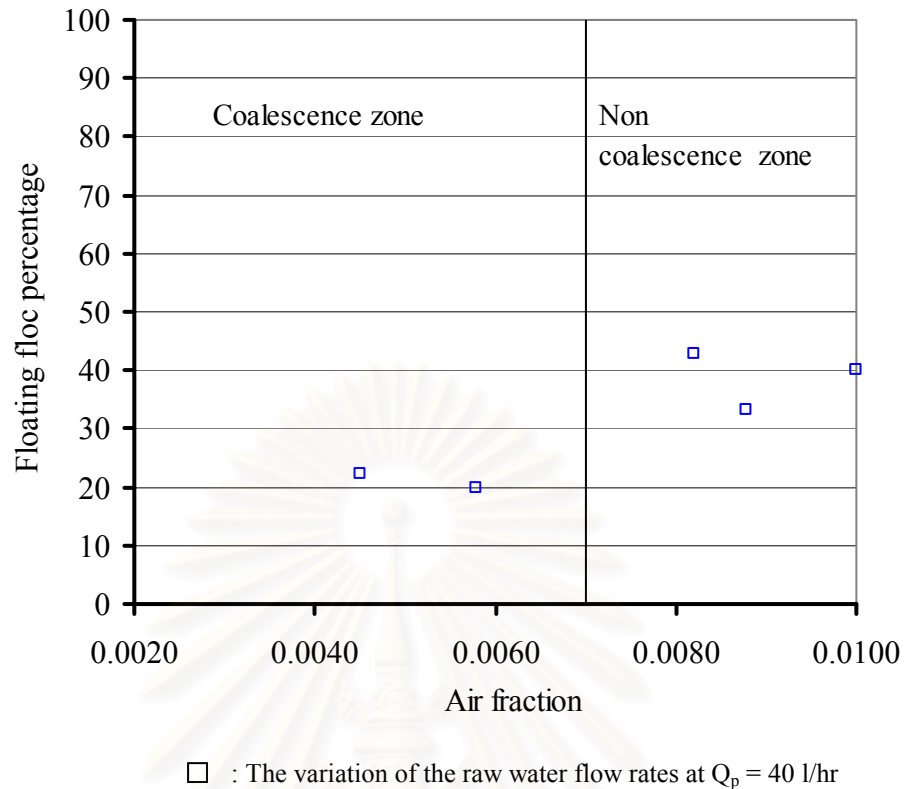
In this study, three different methods were used to modify the air fractions:

1. The raw water flow rate was increased while both the flow rate and total pressure in the tank of the pressurized water were kept constant.
2. The total pressure in the pressurized tank was increased while the pressurized water flow rate was kept constant.
3. The pressurized water flow rate was increased while the total pressure in the pressurized tank was kept constant.

In order to study the effects of air fraction variations on the floating floc percentage, the three methods were used; they involved (1) varying the raw water flow rate (175, 200, 250, 300, and 350 l/hr), (2) varying the total pressure (3.5, 4.0, and 5.0 bar), and (3) varying the pressurized water flow rate (40, 60, and 80 l/hr).

2.2.3.2 Modification of air fractions by varying the raw water flow rates

These experiments were performed to study the effects of air fraction variations (by increasing the raw water flow rate) on the floating floc percentage while the pressurized water flow rate and total pressure of pressurized tank were kept constant. In these experiments, the pressurized water flow rate was studied at 40 l/hr, the total pressure in the pressurized tank was maintained at 3.5 bars, and the coagulant concentration was maintained at 1.0 mg/l. The obtained results of HC3 were presented in Figure IV-29



(Note: The operating condition: $Q_p = 40$ l/hr, $P_t = 3.5$ bars, $C_c = 1.0$ mg/l, and $D_i = 0.50$ cm.)

Figure IV-29. The relation of the floating floc percentage and air fraction at different raw water flow rates for HC3.

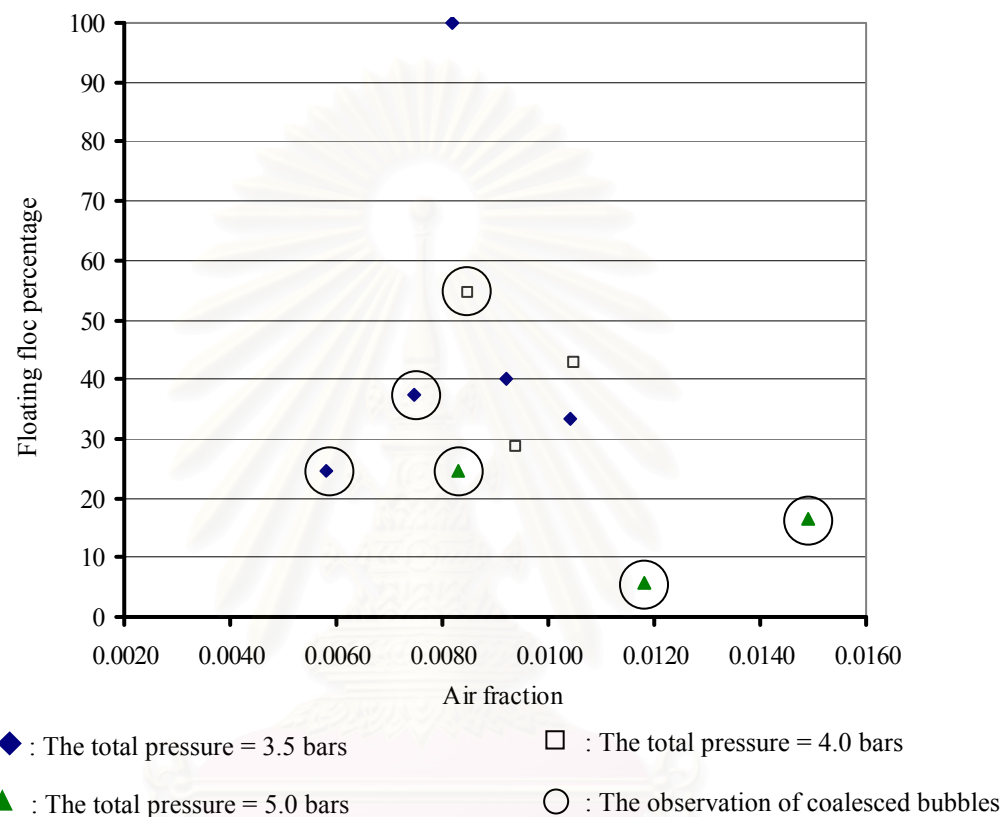
In this figure, coalesced bubbles were categorized into two zones, which were those formed at the low air fraction (high raw water flow rate) and the high air fraction (low raw water flow rate). It can be observed that the high raw water flow rate induced the coalescence bubble even when the air fraction was low.

On the other hand, when bubble coalescence did not occurred (i.e. at low raw water flow rate that produced a higher air fraction), the production of floating flocs was better. This emphasizes that the high water flow rate is not suitable for the production of floating flocs in the hybrid process.

2.2.3.3 A variation of the total pressure in pressurized tank

This study was performed in HC3 to study the effect of the total pressure in the pressurized tank on the amount of floating floc. The experiments were performed by using different total pressures in the pressurized tank (i.e., 3.5, 4.0 and 5.0 bars) while the pressurized water flow rate was kept constant at 40 l/hr. At each total pressure in the pressurized tank, the various air fractions were obtained by the

variation of the raw water flow rates. The coagulant concentration was 2.0 mg/l and the raw water inlet diameter was 0.50 cm. It was noticed that the pilot equipment's total pressure capacity in the pressurized tank was limited to 5 bars and the raw water flow rate was limited to 400 l/hr. Therefore, the variation of the air fraction gave a higher range than variation of that of the raw water flow rate.



(Note: The operating condition: $Q_p = 40$ l/hr, $C_c = 2.0$ mg/l, $D_i = 0.50$ cm)

Figure IV-30. The relation of the floating floc percentage and air fraction at different total pressures in the pressurized tank for HC3.

From Figure IV-30, it could be seen that the percentages of floating floc at 3.5 and 4.0 bars of total pressures were not significantly different; meanwhile, an outstanding result of 100% of floating floc was provided by 3.5 bars in the pressurized tank.

On the other hand, the experimental results of a high total pressure, 5 bars, produced a low floating floc percentage. This could be explained by the coalescence of microbubbles at the lower part of the hydrocyclone (in all operating conditions) that blocked the entering of microbubbles into the floc structure. Therefore, aerated

flocs could not be created. It could be concluded that a total pressure that is too high is not suitable for the hybrid process.

2.2.3.4 The synthesis the global range of air fraction

Figure IV-31 presents the relations of the floating floc percentage versus air fractions in HC3. These experiments were performed at different raw water flow rates (175, 200, 250, 300, and 350 l/hr) and different pressurised water flow rates (40, 60, and 80 l/hr). The total pressure in the pressurized tank was kept constant at 3.5 bars, and the coagulant concentration was kept constant at 1.0 mg/l.

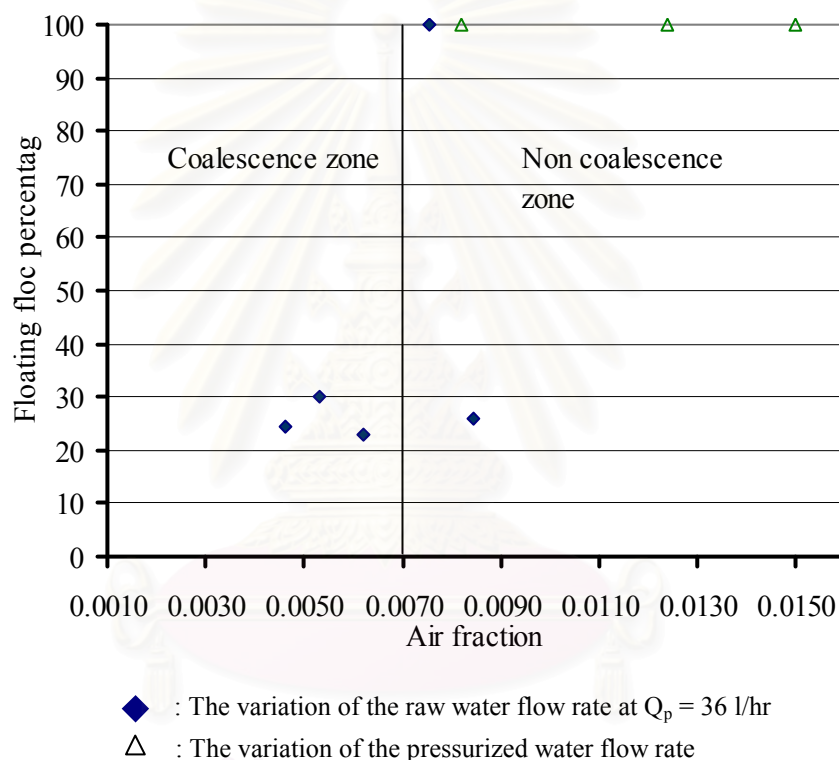


Figure IV-31. The relationship of the floating floc percentage and different air fractions of HC3

In this graph, the experimental results on bubble coalescence were added. Hence, two zones can be distinguished at the air fraction equal to 0.007:

(1) The low air fraction zone, which corresponds to the high raw water flow rate, in which bubble coalescence was observed.

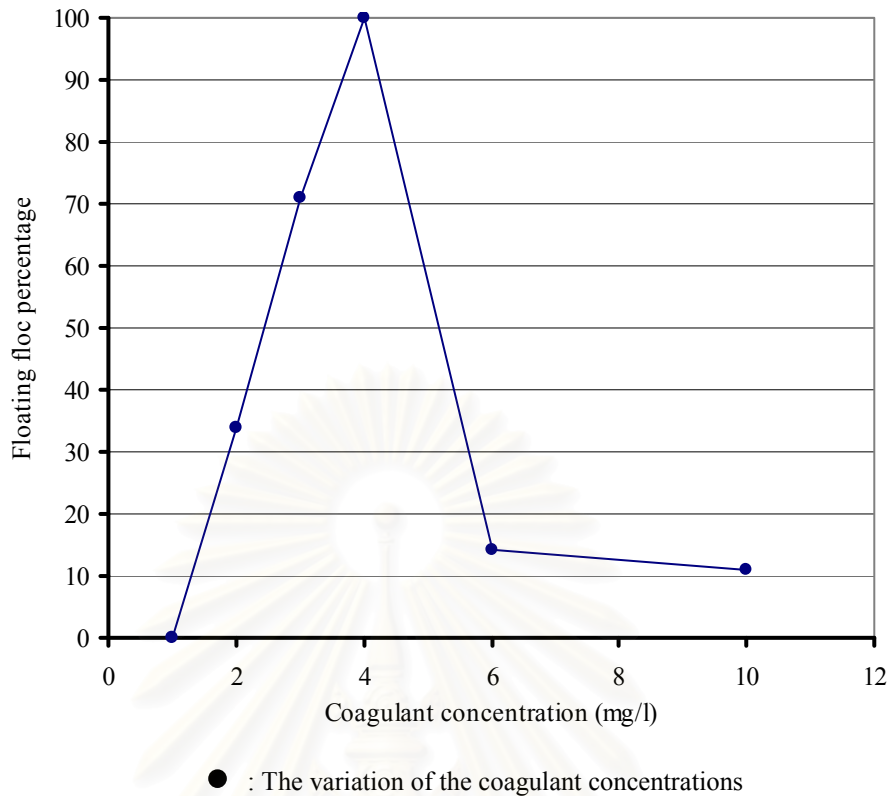
(2) The high air fraction zone, which corresponds to the higher pressurized water flow rate or the low raw water flow rate. This area did not contain bubble coalescence.

Firstly, concerning the low air fraction zone, it was observed that regardless of the air fraction, coalesced bubbles were still found. Therefore, air fraction is not the only parameter for bubble coalescence. Bubble coalescence is also controlled by the raw water flow rate and the downward flow of liquid as previously observed. In the low air fraction zone, the obtained results were unsatisfactory for the hybrid process since the floating floc percentage was low at 25.9 % (on average).

In the high air fraction zone, coalesced bubbles were not found and the floating floc percentage was outstanding at 100 %. This result corresponded to an air fraction of 0.0082, a raw water flow rate of 200 l/hr, and a total pressure of 3.5 bars in the pressurized tank.

2.2.4 The influence of the coagulant concentration on the floating floc production

This experiment was performed to study the influence of the coagulant concentration of the polymer FO 107 in the hydrocyclone on the percentage of floating floc. Coagulant concentrations were varied at 1.0, 2.0, 3.0, and 4.0 mg/l. The experiments were performed in HC3: the air fraction was maintained at 0.0086, the total pressure was kept constant at 3.5 bars, the water flow rate was 200 l/hr, and the raw water inlet diameter was 0.50 cm.



(Note: The operating conditions: $Q = 200$ l/hr, $P_t = 3.5$ bars, $Q_p = 40$ l/hr, and $D_i = 0.50$ cm)

Figure IV-32. The relation between the floating floc percentage and coagulant concentration in HC3.

From Figure IV-32, it could be seen that the floating floc percentage increased progressively, from 0 to 100 %, when the coagulant concentrations were increased from 1.0 to 4.0 mg/l. However, it decreased to 12 % (on average) when excess coagulant concentrations were used (i.e. 6.0 and 10.0 mg/l).

It could be explained that the surface areas of the created flocs of high coagulant concentrations were larger than those of low coagulant concentrations. Consequently, the collision and adhesion of bubbles and flocs were high, the injected microbubbles became entrapped, and aerated flocs were created.

However, the excess coagulant concentrations made the density of the created floc too high, and most of them settled down to the bottom of the hydrocyclone at the end of experiment.

2.2.5 Influence of the location of pressurized water on the floating floc percentage

This experiment was performed in HC3 and HC4 to study the effects of the position of the pressurized water injection, which was injected at the bottom of the hydrocyclone. The pressurized water injected ports were placed close to the wall and at the center of hydrocyclone for HC3 and HC4, respectively.

In this experiment, the raw water flow rate was kept constant at 200 l/hr, the air fraction was 0.0086, and raw water inlet was 0.50 cm. The experimental results of bubble coalescence observations and the percentage of floating floc for HC3 and HC4 at different coagulant concentrations are presented in Table IV-10.

Table IV-10. Bubble coalescence observations and the percentage of floating floc in HC3 and HC4 at different coagulant concentrations.

(Note: The operating conditions: $Q = 200$ l/hr, $P_1 = 3.5$ bars, $Q_p = 40$ l/hr, and $D_i = 0.50$ cm, Method II: progressive start-up)

Parameters	HC3	HC4
Bubbles coalescence	No coalescence	No coalescence
Coagulant concentration (mg/l)	Percentage of floating floc (%)	
1.0	0	0
2.0	34	40
3.0	71	100
4.0	100	100

In this table, it can be observed that the influence of the coagulant concentration is related to the position of the pressurized water injection. Indeed, one can deduce that microbubbles were entrapped by floc in HC3 quicker than in HC4 because the injection location of the pressurized water in HC3 was placed close to the wall where the mixing intensity or velocity gradient was higher than in the center of the hydrocyclone. The resulting trapped bubbles were small in size and the floc formation was stable, which was a required condition.

Under these conditions the control of the coagulant's contact with the flocs and bubbles was more significant in HC3 than in HC4. The difference between both hydrocyclones at 3.0 mg/l may be explained by the bigger bubbles in HC4, which increased the probability of floating flocs.

2.2.6 The conclusions and selection of HC3 or HC4

The tangential velocity in HC2 was higher than that of HC3; therefore, the higher tangential velocity induced the coalescence of bubbles. This result directly affected the percentages of floating floc: 0 and 22 % for HC2 and HC3, respectively. Therefore, HC2 does not have a suitable geometry for the hybrid process.

Based on the same tangential velocity and tangential velocity gradient in HC1, the axial velocity of the 0.30 cm water inlet was higher than that of the 0.50 cm water inlet. The coalescence of bubbles was induced by the small water inlet, which gave an unsatisfactory result for the hybrid process. Therefore, the water inlet of 0.50 cm was used in the hybrid process.

Even when the air fraction was low (high water flow rate), bubbles still coalesced due to the high water flow rate that induced bubble coalescence. Therefore, a high water flow rate (> 200 l/hr) is not suitable for the production of floating flocs in the hybrid process.

It was found that a total pressure equal to 3.5 bars provided a good result for floating floc at 100% at the air fraction of 0.0082 and pressurized water flow rate of 200 l/hr. Whereas, a high total pressure at 5.0 bars, gave a poor result for floating floc due to the coalescence of bubbles at all raw water flow rates. Therefore, the total pressure of 3.5 bars, raw water flow rate of 200 l/hr, and pressurized water flow rate of 40 l/hr provide a suitable condition for the hybrid process. This condition corresponded to 0.0082 of air fraction.

The coagulant concentrations of 3.0 and 4.0 mg/l provided good results for floating floc at the respective percentage of 70 and 100 %.

Pressurized water injections should be placed close to the wall of a hydrocyclone (as in HC3) because this allows the injected microbubbles to reach the high mixing intensity zone more quickly.

2.3 The effects of the significant parameters on the separation efficiency

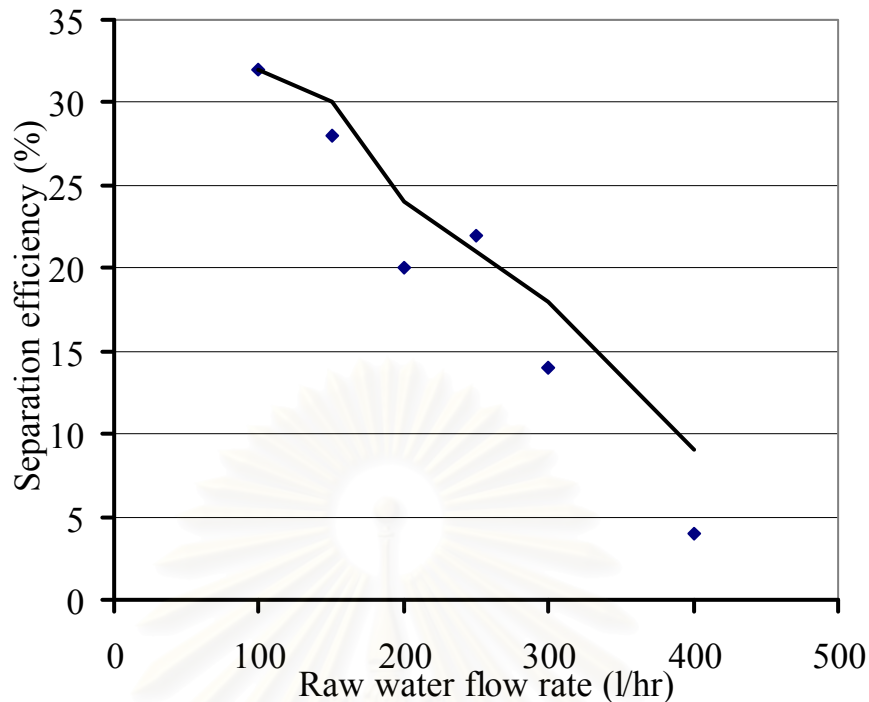
In the previous part, the effects of several parameters on the floating floc percentage were studied, and HC3 was selected for this study. In this section, some operational conditions were tested in HC3 in order to find out the optimum operating conditions. The effects of the water flow rate, air fraction, and coagulant concentration were investigated.

2.3.1 The influence of the raw water flow rate in HC3

In order to determine the effects of the raw water inlet diameter and the raw water flow rate on the separation efficiency of the hybrid process, this experiment was performed using two inlet diameters, 0.50 and 0.30 cm. The air fraction was maintained at 0.0100, which was performed by keeping the total pressure constant at 3.5 bars, and the pressurized water flow rates were varied at 28, 40, 55, 65, 80, and 110 l/hr for raw water flow rates of 100, 150, 200, 250, 300, 400 l/hr. The coagulant concentration was maintained at 3.0 mg/l.

2.3.1.1 Raw water inlet diameter = 0.50 cm

In this experiment, the water inlet diameter was maintained at 0.50 cm, the coagulant concentration was 3.0 mg/l, and the raw water flow rate was varied at 100, 200, 300, and 400 l/hr. The separation efficiency percentages in the hydrocyclone are presented in Figure IV-33 as a function of the raw water flow rate.



◆ : The separation efficiency for $D_i = 0.50$ cm — : The trend line (moving average)

(Note: The operating condition: $C_c = 3.0$ mg/l, $D_i = 0.50$ cm, and air fraction = 0.01)

Figure IV-33. The relationship of the raw water flow rate and separation efficiency (%) in HC3 using a raw water inlet diameter equal to 0.50 cm.

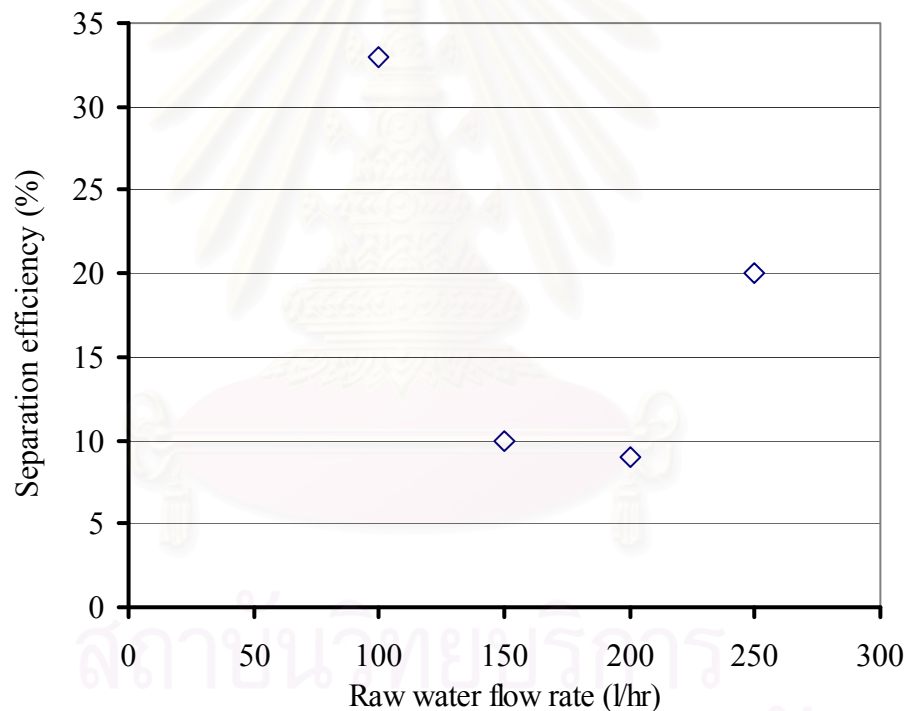
In this figure, the trend of the separation efficiency reduced as the water flow rate increased because coalesced bubbles were formed. It could be observed that the 100 l/hr raw water flow rate gave a higher separation efficiency than the 400 l/hr raw water flow rate: 32 and 4%, respectively. This result could be explained by the detention time of the floc in the hydrocyclone. The detention time of the low water flow rate, 100 l/hr, was 4 times higher than that of the high water flow rate, 400 l/hr: 1.18 and 0.29 minutes, respectively.

In this case, the experimental results of 100 l/hr and 200 l/hr were not significantly different; their separation efficiencies were 33 and 20%, respectively. Moreover, by visual observation, a medium-strong vortex was observed at the 200 l/hr flow rate in the upper part of the hydrocyclone, and the created flocs swirled circularly under the influence of the vortex flow. In contrast, a very weak vortex flow was observed at the 100 l/hr flow rate, and the created floc rose to the upper part without being influenced by the vortex flow.

In addition, the problem of bubble coalescence was not found in the range of 100 to 200 l/hr. Therefore, the water flow rate of 200 l/hr was found to be suitable for the hybrid process.

2.3.1.2 For raw water inlet diameter = 0.30 cm

In this experiment, the raw water inlet diameter was reduced to 0.30 cm, and the raw water flow rate was varied at 100, 150, 200, and 250 l/hr. Due to the capacity of equipment (the pressure drop), when the 0.30 cm water inlet was used, the raw water flow rate was limited to 250 l/hr. The air fraction was maintained at 0.01 and the coagulant concentration was 3.0 mg/l. In Figure IV-34, the relationship of the separation efficiency percentage in the hydrocyclone is presented as a function of the raw water flow rate.



◇ : The separation efficiency for $D_i = 0.30$ cm

(Note: The operating condition: $D_i = 0.30$ cm, $C_c = 3.0$ mg/l, and air fraction = 0.01)

Figure IV-34. The relationship of the raw water flow rate and the separation efficiency (%) in HC3 using a raw water inlet diameter equal to 0.30 cm..

As seen in Figure IV-34, the separation efficiency of the 100 l/hr raw water flow rate was higher than that of the higher raw water flow rates (150 to 250 l/hr), which were 33 and 13%, respectively. This result could be explained by the bubble

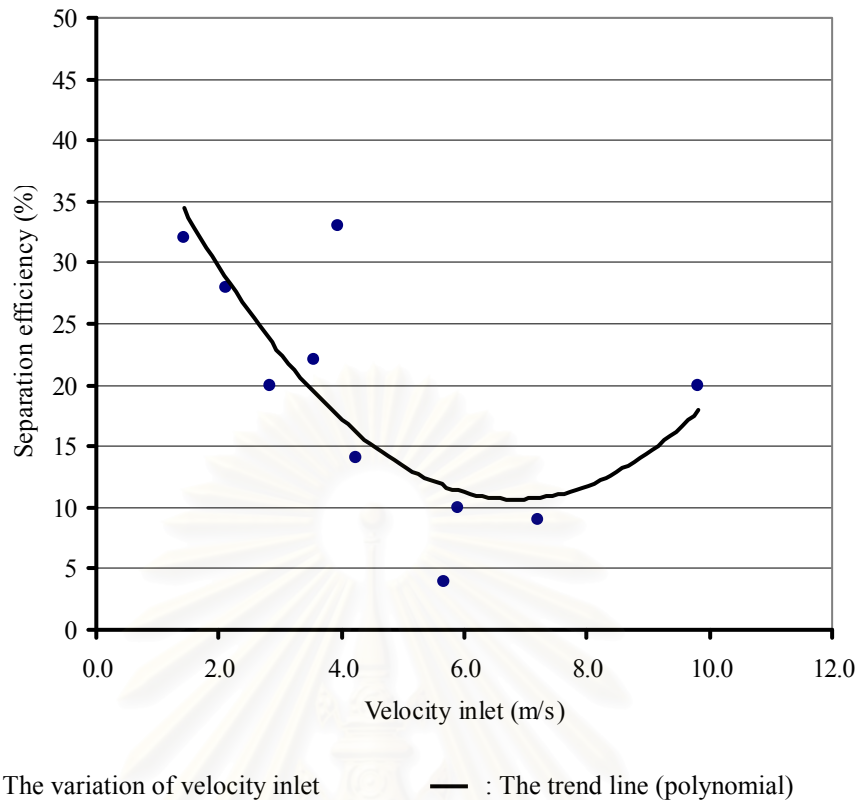
coalescence that was induced by the strong velocity gradient of the higher raw water flow rates.

In addition, it could be explained that the detention time can influence the separation efficiency of the floc in the hydrocyclone. The detention time was 1.18 minutes at the 100 l/hr flow rate, and its average was 0.61 minutes for the higher water flow rates (150, 200, and 250 l/hr).

However, the separation efficiency percentages of this operating condition were still low, as they averaged to 18 % (for all raw water flow rates). More, it was noted that a separation line was not observed.

2.3.2 The influence of the velocity inlet

The objective of this section was to understand the effects of the velocity inlet on the phenomenon in the hydrocyclone. The results are presented in terms of the separation efficiency. The raw water flow rates at 100, 150, 200, 250, 300, and 400 l/hr and the raw water inlet diameters of 0.50 and 0.30 cm results from section 2.3.1 were used to calculate the velocity inlets in this section. The experiments were performed at the air fraction equal to 0.0100 (using the same preparation method as in section 1.3.1); the coagulant concentration was 3.0 mg/l.



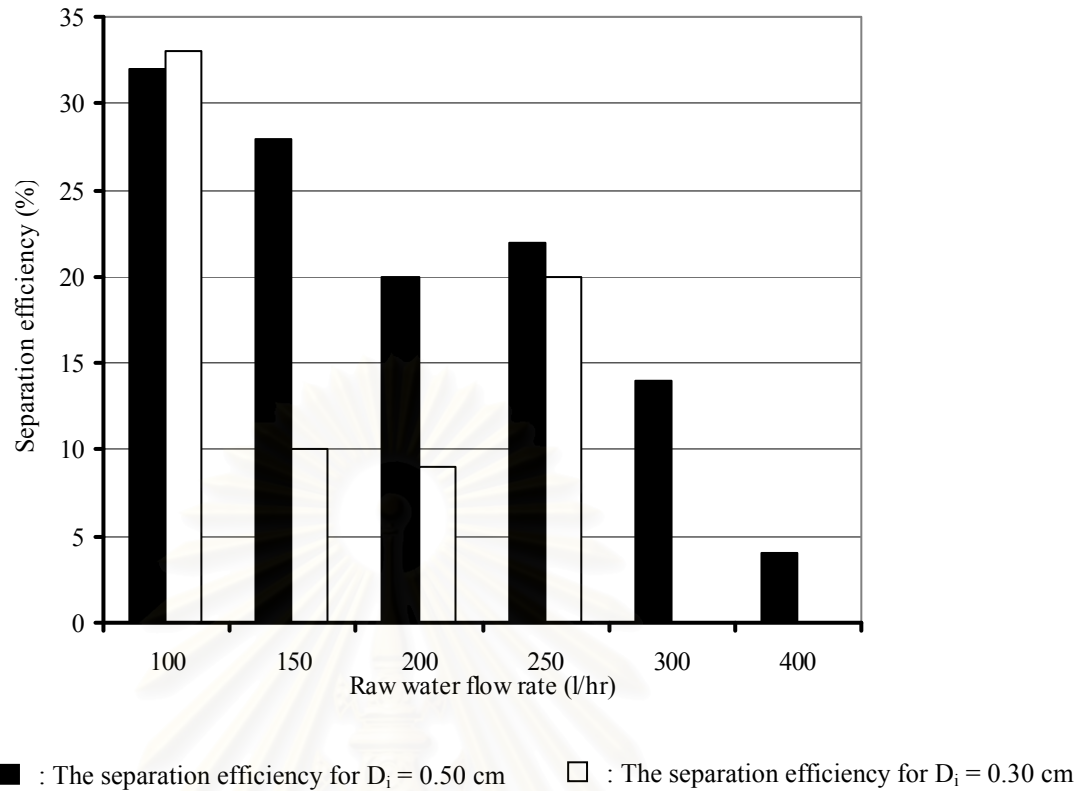
(Note: the operating condition: $C_c = 3.0$ mg/l and air fraction = 0.01)

Figure IV-35. The relationship of the velocity inlet and separation efficiency at different raw water flow rates and different water inlet diameters.

In Figure IV-35, the separation efficiency decreased constantly when the velocity inlet increased from 1.42 to 7.86 m/s. It increased only slightly at high velocity inlet of 9.83 m/s. From these results, it could be concluded that the separation efficiency decreased when the velocity inlet increased.

2.3.3 The influence of the raw water flow rate

To clearly compare the influence of the raw water flow rates on the separation efficiency in the hydrocyclone, two operating conditions were tested using two different raw water inlet diameters, 0.50 and 0.30 cm. The raw water flow rate was varied at 100, 150, 200, 250, 300, and 400 l/hr; the air fraction was fixed at 0.0100, which was carried out by the same method as mentioned in section 2.3.1, and the coagulant concentration was 3.0 mg/l.



(Note: The operating condition: HC3, $C_c = 3.0$ mg/l and air fraction = 0.0010)

Figure IV-36. Relationship of raw water flow rate and separation efficiency in the HC3 at different water inlet (0.50 and 0.30 cm)

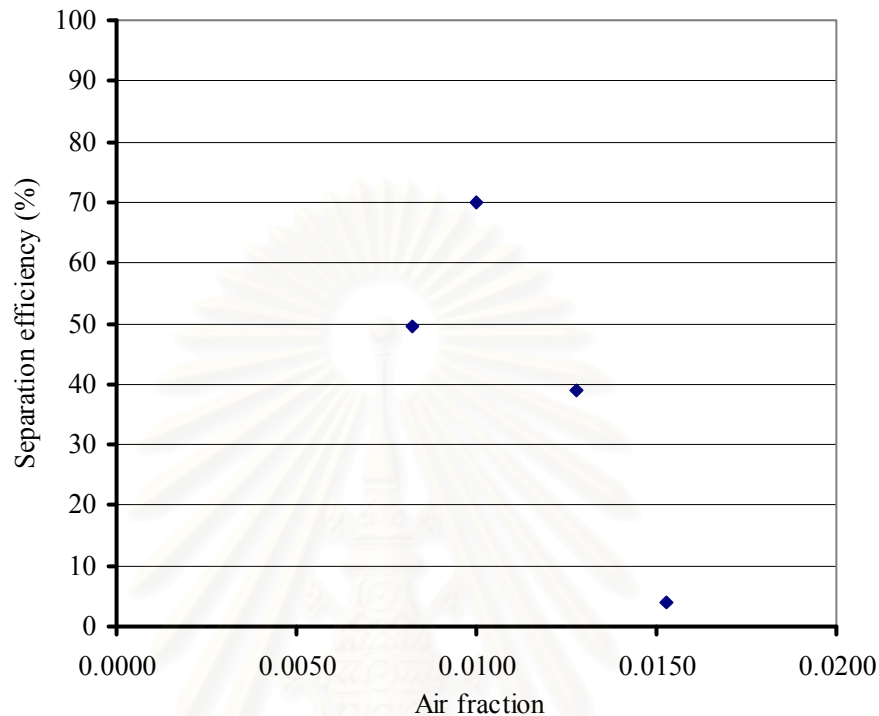
Regarding Figure IV-36, the separation efficiency for the 0.50 cm raw water inlet diameter decreased when the raw water flow rate increased; however, the separation efficiency of the 0.30 cm raw water inlet was different. Its separation efficiency at 100 l/hr was higher than that of the higher raw water flow rates (150 to 250 l/hr).

With regard to the raw water flow rates of 100 l/hr to 250 l/hr, it could be seen in the figure that the global separation efficiency produced by the 0.50 cm inlet was higher than of the global separation efficiency produced by the 0.30 cm inlet.

2.3.4 The influence of the air fraction

This part presents the influence of air fraction variations on the separation efficiency of HC3. In this experiment, air fractions were varied at 0.0082, 0.010, 0.0128, and 0.0150 by adjusting the pressurized water flow rates to 40, 55, 70, and 90 l/hr, respectively. The 0.50 cm raw water inlet was used, the coagulant concentration

was 3.0 mg/l, the total pressure was kept constant at 3.5 bars, and the raw water flow rate was maintained at 200 l/hr. The relationship of the separation efficiency and air fraction is presented in Figure IV-37.



(Note: The operating condition: $Q = 200$ l/hr, $D_i = 0.50$ cm, $P_i = 3.5$ bars, and $C_c = 3.0$ mg/l)

Figure IV-37. The variation of the air fraction and separation efficiency (%) at the different pressurized water flow rates of 40, 55, 70 and 90 l/hr.

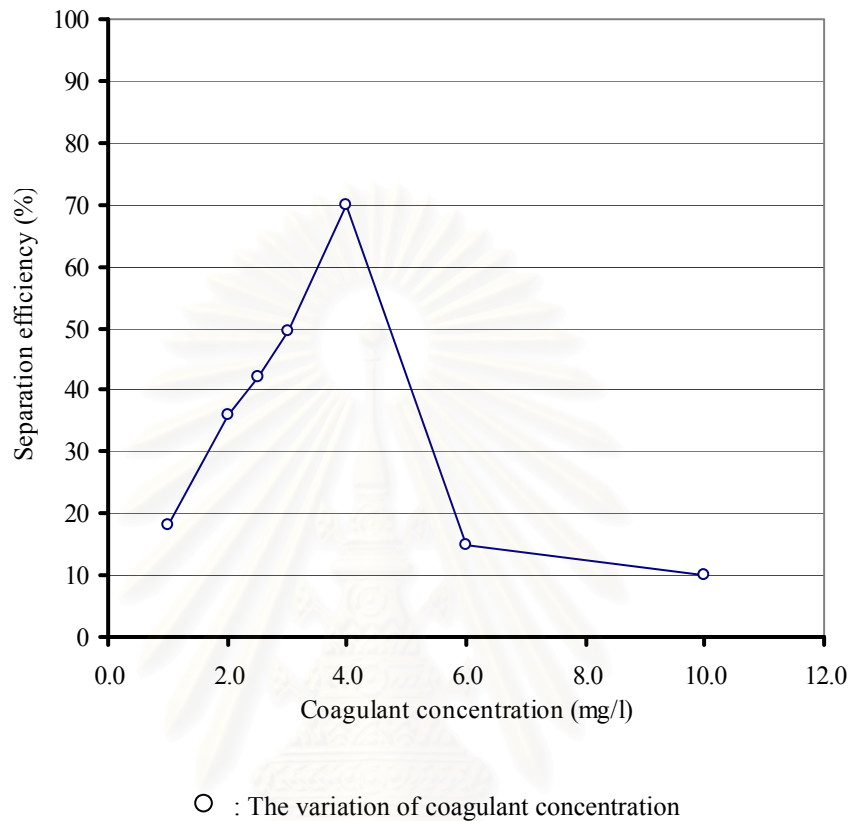
In Figure IV-37, it could be seen that the separation efficiency decreased when the air fraction increased. The separation efficiencies were varied in the range of 39 to 70 % for the air fraction range of 0.0082 to 0.0124.

The separation efficiency of the highest air fraction, 0.0153, was significantly low. These results could be explained by the excess air fraction in the hydrocyclone, which caused the problem of bubble coalescence that obstructed the creation of aerated floc.

2.3.5 The influence of the coagulant concentration

In order to study the influence of coagulant concentration on the separation efficiency, the experiment utilized four different coagulant concentrations: 1.0, 2.0, 3.0, and 4.0 mg/l. The raw water inlet was 0.50 cm, the raw water flow rate was

maintained at 200 l/hr, the total pressure was kept constant at 3.5 bars, and the air fraction was fixed at 0.0082. These experiments were performed by the progressive start-up method.



(Note: The operating condition: $Q = 200$ l/hr, $P_t = 3.5$ bars, and air fraction = 0.0082)

Figure IV-38. The relation of the coagulant concentration and separation efficiency in HC3

In Figure IV-38, the separation efficiency in the hydrocyclone increased from 18 to 70% when the coagulant concentration was increased from 1.0 to 4.0 mg/l. Then, it decreased sharply to 12.5 % (on average) when excess coagulant concentrations were used, i.e., 6.0 and 10.0 mg/l.

Regarding to the relation of coagulant concentration on the floating flocs percentage in Figure IV-32, it was found that it was similar to trend of coagulation concentration on the separation efficiency. Therefore, it could be concluded that in general, a high amount of floating floc produces a high separation efficiency.

2.3.6 The influence of G^*t on the separation efficiency

The objective of this study was to present the effects of the mixing intensity inside the hydrocyclone ($G_{z,exp}^*t$) on the separation efficiency. The experimental velocity gradient results at the wall zone of the hydrocyclone and the detention time of each raw water flow rate were taken into account to calculate the $G_{z,exp}^*t$.

In this experiment, the 0.50 cm raw water inlet diameter was used and the coagulant concentration was maintained at 3.0 mg/l. The experimental results of $G_{z,exp}^*t$ and the separation efficiency at each raw water flow rate are presented in Table IV-11.

Table IV-11. The relationship of $G_{z,exp}^*t$ and the separation efficiency of each raw water flow rate.

(Note: the operating condition: $D_i = 0.50$ cm, $P_t = 3.5$ bars, $C_c = 3.0$ mg/l, rapid start-up)

Raw water flow rate (l/hr)	Velocity gradient, $G_{z,exp}, s^{-1}$	Detention time, s	$G_{z,exp}^*t$	Separation efficiency (%)
200	80.4	35.4	2846.2	20
400	26.0	17.4	453.1	4

From this table, it could be observed that the separation efficiency was high at the high G^*t value. At the low raw water flow rate, 200 l/hr, the G^*t value was higher than at the high water flow rate, 400 l/hr, due to the coagulation process that was carried out at the high G^*t .

In this table, the velocity gradient of the low water flow rate, 200 l/hr was higher than that of the high water flow rate, 400 l/hr. It could be explained that the difference of the tangential velocity of low water flow rate between two points, 2 cm and wall of hydrocyclone, was higher than that of high water flow rate as presented in Figure IV-22 and Figure IV-23 in the hydrodynamics study.

2.4 Global performances of the hybrid process for the optimum conditions.

Many parameters were tested to find out the optimal operating conditions for the hybrid process. The optimum conditions to operate the hybrid process were concluded. Parameters such as the geometry of the hydrocyclone and the coagulant concentration were determined. In this section, an important performance to carry out the hybrid process which was the start-up method was described

2.4.1 The influence of the start-up method

In this study, many parameters were tested step-by-step to find out the optimal operating conditions for the hybrid process. An important parameter for carrying out the hybrid process is the start-up method. The experimental results of the start-up method using different water inlet diameter are presented in Table IV-12

Table IV-12. The influence of the start-up method on the separation efficiency.

(Note: The operating condition: HC3, $C_c = 3.0$ mg/l, $Q = 200$ l/hr, air fraction = 0.0100, $Q_p = 55$ l/hr, and $P_t = 3.5$ bars)

Water inlet diameter (cm)	Separation efficiency (%)	
	Rapid start-up	Progressive start-up
0.30	9	23
0.50	20	70

As can be seen in Table IV-12, the separation efficiency of the progressive start-up method was significantly higher than that of the rapid start-up method. When the water inlet was equal to 0.50 cm, the separation efficiencies were 70 and 20% for the progressive start-up and rapid start-up methods, respectively.

Figure IV-39 presented the photo of the settled flocs in the sampled waters from the center and wall zones of the hydrocyclone. It showed the significantly different in the amount of floc of the optimum operating condition, 70% of separation efficiency.

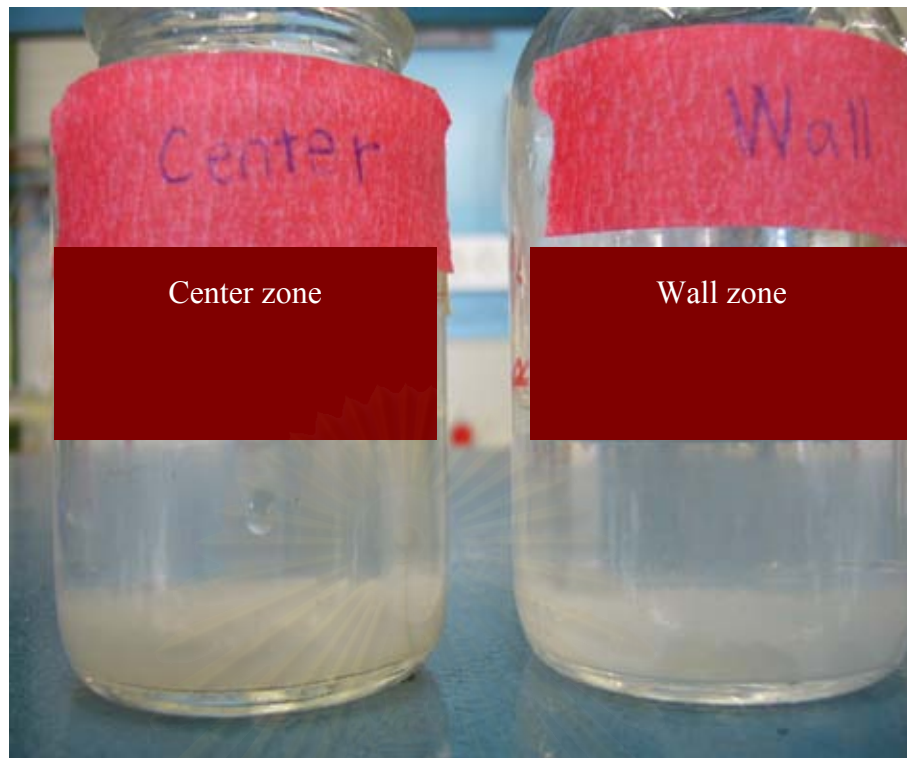


Figure IV-39. Photo of the settled flocs in the sampled waters from in the center and wall zones of the hydrocyclone that show a 70% separation efficiency.

2.4.2 Optimum condition for the hybrid process in HC3

The optimum conditions for implementing the hybrid process are as follows:

Hydrocyclone geometry	= HC3
The raw water flow rate	= 200 l/hr
The raw water inlet	= 0.50 cm
Coagulant concentration	= 3.0 – 4.0 mg/l
Total pressure	= 3.5 bars
Air fraction	= 0.0082 – 0.0100
Start-up method	= the progressive start-up method

However, the floc sizes in the wall zone of the optimum operating condition, 70 % separation efficiency, were still large, 0.1 to 0.5 cm, as presented in Figure IV-27. The higher separation efficiency was difficult in this hydrocyclone geometry (HC3) therefore, the enlargement of hydrocyclone diameter was proposed. The cylindrical

hydrocyclone geometry was kept constant. The details of this new reactor were presented in the perspective section.



สถาบันวิทยบริการ
จุฬาลงกรณ์มหาวิทยาลัย

CHAPTER V

GENERAL CONCLUSION AND PERSPECTIVES

General conclusions

The mission of this thesis research was to create a new separation process for water treatment. This new hybrid process combined the use of coagulation, and flocculation in a hydrocyclone to eliminate water turbidity.

As underlined in the literature review section, the original principle of this hybrid process was the integration of coagulation and flocculation in a hydrocyclone reactor. The strong and low velocity gradients, which characterized the respective external and internal vortexes, were employed to perform coagulation and flocculation. Pressurized water was injected simultaneously with raw water and the coagulant to initiate floc formation around microbubbles. Then, these aerated flocs, with low density were centrifuged in the internal vortex where the velocity gradient was weak. Their growth and separation were achieved in the upper part of the hydrocyclone. Moreover, the hydraulic retention time for performing the coagulation, flocculation and separation in the hydrocyclone was lower significantly that that of classical water treatment process.

The principle objectives of this study were the characterization of the hydrodynamics in the hydrocyclones and the quantification of the optimum conditions for the hybrid process. In this study, the new and simple method was developed to characterize the hydrodynamic condition. This is the simple, effective and reliable method due to the experimental results agreed with the previous studies in the literature reviews and the experimental results were repeatable. Therefore, this method could be used commonly as the experimental method to study the hydrodynamics for another research.

By this method, the experimental results of the hydrodynamics study such as the tangential velocity, axial velocity and the tangential velocity gradient were characterized at the lower part of the hydrocyclones. The result presented that the mixing intensity of the wall zone was higher than that of the center zone. This information was used to design the suitable position of the pressurized water injection

for the hybrid process. In addition, the results of axial velocity and tangential velocity could be used to explain the found phenomenon of coalescence bubbles which was an important parameter that obstructed to the aerated floc formation. By this result, the suitable geometry of hydrocyclone, HC 3, was selected for the hybrid process.

Therefore, the obtained experimental results of hydrodynamics related with the hybrid process due to they were used as the essential information to explain the found phenomena and the mechanisms in the hydrocyclone. Finally, the suitable operating conditions were quantified.

Regarding to the experimental results of the hybrid process, it was found that the optimum operating condition was reported at 70% of the separation efficiency. It can be stated that this was the satisfied result for the innovative reactor in water treatment. The list of optimum operating conditions in this study was presented in Table V-1

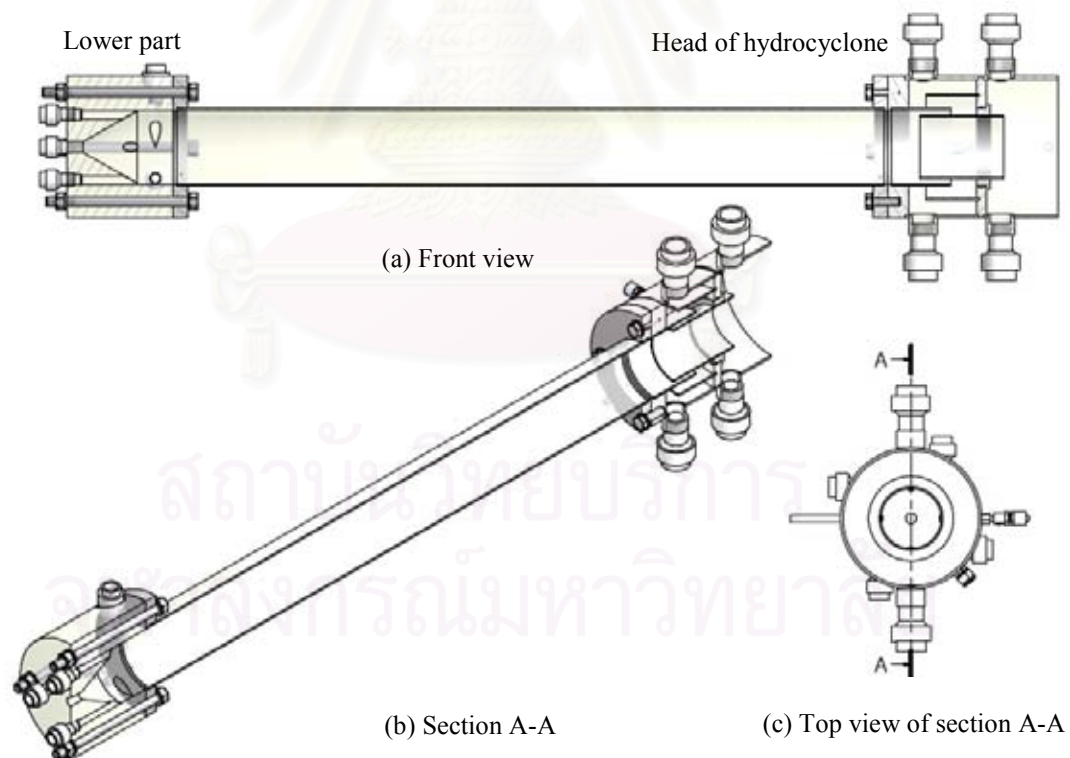
Table V-1. The optimum operating condition for the hybrid process

Parameter	Recommended value
Hydrocyclone geometry	HC3, a 100-cm high cylindrical hydrocyclone with a pressurized water wall injection port.
Raw water flow rate	200 l/hr
Raw water inlet	0.50 cm
The coagulant concentration	3.0 – 4.0 mg/l
Total pressure in the pressure tank	3.5 bars
Air fraction	0.0082 – 0.0100
Start-up method	Progressive start-up method

This optimum operating condition was studied step by step to quantify the optimum value of each parameter. However, the separation of the floc from water was difficult in this small hydrocyclone geometry (HC3), therefore proposed method to solve this problem was to enlarge the hydrocyclone diameter as presented.

Perspective of this study

Both of experimental results of the hydrodynamics characterization and the hybrid process study were realized to develop the new hydrocyclone geometry. Due to the separation of floc in the small geometry of HC3 was difficult, therefore, the enlargement of hydrocyclone diameter was proposed as the perspective for the future research. For this reactor, the cylindrical hydrocyclone geometry should be kept as same as the optimum hydrocyclone (HC3) and the diameter should be increased to 10 cm for the larger separation area. The head of reactor should be constructed to convey easily the separated flocs in the center zone from the clear water in the wall zone of hydrocyclone. In addition, this reactor should have the possibility to study the influence of position of the pressurized water injection; therefore, the pressurized injection port should be constructed at the center and wall zone. The sketch of the front view and the details of section A-A of the proposed hydrocyclone geometry for the hybrid process were presented in **Error! Not a valid bookmark self-reference..**



(Note: (a) the front view, (b) section A-A, and (c) top view of section A-A)

Figure V-1. The sketch of perspective reactor of this study

REFERENCES

- Bank N. and Gauvin, W. H. (1977). Measurement of flow characteristics in a confined vortex flow. Can. J. Chem. Eng **55** : 397–402.
- Bennette, M.A. and Williams, R.A. (2004). Monitoring the operation of an oil/water separator using impedance tomography. Minerals Engineering **17**: 605-614.
- Bradley, D. (1965). The hydrocyclone. New York: Pergamon Press Ltd.
- Burt, M.P. and Thomas, P.R. (2002). Analysis of the hydrocyclone stock cleaning process for wasted fibre in a paper mill. Journal of Cleaner Production **10**: 573-579.
- Bhole, A.G. (1993). Performance of static flocculators. Proceeding Chemistry for the Protection of the Environment 2. Edited by Pawloski et al., IWAQ: 181–194.
- Camp, T. R., and P. C. Stein. (1943). Velocity gradient and internal work in fluid motion. J. Boston Soc. Civ. Eng **30**: 209.
- Carissimi, E. and Rubio, J. (2005). The flocs generator reactor-FGR: a new basis for flocculation and solid-liquid separation. International Journal Mineral Process **75**: 237-247.
- Changirwa, R., et al. (1999). Hybrid simulation for oil-solids-water separation in oil sands production. Minerals Engineering **12**, **12**: 1459-1468.
- Chiné, B. and Concha, F. (2000). Flow patterns in conical and cylindrical hydrocyclones, Chemical Engineering Journal **80**: 267–273.
- Cliff, R. (1978). Bubbles, Drops, and Particles. (Academic, New York).
- Cumming, I. W. et. al. (1999). The rejection of oil using an asymmetric metal microfilter to separate and oil in water dispersion. Water Resource **33**, **17**:3587-3594.
- Degrémont SA. (2005). Mémento technique de l'eau/ Degrémont. 2 Vol. 10th edition. France.
- Franks G. V. et al. (2005). Aggregate size and density after shearing, implications for dewatering fine tailings with hydrocyclones. International Journal Mineral Process Article in Press.

Gil, A., et al. (2002). Gas-particle flow inside cyclone diplegs with pneumatic extraction. Powder Technology 128: 78-91.

Honaker, R.Q. et al. (2001). Apex water injection for improved hydrocyclone classification efficiency. Minerals Engineering 14, 11: 1445-1457.

Jonas, B. et al. (2007). Tangential velocity measurements in a conical hydrocyclone operated with a fibre suspension. Minerals engineering 20: 407-413.

Jonas, B. and Hannes, V., (2004). Velocity measurements in a cylindrical hydrocyclone operated with an opaque fiber suspension. Minerals engineering 17: 599-604.

Khalid et al. (2004). CANMET hydrocyclone: an emerging alternative for the treatment of oily waste streams. Minerals Engineering 17: 643-649.

MA, B. F. (1993). Épuration des eaux résiduaires de l'industrie pétrolière par hydrocyclonage. Thèse de doctorat. I.N.S.A. Toulouse.

Modge D.N. et al. (2004). Hydrocarbon cyclones in hydrophilic oil sand environments. Minerals Engineering 17: 625-636.

Parga, J.R., et al. (2003). Destruction of cyanide waste solutions using chlorine dioxide, ozone and titania sol. Waste Management 23: 183-191.

Puprasert, C., et al. (2004). Potential of using hydrocyclone and hydrocyclone equipped with grit pot as a pre-treatment in run-off water treatment. Chemical Engineering and Processing 43: 67-83.

Puprasert, C. (2004). Contribution a la mise au point d'application spécifique des hydrocyclones en traitement des eaux. 722. Thèse de doctorat. I.N.S.A. Toulouse.

Rafael Teixeira Rodrigues and Jorge Rubio. (2006). DAF- dissolved air flotation: potential applications in the mining and mineral processing industry. International Journal of Mineral Processing 82, 1 (February 2007): 1-13.

Reynolds and Richards (1995). Unit operation and processes in environmental engineering. 2nd edition. Cengage Engineering.

Rivier, L., and Garland, E. (1994). Experience of produced water treatment in the North Sea. Marine Pollution Bulletin 19, 6-12: 312-316.

Rodrigues, R.T. and Rubio, J. (2003). New basis for measuring the size distribution of bubbles. Mineral Engineering 16: 757-767.

Roldán-Villasana, E.J. and Williams, R.A. (1999). Classification and breakage of flocs in hydrocyclones. Minerals Engineering 12: 1225-1243.

Rosa, J. J. and Rubio, J. (2005). The FF (Flocculation-flotation) process. Mineral Engineering 18: 701-707.

Schuetz, S. et al. (2004). Investigations on the flow and separation behavior of hydrocyclones using computational fluid dynamics. International Journal of Mineral Processing 73: 229-237.

Siangsanun, V. (2006). Hybrid process: hydrocyclone, coagulation-flocculation and floatation in water treatment process. Thesis (M. Eng), Department of Environmental Engineering. Faculty of Engineering. Chulalongkorn University.

Svarovsky, L. (1984). Hydrocyclone. Pennsylvania: Rinehart and Winston.

Tchobanoglous, G. et al. (2004). Wastewater engineering: treatment, disposal, and reuse. 4th ed. Singapore: Metcalf & Eddy, Inc. McGraw-Hill

Woodfield, D. and Bickert, G. (2004). Separation of flocs in hydrocyclones-significance of floc breakage and floc hydrodynamics. International Journal of Mineral Processing 73: 239-249.



APPENDICES

สถาบันวิทยบริการ
จุฬาลงกรณ์มหาวิทยาลัย

Appendix A

The calculations of terminal velocity of droplets

Table A - 1. The calculated values of Reynolds number, drag coefficient, and terminal velocity for HC1

HC1									
Injected position	Q = 200 l/hr, D _i = 0.50 cm			Q = 200 l/hr, D _i = 0.30 cm			Q = 400 l/hr, D _i = 0.50 cm		
	Re	C _d	V _d	Re	C _d	V _d	Re	C _d	V _d
Center	149	0.91	5.80	870	0.45	13.22	368	0.63	8.87
1 cm	98	1.10	4.74	798	0.45	12.85	368	0.63	8.87
2 cm	27	2.20	2.40	96	1.12	4.68	23	2.40	2.26
Wall	11	4.00	1.47	92	1.14	4.59	332	0.65	8.46

Table A - 2. The calculated values of Reynolds number, drag coefficient, and terminal velocity for HC2

HC2									
Injected position	Q = 200 l/hr, D _i = 0.50 cm			Q = 200 l/hr, D _i = 0.30 cm			Q = 400 l/hr, D _i = 0.50 cm		
	Re	C _d	V _d	Re	C _d	V _d	Re	C _d	V _d
Center	187	0.83	6.47	344	0.65	8.59	172	0.86	6.21
1 cm	296	0.69	8.01	200	0.81	6.68	342	0.65	8.57
2 cm	63	1.36	3.82	141	0.93	5.70	64	1.36	3.82
Wall	22	2.45	2.21	92	1.14	4.59	22	2.45	2.21

Table A - 3. The calculated values of Reynolds number, drag coefficient, and terminal velocity for HC3

HC 3									
Injected point	Q = 200 l/hr, D _i = 0.50			Q = 200 l/hr, D _i = 0.30			Q = 400 l/hr, D _i = 0.50		
	cm			cm			cm		
	Re	C _d	V _d	Re	C _d	V _d	Re	C _d	V _d
Center	660	0.51	11.6	200	0.81	6.68	312	0.67	8.20
1 cm	640	0.51	11.4	200	0.81	6.80	226	0.76	7.07
2 cm	410	0.61	9.32	164	0.88	6.07	111	1.04	5.02
Wall	75	1.25	4.10	59	1.41	3.68	92	1.14	4.60

สถาบันวิทยบริการ
จุฬาลงกรณ์มหาวิทยาลัย

Appendix B

Air fraction calculation

The example of air fraction and treated water calculation in this study was determined by Henry's law for dissolved gas as described.

- Henry's law for dissolved gases.

The equilibrium or saturation concentration of gas dissolved in a liquid is a function of the type of gas and the partial pressure of the gas in contact with the liquid. The relationship between the mole fraction of the gas in the atmosphere above the liquid and the mole fraction of the gas in the liquid is given by the following from of Henry's law as presented in Equation III-17:

$$p_g = \left(\frac{H}{P_T}\right) \cdot x_g \quad \text{Equation III-17}$$

When P_T = total pressure, usually 1.0 atm

x_g = mole fraction of gas in water, *moleGas / moleWater*

$$= \frac{\text{moleGas}(n_g)}{\text{moleGas}(n_g) + \text{moleWater}(n_w)}$$

- For air p_g = 1.0 mole Air/mole Air

$$H = 66400 \frac{\text{atm}(\text{moleGas} / \text{moleAir})}{(\text{moleGas} / \text{moleWater})}$$

$$x_g = \frac{p_g \times P_T}{H}$$

$$x_g = \frac{1.0(\text{moleAir} / \text{moleAir}) \times 1.0 \text{atm}}{66400 \text{atm} \frac{(\text{moleGas} / \text{moleAir})}{(\text{moleGas} / \text{moleWater})}}$$

$$= 1.506 \times 10^{-5} \text{ mole air/mole water}$$

➤ Air mole calculation:

In this section, amount of air (in mole unite) in 1 litre of water was calculated which depending on the total pressure (P_T) in the reactor tank. The calculated air mole of different total pressure is presented in **Error! Reference source not found.**

- 1 Litre of water contains $\frac{1000g}{18g/mole} = 55.6mole$

$$\frac{n_g}{n_g + n_w} = 1.506 \times 10^{-5} \text{ mole Air/mole Water}$$

$$\frac{n_g}{n_g + 55.6} = 1.506 \times 10^{-5} \text{ mole Air/mole Water}$$

$$n_g = 8.373 \times 10^{-4} \text{ mole Air/L}$$

Table A - 4. Amount of air in 1 litre of water at different total pressure

Total pressure, P_T , (bars)	n_g (mole Air/L)
1.0	0.837×10^{-3}
2.0	1.675×10^{-3}
2.5	2.093×10^{-3}
3.0	2.512×10^{-3}
3.5	2.931×10^{-3}
4.0	3.350×10^{-3}

➤ Determination of the saturation concentration of Air.

In this section, the saturated concentration of air is determined which relates to the molecular weight of air and total pressure in the reactor. The results presented in Table A - 5

- Firstly, at total pressure = 1 atm
- Molecular weight of Air = 28.97 g/mole

The concentration of air (C_s) can be calculated by

$$C_s \approx \frac{0.837 \times 10^{-3} \text{ mole Air / L} (28.97 \text{ g / mole Air})}{(1g / 10^3 \text{ mg})}$$

$$C_s \approx 24.26 \text{ mg/l}$$

Table A - 5. The saturated concentration of air at different total pressure

Total pressure, P_T , (bars)	Concentration of Air (mg/L)
1.0	24.26
2.0	48.52
2.5	60.63
3.0	72.77
3.5	84.91
4.0	97.05

➤ Air volume calculation at 3.5 bars

In this section, the total pressure at 3.5 bars and flow rate of pressurized water at 40 l/hr was selected to calculate the air volume.

- At total pressure = 3.5 bars
- The concentration of air = 84.91 mg/l from Table A - 5
- The pressurized water flow rate = 40 l/hr
- The concentration of air volume = 84.91 mg/l * 40 l/hr
- = 3396.4 mg/hr = 3.396 g/hr
- From molecular weight of air = 28.97g/mol
- Amount of air = $\frac{3.396\text{g/hr}}{28.97\text{g/mol}}$
- = 0.117 mol /hr
- From volume mole of air = 24.1 l/ mol
- Air volume = 0.117 mol/hr * 24.1 l/mol
- Air volume = 2.81 l/hr
- With 70 % efficiency of saturated tank,
- Air volume = 2.81 l/hr * 0.70
- Therefore, Air volume = 1.97 l/hr

➤ Air fraction calculation

For operating condition at raw water = 200 l/hr and pressurized water flowrate = 40 l/hr, The fraction of air and treated water could be calculated by

$$\begin{aligned} \text{Fraction of air and treated water} &= \frac{1.97 \text{ l/hr}}{(200 + 40) \text{ l/hr}} \\ &= 0.0082 \end{aligned}$$

Table A - 6. The summarized of air fraction for each operating condition

Total pressure (bars)	Pressurized water flow rate (l/hr)	Raw water flow rate (l/hr)	Air fraction
3.5	36	150	0.0096
		175	0.0084
		200	0.0075
		250	0.0062
		300	0.0053
		350	0.0046
3.5	40	150	0.0100
		185	0.0088
		200	0.0082
		225	0.0075
		300	0.0058
		400	0.0045
3.5	28	100	0.0100
	40	150	
	55	200	
	65	250	
	80	300	
	110	400	
3.5	70	200	0.0128
	90	200	0.0153

4.0	40	175	0.0105
		200	0.0094
		225	0.0085
5.0	40	150	0.0149
		200	0.0118
		300	0.0083



สถาบันวิทยบริการ
จุฬาลงกรณ์มหาวิทยาลัย

Appendix C

The calculation of Tangential velocity gradient

In this study, there are 4 methods to calculate the velocity gradient. First, the velocity gradient was measured from the experiment. Second, it was calculated from the differential of the tangential velocity. Third, it was calculated based on the intensity in the mixing tank. Fourth, it was calculated from a modification of Bradley's equation.

(1) The velocity gradient by the experimental method which could be calculated by Equation III-12

$$G_{z,\text{exp}} = \frac{\delta V_z}{\delta R} = \frac{V_{z2} - V_{z1}}{R_2 - R_1} \quad \text{Equation III-12}$$

The calculation of experimental velocity gradient for all operating condition in HC 1 which was presented in Table A - 7.

Table A - 7. The summarized calculation of experimental tangential velocity gradient in HC1.

HC 1					
Q = 200 l/hr and D_i = 0.30 cm					
Position	V_y	V_{y2} - V_{y1}	R	R₂-R₁	G_{exp}
center	2.95		0		0
1 cm	5.41	2.46	1	1	2.46
2 cm	8.62	3.21	2	1	3.21
wall	24	15.38	2.25	0.25	61.52
Q = 200 l/hr and D_i = 0.50 cm					
Position	V_y	V_{y2} - V_{y1}	R	R₂-R₁	G_{exp}
center	8.92		0		0

1 cm	7.74	-1.18	1	1	-1.18
2 cm	23.28	15.54	2	1	15.54
wall	34.92	11.64	2.25	0.25	46.57
Q = 400 l/hr and D_i = 0.50 cm					
center	7.48				0
1 cm	7.73	0.25	1	1	0.25
2 cm	31.86	24.13	2	1	24.13
wall	43.97	12.11	2.25	0.25	48.44

(2) The calculation of velocity gradient from the tangential velocity correlation which was expressed in Equation III-13

$$G_z = \frac{\delta V_z}{\delta R} = \frac{\delta(K.R^n)}{\delta R} = n.K.R^{n-1} \quad \text{Equation III-13}$$

By this method, calculation of the velocity gradients could be summarized in Table A - 8

Table A - 8. The summarization of velocity gradient for all types of hydrocyclone

Type of hydrocyclone	n	K	Correlations	G_z (s⁻¹)
HC1	1.0	15	$V_z = 15.R$	15
HC2	1.3	26	$V_z = 26.R^{1.3}$	10
HC3	0.6	2	$V_z = 2.R^{0.6}$	6

(3) The velocity gradient based on the principle of the mixing tank ($G_{a, m}$)

In the water treatment process, the average velocity gradient is calculated with Equation III-14; it is used to quantify and verify the mixing performance of the agitator in the mixing tank, it can be also applied to calculate the average velocity gradient in the hydrocyclone.

$$G_{a,m} = \sqrt{\frac{P}{\mu_w \cdot V_{hc}}} \quad \text{Equation III-14}$$

This was an example to calculate the velocity gradient based on the principle of the mixing tank.

The calculation of dissipated energy

- At raw water flow rate = 200 l/hr = $5.55 \cdot 10^{-5} \text{ m}^3/\text{s}$
- The obtained pressure from the pressure gauge = 0.07 bars
- The calculated head loss in the tube between pressure gauge and water inlet port = 0.035 bars
- Head loss at the water inlet port (h_f) = 0.07 - 0.035 bars
= 0.035 bars
= $0.035 \cdot 10^5 \text{ Pa}$
- The dissipated energy = Headloss * raw water flow rate
= $(0.035 \cdot 10^5 \text{ Pa}) \cdot (5.55 \cdot 10^{-5} \text{ m}^3/\text{s})$
= $0.194 \frac{\text{m}^2 \cdot \text{kg}}{\text{s}^3}$

The calculation of velocity gradient

- In HC1, volume of hydrocyclone = $4.31 \cdot 10^{-3} \text{ m}^3$
- The dynamic viscosity of water (μ_w) = $0.001 \text{ kg} \cdot \text{m}^{-1} \cdot \text{s}^{-1}$

From Equation III-14, velocity gradient could be calculated

$$G = \sqrt{\frac{(0.0194 \text{ m}^2 \cdot \text{kg} \cdot \text{s}^{-3})}{(0.001 \text{ kg} \cdot \text{m}^{-1} \cdot \text{s}^{-1}) \cdot (4.31 \cdot 10^{-3} \text{ m}^3)}}$$

$$= 213 \text{ s}^{-1}$$

Summarized table of velocity gradient calculation

Table A - 9. This was the summarization velocity gradient for all operating condition

Hydrocyclone	Q (l/hr)	h_f (bars)	Pressure in tube (bars)	P, $\frac{m^2 \cdot kg}{s^3}$	V_{hc} , (l)	$G_{a, m}$ (s^{-1})
HC1	200	0.035	0.07	0.194	4.31	213
HC2					7.26	164
HC3					1.96	315
HC1	400	0.009	0.07	0.678	4.31	397
HC2					7.26	306
HC3					1.96	588

(4) The calculation of velocity gradient by the modification of Bradley equation was summarized in Table A-10.

Table A - 10. The summarized results of the tangential velocity by the modification of Bradley equation

Hydrocyclone	Q (l/hr)	D_i (m)	R (m)	α	n	G (s^{-1})
HC1	200	0.005	0.0225	0.37	1.0	47
HC2					1.3	61
HC3					0.6	28
HC1	400	0.005	0.0225	0.37	1.0	93
HC2					1.3	121
HC3					0.6	56

Appendix D

The experimental results of hybrid process

These are the experimental result for all types of hydrocyclone

Table A - 11. The summarization of experimental results of HC1

HC1									
Di (cm)	Q (l/hr)	Controlled Parameter		Observing Results					Floated floc percentage
		Cc (mg/l)	Raw water con.(g/l)	Vortex strength	Bubbles coalescence (mm)	Floating floc (cm)	Settle floc (cm)	Separation efficiency (%)	
Air fraction = 0.0100									
0.5	150	1.0	0.5	weak	no	1	2.5	27	29
	200			weak	no	0	5	0	0
	300			strong	no	1	5	0	17
	400			strong	yes	0.8	5	0	14
Qp = 40 l/hr and Pt = 3.5 bars									
0.5	150	1.00	0.5	weak	no	0.4	5	0	7.5
	200			weak		0.6	4		13
	300			medium	yes	0	7		0
	400			strong	0	10	0		
0.3	100	1.00	0.3	weak	no	0	all	0	0
	150			weak	1 to 2				
	200			medium	2 to 4				
	250			strong	2-6 mm				

Note: The separation line was not observed in this hydrocyclone

Table A - 12. The summation of experimental results for HC2

HC2

Pt = 3.5 bars, Qp = 36 l/hr

Di (cm)	Q (l/hr)	Controlled Parameter		Observing Results			
		Cc (mg/l)	Raw water concentration (g/l)	Vortex strength	Bubbles Coalescence	Floating floc	Separation efficiency (%)
0.50	100	No	No	no	no		
	150			no	no		
	200			no	no		
	250			very weak	no		
	300			strong	no		
	400			very strong	1-5 mm		
	100	1.0	Yes, 0.5	no	no	a little bit	32.0
	150			no	no	a little bit	8.8
	200			no	no	a little bit	20.0
	250			very weak	no	some	6.4
	300			strong	no	a little bit	6.0
	400			very strong	3-5 mm	0	9.0
0.30	100	No	No	no	no		
	150			a little bit	1-6 mm		
	200			weak	2-10 mm		
	250			strong	2-15 mm		
	300			very strong	3-15 mm		
	100	1.0	Yes, 0.50	no	no	no/a little bit	15
	150			no/Very weak	1-5 mm	no/a little bit	17
	200			weak	2-10 mm	No	17
	250			strong	2-10 mm	No	12
	300			very strong	3-15 mm	No	10

Note: The separation line was not observed in this hydrocyclone

Table A - 13. The summation of experimental results for HC3

HC3											
Di (cm)	Q (l/hr)	Controlled		Observing Results						Floated floc (%)	
		Cc (mg/l)	Raw water conc. (g/l)	Vortex strength	Bubbles coalescence (mm)	Floating floc (cm)	Settle floc (cm)	Sep. eff (%)	Separation line		
Pt = 3.5 BARS, Qp = 36 l/hr											
0.5	150	1.0	0.5	Very weak	no	0.6	0		no	-	
	175			weak		0.7	2			26	
	200			weak medium		1.0	0			100	
	250			strong		2	0.6			2	23
	300			strong		3 to 5	1.3			3	30
	350			strong		3 to 5	1.3			4	25
Pt = 3.5 BARS, Qp = 40 l/hr											
0.5	150	1.0	0.5	Very weak	no	1.0	1.5		no	40	
	185			weak		1.0	2.0			33	
	200			medium strong		1.5	2.0			43	
	300			very strong		2	1.0			4.0	20
	400			very strong		2 to 3	1.0			3.5	22
	150			0		0	Very weak			0.5	
185	weak	0.5									
200	medium strong	1									
300	very strong	3 to 4									
400	very strong	4 to 5									
Pt = 3.5 BARS, Qp = 40 l/hr											
0.5	150	2.0	0.5	very weak	no	1.0	2.0		no	33	
	175			medium strong	no	1.0	1.5			40	
	200			medium strong	no	1.3	0.0			100	
	225			medium strong	1 to 2	1.2	2.0			38	
	300			strong	7 to 8	1.3	4.0			25	
note: floc of 2 mg/l > floc size of 1 mg/l											
Pt = 4 BARS, Qp = 40 l/hr											
0.5	175	2.0	0.5	medium	0	1.5	2.0		no	43	
	200			medium strong	0	1.0	2.5			29	
	225			medium strong	2.5	1.2	1.0			55	
Pt = 5 BARS, Qp = 40 l/hr											
0.5	150	2.0	0.5	medium	0.6	1.0	5.0		no	17	
	200			medium strong	0.6	0.3	5.0			6	
	300			medium strong	1.2	1.3	4.0			25	
Pt = 3.5 BARS, Qp = 52 l/hr											
0.5	185	2.0	0.5	weak	not clear	0.8	2.0		no	29	
	200			medium strong	2 to 4	1.0	2.5			29	
	250			strong	2 to 5	0.9	2.5			26	
				medium strong	2 to 5	0.8	3.0				
Pt = 3.5 bars, Qp = 40 l/hr											
0.5	progressive start-up	1.0	0.5	medium strong	no	0	5	18	no	0	
		2.0				1.2	2.3	36		34	
		2.5				1.8	2.0	42		47	
		3.0				1.9	0.8	50		70	
		4.0				1.5	0.0	70		100	
		6.0				1.0	6.0	15		14.2	
		10.0				1.0	8.0	10		no	11.1

Table A - 14. The summation of experimental results for HC3 (continuous)

HC3 (continuous)											
Di (cm)	Q (l/hr)	Controlled		Observing Results							Floated floc (%)
		Cc (mg/l)	Raw water conc. (g/l)	Vortex strength	Bubbles coalescence (mm)	Floating floc (cm)	Settle floc (cm)	Sep. eff (%)	Separation line		
Air fraction = 0.0100											
0.5	100	3.0	0.5	Very weak	no	yes	no	32	no		
	150			weak	no	yes	no	28			
	200			medium strong	no	yes	no	20			
	250			strong	yes	yes	no	22			
	300			strong	yes	yes	yes	14			
	400			strong	yes	yes	yes	4			
	progressive start-up			medium strong							
	0.5			no	yes	no	70	yes			
0.5	100	3.0	0.5	Very weak	no						
	150			weak	no						
	200			medium strong	no						
	250			strong	no						
	300				1 to 2						
	400				1 to 5						
	progressive start-up			medium strong							
	0.5			no							
Air fraction = 0.0100											
0.3	100	3.0	0.5	Very weak	no	no	yes	33	no		
	150			weak	no			10			
	200			medium strong	no			9			
	250			strong	yes			20			
	progressive start-up			medium strong							
	0.3			yes	no			23			
0.3	100	3.0	0.5	Very weak	1 to 3						
	150			weak	3 to 4						
	200			medium strong	3 to 5						
	250			strong	5 to 6						
	progressive start-up			medium strong							
	0.3			3 to 4							

Table A - 15. The summarization of experimental results for HC4

HC4										
Di (cm)	Q (l/hr)	Controlled		Observing Results						
		Cc (mg/l)	Raw water conc. (g/l)	Vortex strength	Bubbles coalescence (mm)	Floating floc (cm)	Settle floc (cm)	Sep. eff (%)	Separation line	Floated floc (%)
Air fraction = 0.0100										
0.5	Progressive start-up	1.0	0.5	medium strong	no	0.0	4.0	6	no	0
		2.0				1.0	1.5	36	a little bit	40
		3.0				1.0	0.0	10	no	100
		4.0				1.0	0.0	10	no	100



 สถาบันวิทยบริการ
 จุฬาลงกรณ์มหาวิทยาลัย

BIOGRAPHY

Name Pradipat Bamrungsri
Date and place of birth June 22, 1979, Naknonsawan, Thailand

Education

(1997-2003) Bachelor degree (B. Eng) from Chiang Mai University in Environmental engineering (2000).

(2003-2004) Master degree of Environmental Engineering (M. Eng) in Chiang Mai University (2003).

(2004-2007) double Ph. D. between National Center of Excellence for Environmental and Hazardous Waste Management (NCE-EHWM), Chulalongkorn University, Thailand and Chemical and Environmental Engineering, Institut National des Sciences Appliquées de Toulouse (INSA-Toulouse).

List of publication

- K.SOPAJAREE, A. KLEEPKLANG, P. BAMRUNGSRI.

“Effect of Temperature and Volumetric Loading Rate on Phenol Adsorption Capacity by Granular Activated Carbon”, Songklanakarin J. Sci. Technol., 2004, 26 (Suppl. 1): 97-108.

- J.L. TROMPETTE, H.VERGNES, G.HEBRARD, P.BAMRUNGSRI

“Characteristic Aspects of Bubbles Coalescence during Electrolysis of Ammonium Salt Solution” J. Phys. Chem. C, 2007, 111(13), 5236-5243.

- P. BAMRUNGSRI, C. PUPRASERT, C. GUIGUI, P. MARTEIL, P. BREANT, G. HEBRARD

“Development of a Simple Experimental Method for the Determination of the Liquid Field Velocity in Conical and Cylindrical Hydrocyclones”. Poster presentation in Gas-Liquid-Solid 8. 16-19 December 2007. New Delhi, India.

- P. BAMRUNGSRI, C. PUPRASERT, C. GUIGUI, P. MARTEIL, P. BREANT, G. HEBRARD

“Development of a Simple Experimental Method for the Determination of the Liquid Field Velocity in Conical and Cylindrical Hydrocyclones”. This is publication was accepted by “ChERD: Chemical Engineering Research and Design ”, May 2008.

- G.HEBRARD, C.GUIGUI, C.PUPRASERT, P.BAMRUNGSRI, V.SIANSANUN, L.LOPEZ, P.BREAN, P.MARTEIL.

“Water treatment process by hydrocyclone” Documented date 25 April 2008 at VIDON office for French Patent, number 0852783.



สถาบันวิทยบริการ
จุฬาลงกรณ์มหาวิทยาลัย